Universität für Bodenkultur Wien
University of Natural Resources and Applied Life Sciences, Vienna
Department of Chemistry, Division: Analytical Chemistry

DIPLOMARBEIT

Migration studies of fish by measurement of strontium isotope ratios and multi-elemental patterns in otoliths using LA-ICP-MS

von
Monika Sturm

Betreuer:
Ao. Prof. Dr. Thomas Prohaska
Dr. Andreas Zitek

März 2008

SPECIAL THANKS TO:

THOMAS PROHASKA[1]

ANDREAS ZITEK[1]

THE VIRIS TEAM[2]

MY FAMILY[3]

MY FRIENDS[4]

[1] The best supervisors ever! Thanks for everything!
[2] Special thanks to Marion for helping me to overcome several crises during the diploma thesis!
[3] Thank you for your support and your confidence in my decisions!
[4] Thank you for being there for me in good and bad times!

Table of content

Abstract

Migration studies of fish are used in fisheries management in order to manage and sustain fish stocks by habitat preservation and by implementation of protection areas. Certain structures within the body of fish record the elemental and isotopic patterns of the surrounding water. They can be used as natural tags to investigate population structures and the movement of individual fish. Mostly calcified structures like otoliths and scales have been used as natural tags besides some approaches with eye lenses. Otoliths are ear stones of teleost fish. Since they grow throughout life and are metabolically inert, otoliths are supposed to record environmental variations experienced over the entire life time of an individual fish.

The aim of this work was to examine whether the isotope ratio of Sr in combination with elemental finger prints (Sr, Na) of otoliths from rainbow (*Oncorhynchus mykiss*) and brown trout (*Salmo trutta fario*) obtained by LA-ICP-MS (laser ablation inductively coupled plasma mass spectrometry) can be used to find the natal origin of the fish and to reconstruct eventually its life history. Brown trout and rainbow trout belong to the family of salmonides and they can be found all over Europe. Trout production in fish farms is an economic factor in Austria, e.g. 2.500 tons of salmonides were produced in 2005. Fish from three Austrian fish farms and two rivers were examined.

The clusters formed by nearest neighbour cluster analysis of the water samples based on $^{23}Na/^{43}Ca$, $^{88}Sr/^{43}Ca$ and $^{87}Sr/^{86}Sr$ allowed a retrospective assignment of the otolith regions to water clusters via a nonparametric discriminant analysis to the water clusters with 100% accuracy. Eye lenses and scales were examined by LA-ICP-MS in addition to otoliths. Sr, Na, Mg and Ba concentrations in the scales were significantly above the detection limit. Only Na was above the detection limit in the eye lenses. Differences in the Na content at the surface of eye lenses of fish from two different locations were found.

Zusammenfassung

Migrationsstudien von Fischen werden dazu verwendet, Fischbestände zu managen und dadurch die Erhaltung von Lebensräumen und Schongebieten zu sichern. Bestimmte Strukturen im Fisch speichern Isotopen- und Elementmuster des Wassers. Diese Strukturen können als natürliche Marker zur Untersuchung von Populationsstrukturen und zur Rekonstruktion von Wanderungsbewegung genutzt werden. Neben Linsen werden vor allem kalkhaltige Strukturen wie Otolithen und Schuppen als Marker verwendet. Otolithe sind Gehörsteine von Knochenfischen. Sie wachsen während des gesamten Lebens und sind metabolisch inert. Daher zeichnen sie Umweltveränderungen auf, die der Fisch im Laufe seines Lebens erfährt.

Das Ziel dieser Diplomarbeit war festzustellen, ob Strontiumisotopenverhältnisse und elementaren Fingerabdrücken (Sr, Na) von Otolithen von Regenbogen- (*Oncorhynchus mykiss*) und Bachforellen (*Salmo trutta fario*), die mit LA-ICP-MS (Laserablation mit induktiv gekoppelter Plasma Massenspektrometrie) bestimmt wurden, dazu benutzt werden können, den Geburtsort und die Lebensgeschichte der Fische zu rekonstruieren. Regenbogen- und Bachforelle gehören zu den Salmoniden und kommen in ganz Europa vor. Die Forellenzucht ist in Österreich von wirtschaftlicher Bedeutung, so wurden 2005 2.500 Tonnen Salmonide produziert. Fische von drei Fischzüchten und von zwei Flüssen wurden im Rahmen dieser Arbeit untersucht.

Die Cluster, die durch nächster Nachbar Clusteranalyse der Wasserproben basierend auf $^{23}Na/^{43}Ca$, $^{88}Sr/^{43}Ca$ und $^{87}Sr/^{86}Sr$ gebildet wurden, ermöglichten eine retrospektive Zuordnung der untersuchten Otolithenregionen mittels nicht-parametrischer Diskriminanzanalyse zu den entsprechenden Wasserclustern zu 100%. Zusätzlich wurden Linsen und Schuppen mit LA-ICP-MS untersucht. In den Schuppen lagen Sr, Na, Mg und Ba über dem Detektionslimit. Bei den Linsen lag Na über dem Detektionslimit. Unterschiedliche Na-Gehälter in den Oberflächen der Linsen von Fischen zweier unterschiedlicher Standorte wurden gefunden.

1 Introduction

1.1 General aspects of migration studies of fish

Migration studies of fish are of high importance for fisheries management in order to manage and sustain fish stocks by habitat preservation and implementation of both protection areas and periods. Thus, it is necessary to understand the migration behaviour of a species to get knowledge about the population structure, population dynamics and habitat use [HAMER et al, 2006]. Migration studies of fish and the structure of fish populations are especially of interest when different countries catch fish in the same body of water [MARKWITZ et al, 2000]. In order to discriminate between populations different approaches have been used such as meristics (countable structures like scales are counted for differentiation of species and populations [N. N., 2008c]), morphometrics, parasite loadings, otolith shape and otolith increment patterns as well as genetic approaches examining nuclear and mitochondrial DNA markers. [ASHFORD et al, 2006] Unfortunately, gene flow within a meta-population can prevent the detection of genetic differences. [WRIGHT et al, 2006] Although, fish populations might be discriminable by these methods they do not provide any time resolved information about life history of the fish. For this purpose tagging experiments for example with codes wire tags are used by hydro-biologists to help identify movement patterns of fish. However, tags may distort the natural behavior or increase the chance of being killed. Another problem concerning tag-recapture experiments is that many small larvae with high mortality rates are produced. Apart from that, these artificial tags do usually only provide information about the place and time of tagging and of recapture. Alternatively, structures within the body of the fish which record the natural elemental and isotopic concentration of the surrounding environment can be used as natural tags to investigate population structures and the movement of individuals. Besides some approaches with eye lenses, mostly calcified structures like bone, fin rays, otoliths and scales have been used for this purpose. [CHITTARO et al, 2006, CLARKE et al, 2007 and BROPHY et al, 2003] Otoliths have been extensively used as natural tags, because otoliths grow throughout life and are metabolically inert, while scales and bones have been shown to degrade during stress [WELLS et al, 2003]. Thus otoliths have mostly been used as natural tags for migration studies of fish, since they record environmental variations experienced over the entire life time of an individual

[CAMPANA, 1999]. In order to use natural tags as indicators of migration of fish it must be demonstrated that there are chemical differences that are consistent over time and space. Furthermore, relationships between levels of specific elements in the ambient water and in the natural tag must be established. [HAMER et al, 2006] Additionally, it must be ensured that the incorporation is not biased by ontogeny, temperature variations, stress or physiological changes (e.g. growth) [KALISH 1991 and 1992, SADOVY and SEVERIN, 1994 and 1992].

1.2 Otoliths

1.2.1 Physiological function of otoliths

Otoliths are structures in the ears of teleost fish. Due to their form and function they are also called earstones. There are three pairs of otoliths called lapilli, sagittae and asterisci, which differ in function, size, shape and microstructure. Sagittae are used in most studies concerning otolith chemistry. The three pairs of otoliths are located symmetrically in vestibules which are part of the ear of the fish (Figure 1). These vestibules are filled with endolumphy which are referred to as utriculus, sagitta and langenus for lapilli, sagittae and asterisci, respectively. The otolith containing vestibules are covered with sensory hair cells which are covered by a membrane. This membrane holds the otolith in its place next to the sensory epithelium. Stimulated by head motion or sound the otolith moves relative to the sensory epithelium. As a result the cilia of the sensory hair cells are bent leading to the detection of the mechanical signal by excitation of nerves. Motion and hearing are detected in this way. Shape and size of the three otolith pairs differ considerably between species (Figure 2 and Figure 3). Otoliths of different sizes are believed to have different resonance frequencies, i.e. species with larger otoliths are more sensitive to lower frequencies. Otolith sizes are not related to the body length of different species of fish. For example big ocean fish like swordfish and tuna have small otoliths in relation to their body size compared to reef fish. Commonly, saggitae and lapilli are hard to distinguish in larvae, whereas asterici form later in development. Otoliths continue increasing in mass with time, even after the somatic growth of the fish stopped [SECOR et al. 1992, POPPER et al, 2005].

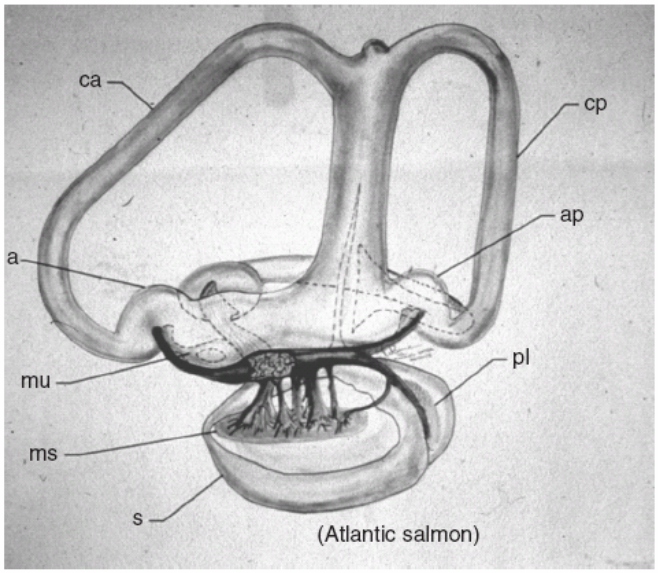

Figure 1. Right ear of atlantic salmon (Salmo salar) [source: POPPER et al, 2005]

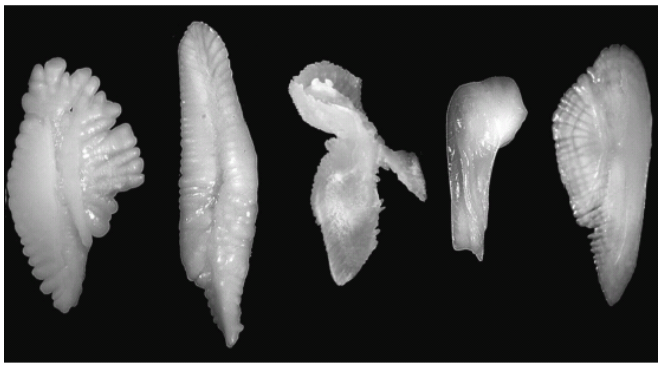

Figure 2. Variety of Shapes of otoliths demonstrated by saggital otoliths of Merluccius bilinearis, Halargyreus johnsoni, Lampris gutattus, Urophycis tenuis and Lophplatilus chamaeleonticeps [source: POPPER et al, 2005]

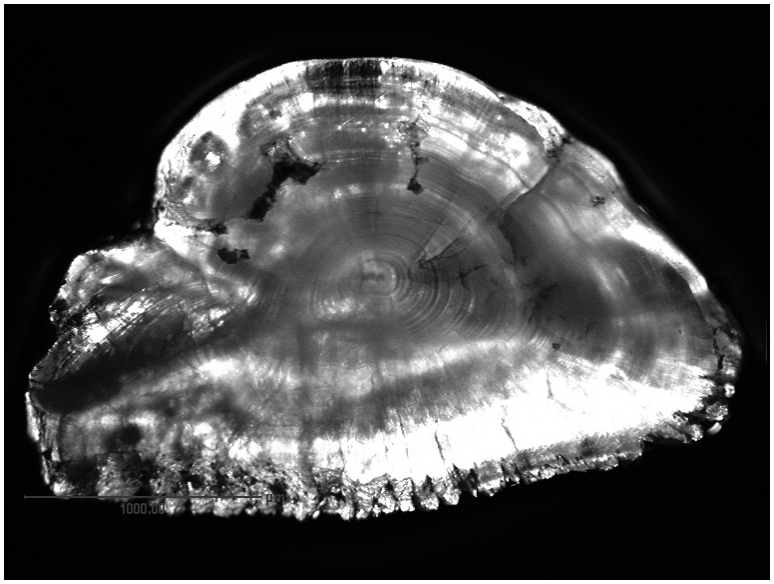

Figure 3.Otolith of a brown trout (Salmo trutta fario) from river Ois grinded to the core level with visible annuli.

1.2.2 Otolith structure and chemistry

Otoliths consist mainly of calcium carbonate. The crystalline form of the calcium carbonate of most lapillus and sagittal otoliths is aragonits, while asterisci are made of vaterite. The aragonite of the otoliths has a chemical purity of about 97 %, the rest consists of organic material and trace elements. [CAMPANA, 1999] Otoliths are acellular, that is they do not contain any cells, and are metabolically inert. Thus, any elements that are incorporated into its growing surface are conserved permanently. Consequently, the entire lifetime of the fish from otolith growth before hatching to the death is reflected in this otolith microstructure. [CAMPANA and NEILSON, 1985] Since otoliths grow in discrete layers, otoliths have been used to determine the age of fish since 1899 when Reibisch discovered these otolith annuli [CAMPANA, 1999]. Pannella discovered that there are daily growth increments 1971 [CAMPANA, 1999]. Therefore, the temperature and composition of the ambient water recorded in the otolith can be linked theoretically to otolith growth increments. However, in practice, the interpretation of this chemical record is more complex since there are e.g. physiological filters between the water and the otolith. [KALISH, 1989]

1.2.2.1 Otolith growth and elemental composition

The major elements calcium, oxygen and carbon are obviously dominant in the calcium carbonate ($CaCO_3$) matrix. The minor elements with a concentration of more then 100 $\mu g\ g^{-1}$ in otoliths are Na, Sr, K, S, N, Cl and P. Trace elements are present in quantities less 100 $\mu g\ g^{-1}$. [CAMPANA, 1999] The calcification of the otolith depends on the composition of the endolymph around the otolith. The pH of the endolymph determines the calcification rate since the concentration of bicarbonate ions (HCO_3^-) changes with the pH, i. e. reduced alkalinity leads to reduced calcification. The calcification is influenced by temperature as well. The proteins in in the otolith are also of vital importance for the otolith growth and composition. Calcium-binding glycoproteins seem to regulate the calcification rate [ASANO and MUGIYA, 1993]. Calcium carbonate can crystallize as calcite, aragonite or vaterite. Presence of divalent ions like Sr or Mg and organic molecules seem to encourage the formation of aragonite [CARLSTRÖM, 1963 and FALINI et al, 1996]. Other elements can be incorporated into the otolith as a substitute for calcium, form an inclusion in the $CaCO_3$ crystal or are associated with the proteins matrix. Additionally, elements can be incorporated through co-precipitation of another carbonate like Mg as $MgCO_3$. Divalent metal ions of

comparable size are prone to substitute for Ca in $CaCO_3$ or to form co-precipitations. Since $SrCO_3$ is practically isostructural with aragonite, strontium substitutes for calcium in the $CaCO_3$, whereas slightly larger ions such as barium and lead are expected to co-precipitate. [GREEGOR et al, 1997 and MORSE and MACKENZIE, 1990] Incorporation of these elements depends often on a temperature-sensitive partition coefficients and precipitation rate. Anions like chloride and sulfate can also co-precipitate in the otolith matrix. Ions like sodium are found in crystal defects [MORSE and MACKENZIE, 1990]. Weakly bound elements like Na, Cl, Zn and K easily leach out of the otolith when stored in fluids like ethanol or formalin. This might be explained by the micro-channel structure of otoliths. [GAULDIE et al, 1998, CAMPANA, 1999 and PROCTOR and THRESHER, 1998] Amino acids in the calcium carbonate matrix consist of C, H, O, N and to a lesser extent sulfur. Other elements found in otoliths might also be associated with or bound to proteins. The rate of otolith precipitation might have a different influence on these elements than on those directly associated with calcium carbonate crystals. Changes in temperature might change the balance between organic matrix and calcium carbonate formation, resulting in a change of the ratio of element incorporation. [CAMPANA, 1999]

1.2.2.2 Regulation of the otolith chemistry

The incorporation of elements from the surrounding environment of the fish into the otolith is a multi-stage process with different barriers since fish are highly osmoregulated. However, it seems that there is relatively little discrimination against the incorporation of at least some of the trace elements into the otolith. Basically, most minor and trace elements enter the blood plasma via gills and intestine in freshwater fish and marine fish, respectively. From the blood the elements enter the endolymph where the otoliths crystallize. [OLSSON et al, 1998] An unknown fraction of the elements incorporated into the otolith originate from food sources. For instance at least some dietary Sr is found in the otolith. However, 80 and 90% of Ca and Sr, respectively, have been shown to originate from the water in freshwater fish. Thus it is hypothesised that the majority of the elements in the otolith come from the water [LIMBURG, 1995; SIMKISS, 1974 and FARRELL and CAMPANA, 1996]. Gills or intestines serve as osmoregulators in freshwater or marine fish, respectively. Thus they are the most important barriers for dissolved ions from the water [OLSSON et al, 1998]. Water properties like salinity, pH, dissolved oxygen and the calcium concentration also influence the receptivity of the fish for different elements. When the ambient concentration of calcium is low, a greater

fraction of the dissolved calcium as well as of other dissolved metals is absorbed by the fish. The calcium concentration is the most influent water property for elemental uptake in freshwater fishes. Thus the element to calcium ratio is often more important for the uptake of elements in freshwater than the concentration of these elements. [MAYER et al, 1994] There is another elemental barrier between the blood plasma and the endolymph, which leads to a decrease of all major elements except potassium. [GAULDIE and ROMANEK, 1998] The final barrier for the elements is the crystallisation process. This seems to be the most important barrier for the uptake of strontium in the otolith. Therefore, it is not surprising that the differences between freshwater and salt water in Ca, Na, K, Mg and Cl concentrations are not reflected in the otolith. Although, patterns of these elements might not reflect the water chemistry due to their physiological regulation, they might be successfully used to differentiate between groups of fish. Elements with physiological importance like P, Cu and S also seem to be uninfluenced by the environment. Summing up, physiological regulated elements cannot be expected to reflect the environmental concentrations. In contrast to that, the concentrations of other elements such as Sr, Zn, Pb, Mn, Ba and Fe in the otholith seem to reflect the environmental concentration which has for instance been shown for differences between freshwater and salt water phases. The uptake of other trace elements like Li, Cd and Ni may also be unregulated compared to the uptake of common salts, but there are only limited data available about the uptake of these trace elements [CAMPANA, 1999]. Given that there are geographic variations in water chemistry, otolith elemental analysis has a limited use to reconstruct environmental history. However, in addition to ambient concentrations temperature and growth rate may also influence the composition of otoliths. [CAMPANA, 1999]

Several studies show the influence of temperature on the composition of otoliths. For example [HOFF and FUIMAN, 1995] showed that Mg, K, Na and Sr are influenced by temperature. However, confounding results are published for the temperature dependence of the Sr:Ca ratio in the otolith, which was studied by several research groups: [HOFF and FUIMAN, 1995] described a relationship between Sr:Ca and temperature to be positive, [SADOVY and SEVERIN, 1992] negative and [GALLAHAR and MINGSFORD, 1996] found no correlation.

Campana also mentions in his review about otolith chemistry that high Sr:Ca ratio in the otolith coincides with a low otolith growth rate [CAMPANA, 1999] and [CHITTARO et al, 2006a] found significant differences in the elemental concentrations of sagittal and lapillar otoliths from the same individual. They report that the concentrations of Li, Mn, Sn, Ba and Ce were two to nine times higher in lapillar than in sagittal otoliths. It must also be noted that

otoliths can differ considerably in elemental concentrations even when different species live in the same habitat [CHITTARO et al, 2006].

Especially elemental pattens in the core region of otoliths must be interpreted carefully, because they need not necessarily reflect the ambient water. Otolith core chemistry might instead be influenced by yolk upon which the larvae feed or by strong physiological effects. [BROPHY et al, 2003] found for instance elevated Mn levels in the otolith cores of Atlantic herring and proofed in with laboratory reared fish that this effect is independent from the ambient conditions of the eggs. Thus they proposed that the elevated Mn levels in the core might be due to physiological effects in embryonic development. Otolith cores of anadromous fish, that hatch in freshwater, like salmon show equally high Sr/Ca core levels as found in marine phases adult salmon, but there are no elevated Sr/Ca core levels observed in fresh water resistant salmon. This fact shows clearly that the otolith core chemistry is influenced by the environment of the mother. The larvae feed on the yolk sac for some time after hatching before they start feeding on their own [ARAI et al, 2007 and WEBER et al, 2005].

1.2.2.3 Isotopic ratios in otoliths

The isotopic ratios of oxygen and strontium in the otolith are almost identical to the ratios expected in aragonite crystallized directly from the ambient water. Thus water is most likely the main source of strontium in the otolith [THORROLD et al, 1997 and KENNEDY et al, 1997]. 10 to 30% of the carbon comes from other sources than the ambient water such as diet [SCHWARCZ et al, 1998]. The strontium isotope system is described in more detail in chapter 1.5 since strontium isotopes have been used in this study.

1.2.3 Methods applied for otolith analysis

Either the whole otolith or just a specific part of the otolith can be sampled. In general, analyses of whole otoliths are useful for stock discrimination, because different fish stocks are expected to show differences accumulated over the whole life span. The advantages of assays of whole dissolved otoliths are generally better accuracy, precision and sensitivity in comparison to micro-sampling. Thus trace elements with lower concentrations can be analyzed. Moreover, sample preparation is easy without the danger of sampling the wrong growth increment and accurate assay protocols exist. In spite of these atvantages, the major

disadvantage of analyses of whole otoliths is that the time resolved information preserved in the otolith increments is lost. The methods applied for analyses of whole otoliths are listed below, but nowadays ICP-MS is the method of choice [CAMPANA, 1999]:

- Atomic absorption spectrometry (AAS) [HOFF and FUIMAN, 1995]
- inductively coupled plasma atomic emission spectroscopy (ICP-AES) [EDMONDS et al, 1995]
- neutron activation analysis [PAPADOPOULOU et al, 1980]
- Raman spectroscopy [GAULDIE et al, 1994]
- inductively-coupled plasma mass spectrometry (ICPMS) [EDMONDS et al, 1991]

Micro-sampling using e.g. a laser beam is the method of choice in studies when the chronological information recorded in the otolith is of importance.

Micro-sampling methods applied for otolith assays are listed below [CAMPANA, 1999]:

- electron probe microanalysis (EPMA): energy-dispersive (ED-EM) and wavelength-dispersive(WD-EM) electron microprobes [GUNN et al, 1992]
- proton-induced X-ray emission (PIXE) [SIE and THRESHER, 1992]
- laser ablation ICP-MS (LA-ICP-MS) [CAMPANA et al. 1994]

Since LA-ICP-MS was the method of choice for this study, a short introduction on ICP-MS and the instruments used can be found in chapter 2.2. Table 1 gives an overview of a selection of recent studies concerning population structure and migration studies using otolith chemistry analysed by solution-based ICP-MS and LA-ICP-MS.

Table 1. Recent studies concerning population structure and migration studies using otolith chemistry analysed by solution-based ICP-MS and LA-ICP-MS

Fish species	elemental pattern/ isotopic system	Aqnalytical method	literature reference
Saltwater fish			
Stock discrimination of saltwater fish			
Patagonian toothfish (*Dissostichus eleginoides*)	$^{55}Mn/^{42}Ca$, $^{88}Sr/^{42}Ca$ and $^{137}Ba/^{42}Ca$	LA-ICP-MS	[ASHFORD et al, 2006]
staghorn sculpin (*Leptocottus armatus*)	^{25}Mg, ^{43}Ca, ^{55}Mn, ^{86}Sr, ^{138}Ba and ^{208}Pb	LA-ICP-MS	[MILLER, 2007]
Schoolmaster (*Lutjanus apodus*)	^{7}Li, ^{25}Mg, ^{65}Cu, ^{66}Zn, ^{85}Rb, ^{86}Sr, ^{120}Sn, ^{138}Ba, and ^{208}Pb	LA-ICP-MS	[CHITTARO et al, 2006]
Atlantic bluefin tuna (*Thunnus thynnus*)	Li, Mg, Ca, Mn, Sr and Ba	Solution based ICP-MS	[ROOKER et al, 2003]

swordfish (*Xiphias gladius*)	^{24}Mg, ^{66}Zn, ^{88}Sr, ^{138}Ba and ^{208}Pb	ID-ICP-MS	[HUMPHREYS et al, 2005]
Patagonian toothfish (*Dissostichus eleginoides*)	δ^{18}O and δ^{13}C	Solution based ICP-MS	[ASHFORD et al, 2007]
damselfish (*Stegastes nigricans*)	Ba, Ca, Li, Mg, Mn, Na, Sr and Y	Solution based ICP-MS	[LO-YAT et al, 2005]
two-banded bream (*Diplodus vulgaris*)	Li, Mn, Sr, Cd and Ba	Solution based ICP-MS	[GILLANDERS et al, 2001]
plaice (*Pleuronectes platessa*)	δ^{18}O and δ^{13}C	Solution based ICP-MS	[AUGLEY et al, 2007]
English sole (*Pleuronectes vetulus*) and speckled sanddab (*Citharichthys stigmaeus*)	Sr, Li, Ba and Mn	Solution based ICP-MS	[BROWN J., 2006]
orange roughy (*Hoplostethus atlanticus*)	Ba, Cd, Cu, K, Mg, Na, Pb, S, Sr and Zn	Solution based ICP-MS	[EDMONDS et al, 1991]
Atlantic cod (*Gadus morhua*)	B, Mg, Ca, Fe, Zn, Rb,Sr, Sn and Ba	LA-ICP-MS	[CAMPANA et al. 1994]
Weakfish (*Cynoscion regalis*)	Mg, Ca, Sr, Mn, Ba, δ^{18}O and δ^{13}C	LA-ICP-MS	[THORROLD et al, 2001]
Atlantic herring (*Clupea harengus*)	Mg, Zn, Sr, Ba and Pb	LA-ICP-MS	[BROPHY et al, 2003a]
Atlantic cod (*Gadus morhua*)	Li, Mg, Mn, Sr, Ba and Zn	Solution based ICP-MS	[CAMPANA et al. 2000]
damselfish (*Pomacentrus coelestis*)	^{26}Mg, ^{43}Ca, ^{55}Mn, ^{88}Sr, and ^{138}Ba	LA-ICP-MS	[PATTERSON et al, 2004]
damselfish (*Parma microlepis*)	Sr, Ba and Mn	Solution based ICP-MS	[KINGSFORD and GILLANDERS, 2000]
damselfish (*Parma microlepis*)	Ba, Co, Mg, Mn, Rb and Ti	Solution based ICP-MS	[KINGSFORD and DOVE, 1998]
Migration studies of saltwater fish			
damselfish (*Pomacentrus coelestis*)	^{26}Mg, ^{43}Ca, ^{55}Mn, ^{88}Sr, and ^{138}Ba	LA-ICP-MS	[PATTERSON et al, 2005]
anadromous fish			
Stock discrimination in anadromous fish			
black bream (*Acanthopagrus butcheri*)	^{44}Ca and ^{88}Sr	LA-ICP-MS	[ELSDON et al, 2006]
Migration studies of anadromous fish			
chum salmon (*Oncorhynchus keta*)	^{24}Mg, ^{43}Ca, ^{52}Cr, ^{55}Mn, ^{64}Zn, ^{86}Sr and ^{138}Ba	LA-ICP-MS + EPMA + solution based ICP-MS	[ARAI et al, 2007]
Sparidae (*Pagrus auratus*)	^{138}Ba	LA-ICP-MS	[HAMER et al, 2006]

chum salmon (*Oncorhynchus keta*)	^{24}Mg, ^{52}Cr, ^{55}Mn, ^{64}Zn, ^{86}Sr and ^{138}Ba	LA-ICP-MS + EPMA + solution based ICP-MS	[ARAI et al, 2006]
chum salmon (*Oncorhynchus keta*)	^{64}Zn, ^{86}Sr and ^{43}Ca	LA-ICP-MS	[ARAI et al, 2007]
barramundi (*Lates calcarifer*)	Cu, Mn, Zn, Cd and Pb	LA-ICP-MS	[MILTON et al, 2000]
Australian grayling (*Prototroctes maraena*)	^{88}Sr, ^{138}Ba and ^{44}Ca	PIXE + LA-ICP-MS	[CROOK et al, 2006]
freshwater fish			
Stock discrimination in freshwater fish			
Allis shad (*Alosa alosa*)	^{55}Mn, ^{59}Co, ^{88}Sr, ^{24}Mg, ^{57}Fe, ^{209}Bi, ^{74}Ge, ^{113}In, ^{98}Mo, ^{232}Th, ^{85}Rb, ^{120}Sn and ^{51}V	Solution based ICP-MS	[TOMAS et al, 2005]
Arctic grayling (*Thymallus arcticus*)	^{25}Mg, ^{43}Ca, ^{55}Mn, ^{86}Sr and ^{137}Ba	LA-ICP-MS	[CLARKE et al, 2007]
Migration studies of freshwater fish			
chinook salmon (*Oncorhynchus tshawytscha*)	^{87}Sr/^{86}Sr	Solution based ICP-MS	[INGRAM and WEBER, 1999]
Dolly varden char (*Salvelinus malma*)	^{87}Sr/^{86}Sr	LA-ICP-MS	[OUTRIDGE et al, 2002]

1.2.4 Applications of otolith chemistry

A variety of applications of otolith chemistry [CAMPANA, 1999] has been used for the following purposes:

- Stock identification (see 1.2.4.1)

- Migration history (see 1.2.4.2)

- Age determination: Age determination based on otolith chemistry is mostly used to validate traditional methods of age determination like counting of otolith increments. Radiocarbon from nuclear testing has been used for this aim. [CAMPANA and JONES, 1998]

- Reconstruction of environmental history: Oxygen isotope ratios in otoliths have been proven to be usable for reconstructing temperature changes. [THORROLD et al, 1997]

- Pollution: Different studies examined the usability of otolith chemistry as a proxy for pollution. Otoliths seem to incorporate an insufficient portion of pollution related metals. [CAMPANA, 1999] Heavy metals like Cu seem to be removed from the blood via liver and kidneys and may therefore not be incorporated into the otolith matrix [MILTON et al, 2000].

- Physiological indicators: Changes in physiology are observed by changes in otolith chemistry such as a decline of the metabolic rate by increased otolith $\delta^{13}C$ [SCHWARCZ et al, 1998]

- Chemical marking experiments: Living fish are exposed to chemicals such as oxytetracycline hydrochloride which produces a mark in the otolith. This approach is for instance used in tag-recapture experiments. [NAGIEC et al, 1995] Another possibility is trans-generational chemical marking. This approach can be used for marking great numbers of larvae. [THORROLD et al, 2006] injected ^{137}Ba enriched $BrCl_2$ into mother fish in order to mark the larval portion of the otoliths of the progeny with ^{137}Ba.

Since migration studies and stock discrimination are the objectives of most studies using otolith chemistry, they are described in more detail below.

1.2.4.1 Stock identification

Groups of fish living in chemically different environments can be identified using otolith chemistry. Elements like Sr, Ba, Mn, Fe and Pb without strong physiological regulation are suitable for this application. The content of these elements in otoliths reflects the water chemistry in contrast to other elements which do not necessarily reflect the water chemistry due to strong physiological regulation. However, even the concentrations of therse strongly regulated elements can vary between groups of fish.[FARRELL and CAMPANA, 1996] The isotopic ratios of strontium und oxygen can also be used. [THORROLD et al, 1997 and KENNEDY et al, 1997] The “elemental fingerprint” composed of selected elements and isotopic ratios can be used to discriminate among groups of fish which have spent at least part of their lives in different environmental conditions. However, fingerprints for fish of different size classes from the same population can differ. [PAPADOPOULOU et al, 1980] Either the

whole otolith or the otolith core is analysed for stock identification. The elemental fingerprint is integrated over the entire life time when the whole otolith is used. The elemental fingerprint can be used as long-term stock discriminator when the spatial environmental differences are more pronounced than those within areas or across year-classes and when fish size related differences in the fingerprint are statistically removed. [CAMPANA, 1999] An overview of a selection of recent stock identification studies using otolith chemistry analysed by solution-based ICP-MS and LA-ICP-MS is given in Table 1.

1.2.4.2 Migration history

The migration history of fish can be reconstructed using the elemental and/or isotopic composition along the growth axis of the otoliths. Therefore the otolith is usually grinded to the core level (see Figure 3) and probed using micro-sampling techniques as described in 1.2.3. The chemical composition of the otolith growth axis is linked to the chronology recorded in the otolith annuli. Consequently, isotopic and elemental pattern of a certain area of the otolith can be linked to a specific time or age. [CAMPANA, 1999] This approach has been used widely for the detection of anadromy. Anadromous fish are fish with the ability to switch between fresh water and saltwater environments like e.g. salmon. Shifts in the Sr:Ca ratio are mostly used for the detection of anadromy since this ratio differs strongly between freshwater and saltwater. [ARAI et al, 2007] Migration in more homogenous environments like freshwater streams can also be detected, but ontogenetic changes in the otolith composition can be misinterpreted since shifts in the otolith chemistry can result from age-related physiological change or from environmental changes. [CAMPANA, 1999] An overview of a selection of recent migration studies using otolith chemistry analysed by solution-based ICP-MS and LA-ICP-MS is given in Table 1.

1.3 Scales

Scales might be used as natural tags for studies concerning fish migration and population structure besides other calcified structures like bone, finrays and otoliths. [CHITTARO et al, 2006, CLARKE et al, 2007 and BROPHY et al, 2003] According to [MUHLFELD and MAROTZ, 2005] scales could become a non lethal alternative to otoliths. That would be a

great advantage in studying rare and endangered fish species. Scales are made of calcified hard tissue and cover the body surface of teleost fish. The scales reduce drag when the fish moves through the water, serve as storage for minerals and nutrients and provide protection for the fish and especially the lateral line organ, which helps to detect vibration and movement in the surrounding water. Fish scales are frequently used for the determination of fish age and in order to identify fish species [ABLE and LAMONACA, 2006].

1.3.1 Growth and structure of fish scales

Scales are composed of internal and an external layers. The external layer is thin and well calcified. This layer is also called bony layer since it consists of hydroxyapatite crystals and type I collagen fibrils. The internal layer is thicker and calcified only partially. This layer is also called basal plate. The basal plate is composed of lamellae made from each containing type I collagen fibrils and amorphous matrix. When a fish looses scales or when they are experimentally removed, they are immediately regenerated. [OHIRA et al, 2007] Each scale lays in a separate scale pocket in the dermis and is covered by the epidermis with the calcified layer facing the epidermis. [PERSSON et al, 1999] Fish scales are mineralized throughout life. The internal layer is build after the mineralisation of the external layer [IKOMA et al, 2003]. The Ca content of scales was determined to be 23% of the weight by [CLARKE et al, 2007]. Around the centre of the scale concentric scale ridges, which are also referred to as growth rings, are visible on scales of a brown trout (*Salmo trutta fario*) in Figure 4. Scales are formed between the larval and the juvenile life stage of a fish. Scale formation starts at a specified place on the surface of the fish for many species [ABLE and LAMONACA, 2006]. [PERSSON et al, 1999] report that scales from adult fish showed more severe signs of resorption than scales from juvenile fish, since more resorption cavities were visible on the surface of the calcified layer of adult fish scales. While ions are incorporated into the otolith matrix form the endolymph, scales incorporate ions from the blood. [CLARKE et al, 2007]

Figure 4. Scale of brown trout (Salmo trutta fario) with an ablated line across the surface.

1.3.2 Usability of scales for stock discrimination and migration studies of fish

There are contradictory opinions in recent literature about the usability of fish scales for migration studies and stock discrimination of fish.

[MUHLFELD and MAROTZ, 2005] found that the elemental signatures in juvenile westslope cutthroat trout scales could be used to accurately assign individual fish to the drainage and stream of capture and that scale and otolith chemistries were highly correlated. Thus, they suggest that elemental signatures in scales offer a useful and non-lethal alternative to elemental analyses of otoliths as natural tags of natal origin in westslope cutthroat trout and other freshwater fishes. [MUHLFELD and MAROTZ, 2005] also state that the Sr:Ca and Ba:Ca ratios in otoliths were significantly correlated with the ratios of the scale cores and edges, while the Mg:Ca, Mn:Ca and Pb:Ca ratios were less consistent between otoliths and scales. [WELLS et al, 2003a] found a high correlation between these ratios in scales and otoliths of westslope cutthroat trout as well, but scales were less accurate than otoliths in determining the natal origin in that study. Nevertheless, elemental signatures in fish scales may not be stable over time because of metabolic resorption of Ca and additional research is needed to assess the stability of elemental signatures in fish scales [MUHLFELD and MAROTZ, 2005]. [WELLS et al, 2003b] concluded that scales are too unstable to be used as

natural tags of natal origin, because they found that elemental signatures in scales of adult weak-fish degraded after the juvenile period and after maturation.

[CLARKE et al, 2007] found that measured Sr, Ba and Mn concentrations by LA-ICP-MS in the scales show little variation over the life of each animal in contrast to otoliths and finrays in the fresh water fish arctic grayling. Sr concentrations in otoliths and scales as well as in scales and water were not correlated significantly. But they were also able assign 96.7% of the fish to the river of origin by linear discriminant function analysis using the multivariate combination of Sr, Ba, Mn and Mg in the scales. In conclusion, however, [CLARKE et al, 2007] state that scales should not be used for the determination of population structure, since water and scale chemistry are not correlated and the regulation of scale chemistry is not yet understood despite the fact that unique elemental signatures were found for different groups of fish.

1.4 Eye lenses

Eye lenses have been used as natural tags, as well. [CHITTARO et al, 2006, CLARKE et al, 2007 and BROPHY et al, 2003] Eye lenses are similar to the cell free otoliths incapable to remove incorporated material actively, since eye lenses are relatively devoid of cell organelles, thus they are capable of recording the environmental history of the individual [HORWITZ, 1993]. [KINGSFORD and DOVE, 1998] showed that eye lenses can be used for population discrimination and [KINGSFORD and GILLANDERS, 2000] used eye lens chemistry by solution base ICP-MS in addition to otoliths for the same purpose. An air dried eye lens of a brown trout (Salmo trutta fario) is shown in Figure 5.

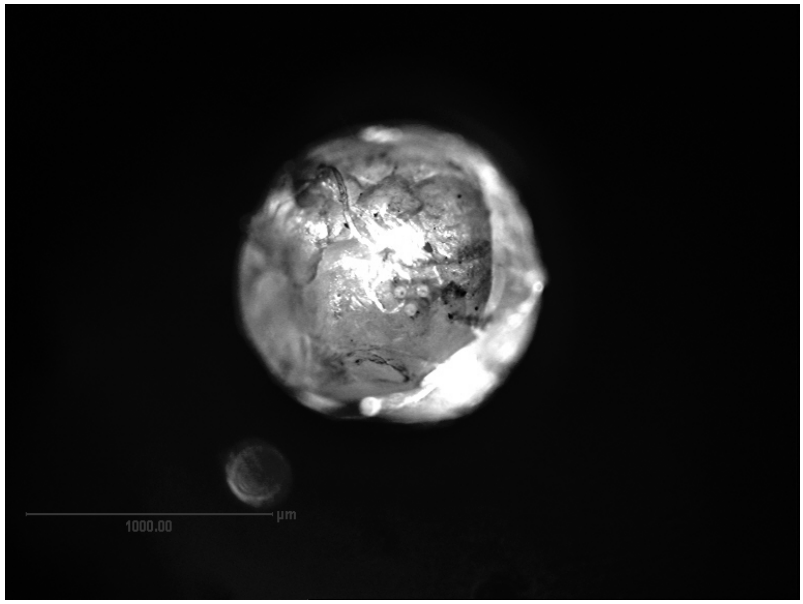

Figure 5. Air tried eye lens of a brown trout (Salmo trutta fario) with three visible laser spots.

1.4.1 Growth and structure of eye lenses

Eye lenses grow by the addition of layers of epithelial cells which differentiate into fibre cells. Only epithelial cells and very young fibre cells contain cell organelles for protein synthesis and some other metabolic and catabolic processes in order to reduce the scattering of light. Thus lens proteins are very stable and the proteins in the mature fibre cells are not catabolized or exchanged once incorporated into the eye lens matrix. [HORWITZ, 1993] Additionally, this lack of organelles in the eye lens leads to the inability of removing incorporated ions. Since eye lenses are made of about 50 % of protein, they are affine to ions like Hg that bind easily ho the sulfhydryl groups of proteins. The matrix of eye lenses differs considerably from other natural tags such as otoliths. Consequently the affinity for cations differs considerably. For example the concentrations ordered from higher to lower concentration for otoliths and lenses of the marine damselfish *Parma microlepis* were Sr > Ba > Pb > Rb > Hg and Hg > Sr > Rb > Pb > Ba, respectively. In addition to that, the concentrations differed strongly in elements accumulated by both structures. The Ba concentrations found in the otoliths were thousand times higher than in the eye lenses. The authors of the study about damselfish *Parma microlepis* also found no difference in Mn levels in eye lenses when Mn concentrations differed in otoliths. This finding is consistent with the theory that concentrations of elements that serve as co-factors in enzymes involved in metabolic processes on the lens surface like Cu, Mn, and Fe are strongly regulated. High Ba

concentrations in eye lenses are accredited to the ability of crystalline proteins to bind divalent cations which would otherwise block the connections between the fiber cells which are called gap junctions [DOVE and KINGSFORD, 1998].

[KINGSFORD and GILLANDERS, 2000] and [DOVE and KINGSFORD, 1998] showed that eye lenses can be used for population discrimination using solution based ICP-MS. However, there are concerns whether eye lenses can be used in studies analyzing only a fraction of the protein layers in spite of their chronological formation. [DOVE, 1999] found that there are differences in the protein composition of the nucleus and the cortex of the eye lens which might be due to changes in protein synthesis and protein degradation.. Thus [DOVE, 1999] suggests "that one should not draw conclusions concerning the trace-metal history of the environment from these chronologically distinct layers".

1.5 The strontium isotope system

There are four naturally occurring isotopes of strontium. The abundances of ^{84}Sr, ^{86}Sr, ^{87}Sr and ^{88}Sr are 0.56%, 9.86%, 7.00% and 82.58%, respectively. [ROSMAN and TAYLOR, 1997] Additionally, there is a small amount of the non natural radioactive isotope ^{90}Sr fond in the environment produced by fission reactions. ^{90} Sr has a half-life of approximately 30 years.

The amount of ^{87}Sr varies, because ^{87}Sr results from the radioactive β-decay of ^{87}Rb.The amount of ^{87}Sr in minerals depends on the geochemical composition and geological age. The Rb-Sr dating method of ingeneous rocks such as granites is based on this fact. certain amounts of Rb and Sr are incorporated when minerals and rocks form. The amount of ^{87}Sr increases with age due to the β-decay of ^{87}Rb. The $^{87}Sr/^{86}Sr$ ratio of minerals and rocks thus depends on the initial Sr/Rb ratio and their age. Strontium from minerals and rocks is present in rivers and other bodies of water because of weathering processes. Therefore the $^{87}Sr/^{86}Sr$ ratios in water from different geographical origin may differ. Since the ionic radius of Sr (1.18 Å) and Ca (1.00 Å) are similar, Sr can not only substitute for Ca in minerals like feldspar but also in calcified structures of animals and humans. [CAPO et al,1998] Thus Sr isotopes are frequently used for migration studies in archaeology [KNUDSON et al, 2005] and animals like chinook salmon. [INGRAM and WEBER, 1999]

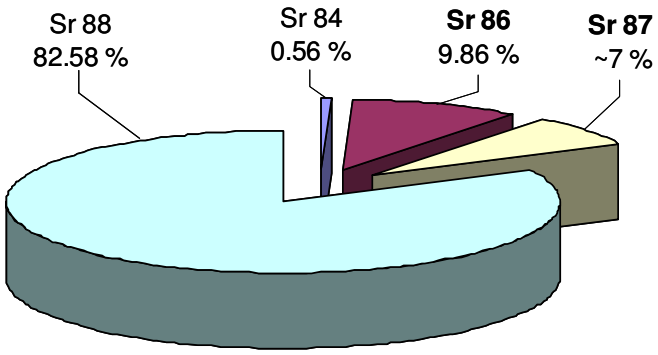

Figure 6. The abundances of the four naturally occurring stable isotopen of strontium according to [ROSMAN and TAYLOR, 1997].

1.6 Objective of this work

The aim of my diploma thesis was to examine whether the isotope ratio of Sr or other and elemental finger prints of otoliths from rainbow (*Oncorhynchus mykiss*) and brown trout (*Salmo trutta fario*) obtained by LA-ICP-MS can be used to determine the natal habitat of the fish where it hatched from the egg and to reconstruct its life history. Therefore validation studies like this are needed to confirm that these markers will in fact distinguish known environmental differences between areas. Consequently, not only fish from natural rivers but also from hatcheries were analyzed along with the water where the fish were caught and the pools were they hatched in case of bred fish. The rim and center of otoliths which were grinded to the core were analyzed. The isotopic an elemental composition of the rim should correspond to the body of water were the fish was caught. The rim of the otoliths from natural rivers is supposed to correspond to the river water and the rim of the otoliths from breeders is supposed to correspond to the water of the pools were the fish were caught. The region around the core should correspond to the water samples taken from the tanks where the fish hatch in case of the fish from breeders. The core itself might be influenced by the environment where the mother lived before she laid the eggs, because the fish larvae feed from the yolk inside the eggs even some time after hatching (PATTERSON et al. 2004). Eye lenses and scales were sampled and analyzed as well.

1.6.1 Rainbow trout (*Oncorhynchus mykiss*) and brown trout (*Salmo trutta fario*)

Brown trout and rainbow trout belong to the family of salmonides (Figure 7). They need clean, oxygen enriched water with an optimal temperature between 8 and 18° C. Since trouts

are predatory fish they feed from insects, larvae and small fish. Trouts are found in rivers and lakes with high water quality. [KÖLBL, 2007]

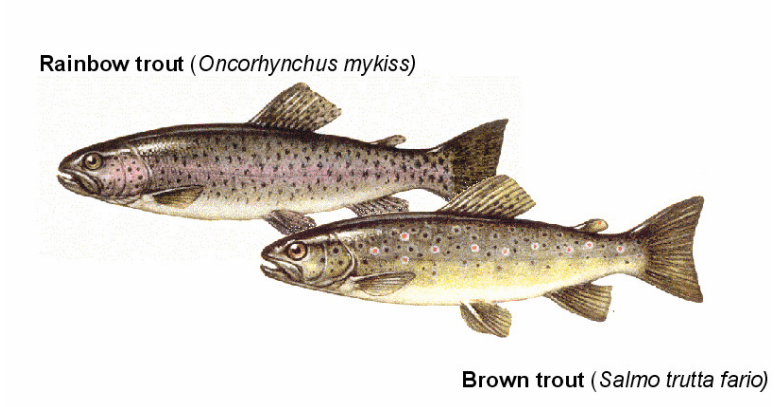

Figure 7:Drawn images of Brown trout and rainbow trout.[source: N. N. , 2008b]

1.6.1.1 Brown trout

Brown trout (*Salmo trutta fario*) can be found all over Europe. They prefer fast flowing cool bodies of water with sandy or gravel grounds. Depending on food availability they reach fork lengths between 20 and 80 cm. Since adult brown trout are territorial, they usually do not leave their place of residence unless for reproduction or when they are disturbed. Brown trout spawn between October and January. The females dig shallow cavities in the gravel or sandy ground in order to put about 1000 reddish eggs in the cavity. The fish larvae hatch after 2 to 4 month. Since the brown trout is also bred in hatcheries for food purposes and is put in rivers in order to reconstitute their trout population. [N. N., 2008]

1.6.1.2 Rainbow trout

Rainbow trout (*Oncorhynchus mykiss*) originally derived from North America. In the 19th century rainbow trout was brought to Europe in order to be bred for the royal court in England and in Württemberg, Germany. Due to a lack of restrictions rainbow trout were also put into natural rivers and lakes for angling. Nowadays rainbow trout are found all over Europe [N. N., 2008a]. Since rainbow trout are less sensitive for water quality and temperature (up to 25° C) and because of their high growth rate, there are concerns that rainbow trout may replace brown trout in European rivers [N. N., 2008]. Rainbow trout are also bred in hatcheries for food. They can reach a length of up to 80 cm and weigh up to 10 kg. [N. N., 2008a] Adult fish are territorial, while juveniles live in swarms. Rainbow trout spawn between December and

May in Europe. The females dig shallow cavities in the gravel or sandy ground in order to put the eggs in the cavity. The eggs are covered with gravel and sand by the female after fertilization by the male. The time until hatching depends on temperature, for instance about 30 days at 10° C. [N. N., 2008]

1.6.1.3 Fish hatcheries in Austria

In 2005 2.500 tons of salmonides (mostly rainbow trout) were produced in Austria. While the amount of freshwater fish produced in Austria declines, the imports of freshwater fish from abroad increase. Most Austrian trout producers are family enterprises producing less than 50 tons per year. Many of them produce trout in addition to conventional farming or to gastronomy. In Austria trout are traditionally kept in natural ponds with rock water supply, which ensures low water temperature throughout the year. In this way the water of the pond is renewed about 4 to 5 times a day. Since trout are predators they need a protein rich diet, there fore they are fed on ready made pellets made of fish meal, fish oil and herbal components. [KÖLBL, 2007]

1.6.1.4 Trout production in hatcheries

The eggs and the milt are extracted from adult fish between October and December. For fertilization the eggs and the milt are mixed and put into water. Water quality and temperature (7 - 8 °C) are of vital importance. After 1 to 2 month the larvae hatch from the eggs. The larvae feed from their yolk sack for 2 to 4 weeks after hatching, before the fed actively. While they feed on the yolk the larvae stay on the ground for their swim bladder is not filled yet. After about 2 month when the fish are about 6 cm long they are put from the tank where they hatch into pools. Fast growing trout can be harvested after 12 month minimum with an approximate weight of 350 g. [KÖLBL, 2007]

1.6.2 Austria,s geology

Since Austria‘s geology consists of different geological units for example granite and gneiss in the north of the river Danube and molasses south of the Danube (Figure 8 and Figure 9). Austria‘s rivers and lakes might therefore have different water properties with respect to their elemental and isotopic composition. Thus there is a high probability that rivers and lakes can be distinguished in migration studies of fish using otolith micro chemistry.

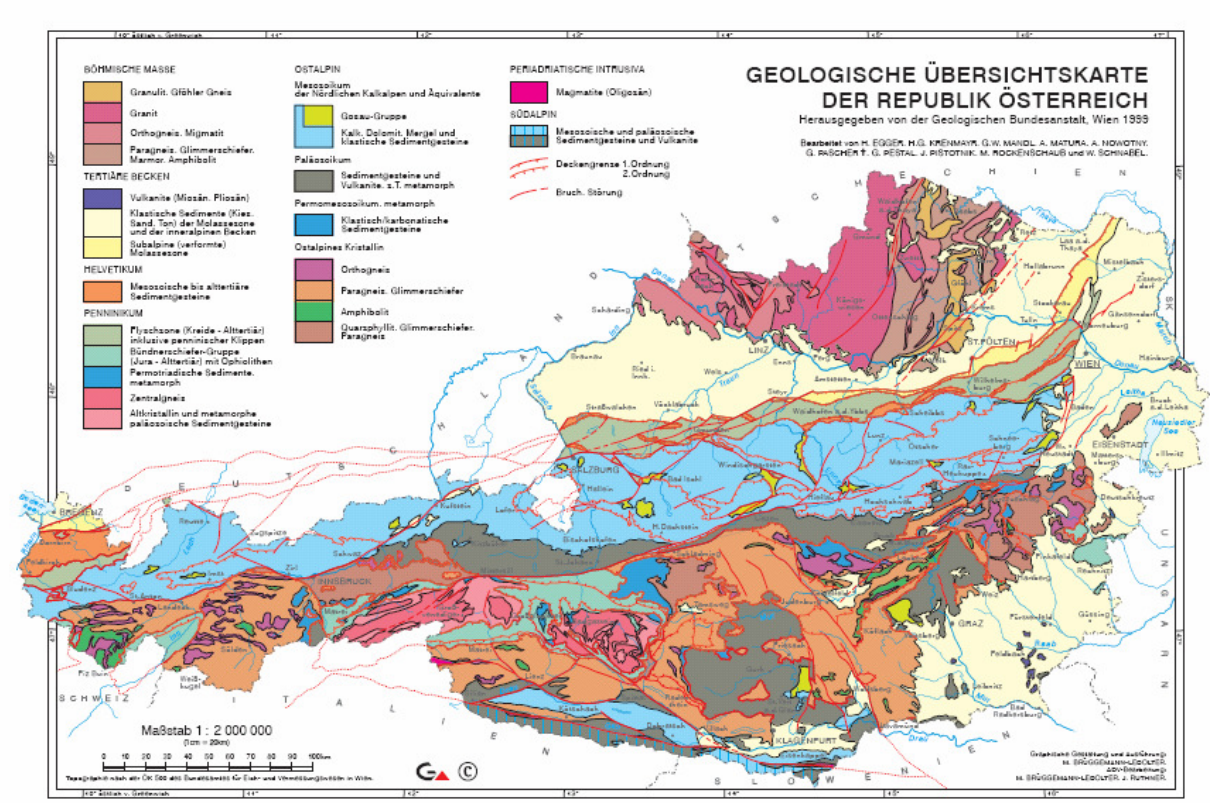

Figure 8: Overview of Austrias geology. Though no details are visible, it is obviouse that Austria's geology is quite diverse.[source: BRÜGGEMANN-LEDOLTER, 1999]

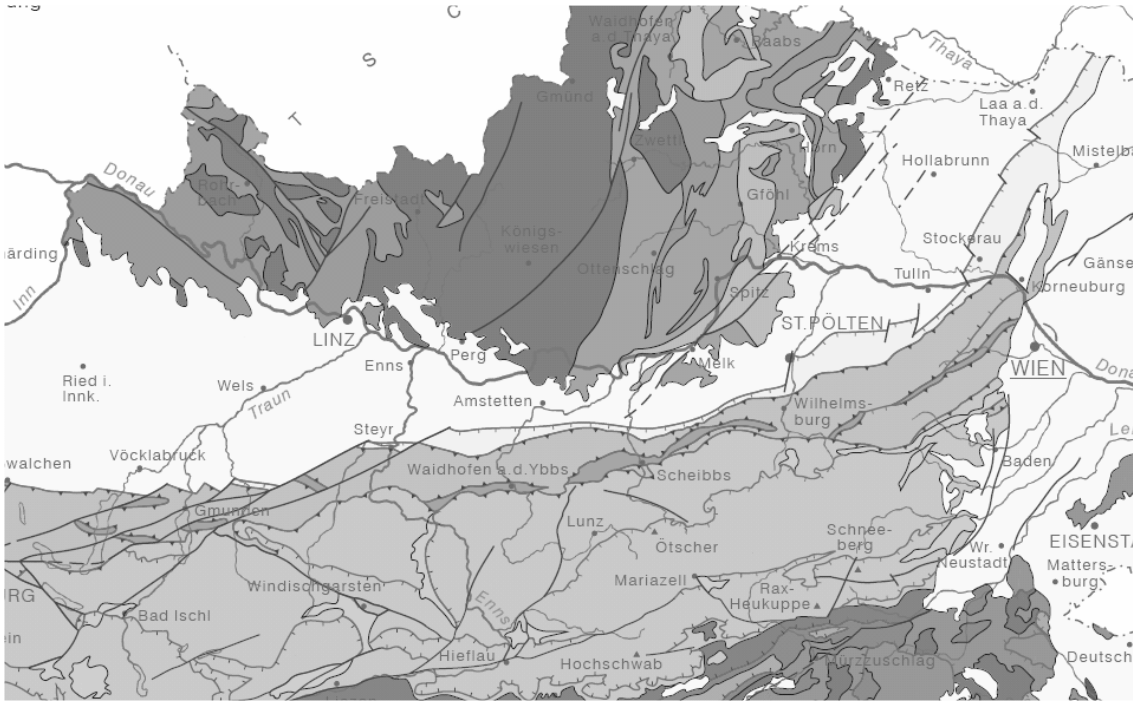

Figure 9. The geology around the river Danube: The granite and gneiss zone in the north of the river Danube (gray colored parts in upper part of the map) and molasses (with colored part in the middle od the map) south of the Danube are indicated by arrows.[source: BRÜGGEMANN-LEDOLTER, 1999]

2 Experimental

2.1 Reagents and Standards

Deionised water (18MΩ) (REWA HQ5, Austria Wasseraufbereitung GmbH, Guntramsdorf, Austria) and nitric acid (65%) (p.A grade, Merck, Darmstadt, Germany) were used for sample preparation. Deionised water and nitric acid were single and double subboiled in an ultrapure quartz apparatus (MLS DuoPur, MLS, Leutkirch im Allgäu, Germany).

Polyethylene flasks and tubes were used for sampling, sample preparation and measurement, and were cleaned with HNO_3 (10% w/w) and HNO_3 (1% w/w) and rinsed with deionised water. All dilution steps for the preparation of water samples and standard solutions for the multi-element measurement were performed with HNO_3 (1% w/w), made of subboiled deionised water and double subboiled HNO_3. Calibration standards for external calibration for the multi-element measurement of the water samples were prepared gravimetrically by a semi-micro balance (BP 210D, Sartorius AG, Göttingen, Germany) from 10^6 ng g^{-1} stock solutions (Merck, Darmstadt, Germany) and a 110 ng g^{-1} solution of indium served as internal standard, which was prepared from a 10^6 ng g^{-1} stock solution (Merck, Darmstadt, Germany), as well. Syringes for filtering the water samples prior to strontium isotope measurement were cleaned in the same way (see chapter 2.4.4).

A solution of NIST SRM 987 in HNO_3 (1% w/w) with a strontium concentration of 5 ng g^{-1} was used (see chapter 2.7.2 and 2.7.3 as quality control for strontium isotope ratio measurement of the water samples and of the solid $CaCO_3$ standard).

The solid $CaCO_3$ standards were made of $CaCO_3$ (p.a., precipitated, Merck, Darmstadt, Germany) plus a solution of NIST SRM 987 in HNO_3 (1% w/w) with a strontium concentration of 5365 ng/g. The absolute abundance ratios in SRM 987 are $^{86}Sr/^{88}Sr$ 0.11935 +/- 0.00325, $^{87}Sr/^{86}Sr$ 0.71034 +/- 0.00026 and $^{84}Sr/^{86}Sr$ 0.05655 +/- 0.00014. The accepted $^{87}Sr/^{86}Sr$ ratio for this standard reported in literature is 0.710245. [FAURE and MENSING, 2005]

2.2 Inductively coupled plasma mass spectrometry (ICP-MS)

All isotopic ratios of strontium and multi-elemental patterns were obtained by inductively coupled plasma mass spectrometry (ICP-MS). Details about the fundamental basics of ICP-MS can be found in literature such as [DEAN, 1997] and [NELMS, 2005]:

Basically, liquid samples are nebulized into droplets by a nebulizer device applying the principles of a venture injector and bigger droplets are removed in a spray chamber device before the sample droplets are transported into the inductively coupled plasma by an argon gas flow. Solid samples can be ablated directly by a laser beam into small particles which are transported by an argon gas flow. Ions are formed from the sample droplets or particles via inductively coupled plasma. The devices used for the generation of the plasma are the plasma torch and an induction coil which is connected to a radio frequency generator. The plasma torch is made of three concentric glass tubes. Argon gas flows through these tubes and the sample aerosol is transported into the ICP-MS device by the argon gas flow through the inmost of the three glass tubes. The induction coil produces a high frequency electromagnetic field leading to the formation of argon plasma with temperatures between 7,000 and 10,000 K. The sample is ionised under environmental pressure in this plasma. Then the ions pass the interface region consisting of sampler cone and skimmer cone with small orifices. The interface region provides the transfer of the ions from atmospheric pressure to the high vacuum in the mass spectrometer. A system of electric lenses directs the ions to the mass analyser. The ions are separated according to their m/z ratio in the mass analyser and detected by the detection unit.

2.2.1 Setup of the ICP-QMS

The inductively coupled plasma quadrupole mass spectrometers ELAN DRC-e (Perkin Elmer, Ontario, Canada) and ELAN DRC II (Perkin Elmer, Ontario, Canada), respectively, were used for the multi-element measurements of the water samples and the otoliths. The instruments have basically the same setup and a scheme of the latter is shown in Figure 10.
A cyclonic spray chamber (CPI International, Amsterdam, The Netherlands) in combination with a PFA nebuliser (PFA ST nebuliser, Amsterdam, The Netherlands) was used for the sample introduction of the water samples. The operational parameters for the multi-element analysis of the water samples are given in chapter 2.6.4.
A laser ablation system (UP-193 Laser Ablation System, New Wave Research Inc, Fremont, CA, USA) was used for the sampling and sample introduction of the otolith samples. The operational parameters for the multi-element analysis of the otolith samples are given in chapter 2.6.1.

The mass analyser of inductively coupled plasma quadrupole mass spectrometers is a quadrupole which consists of two pairs of orthogonally arranged rods. When one pair of these

rods is charged with a positive DC voltage, the other pair is charged negatively and vice versa. Thus a complex electromagnetic field is generated which controls the pathway of the entering ions. Only ions with a particular mass to charge ratio can pass through the quadrupole mass analyser to the detector while all other ions are lost. A discrete dynode electron multiplier serves as detector.

The discrete dynode detector consists of 22 dynodes. Since the first dynode is connected to negative voltage, the positively charged ions are drawn to the dynode. When an ion hits the dynode surface electrons are emitted. The electrons are accelerated to the next dynode, because the voltage on the dynodes gets more and more negative from the beginning to the end of the detector. About 10^8 electrons are produced from one ion in the end of the detector. This detection mode is named pulse mode because for each ion an electric pulse is registered. This detection mode is used for ion currents of up to $2*10^6$ counts ions per second. When ion currents with higher count rates occur, the rear part of the detector is shut down in order to protect the detector from damage and the current is measured in the middle of the detector between dynode 10 and 11. This detector mode is called analogue mode. The current measured in the analogue mode can be converted into counts per second. If the ion current exceeds $2*10^9$ ions per second the whole detector is shut down in order to avoid damage.

Depending on the concentration of the analyte pulse or analog mode are used in the dual mode. A wide range of concentrations can be measured in the dual mode, because the pulse mode measures up to $2*10^6$ counts per second, while 10^6 to 10^9 are measured with the analogue mode. The dual detector calibration is needed for the dual mode in order to determine a conversion factor to convert the analogue mode signal into a pulse signal, because the slopes of the calibration curves of both modes differ (Figure 11). During the dual detector calibration sample solutions with different concentrations in the dual range of the detector are simulated by the autolens.

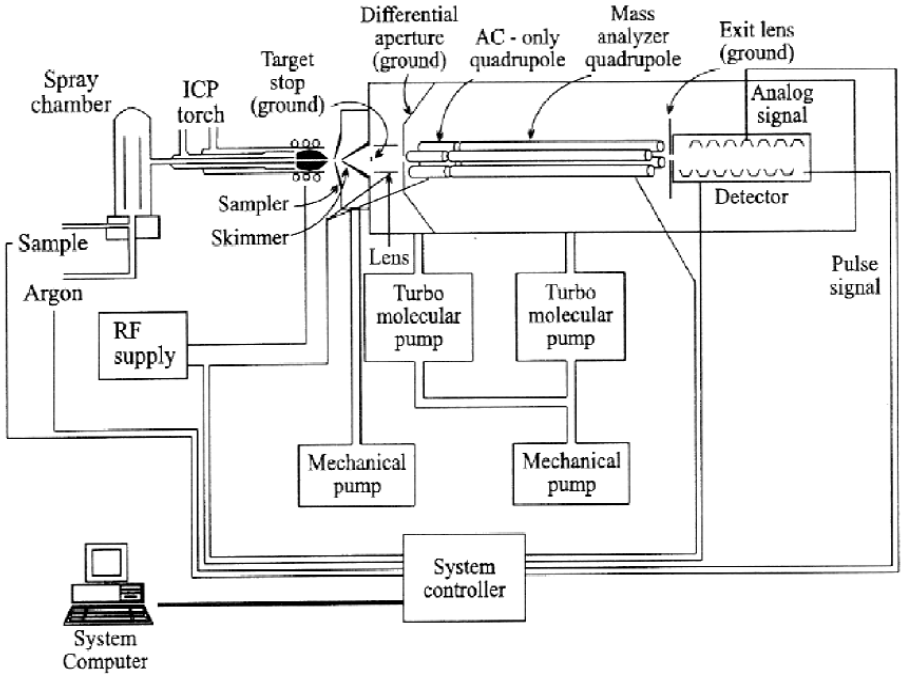

Figure 10. Scheme of inductively coupled plasma mass spectrometer ELAN DRC II (Perkin Elmer, Ontario, Canada) [source: MONTASER 1989]

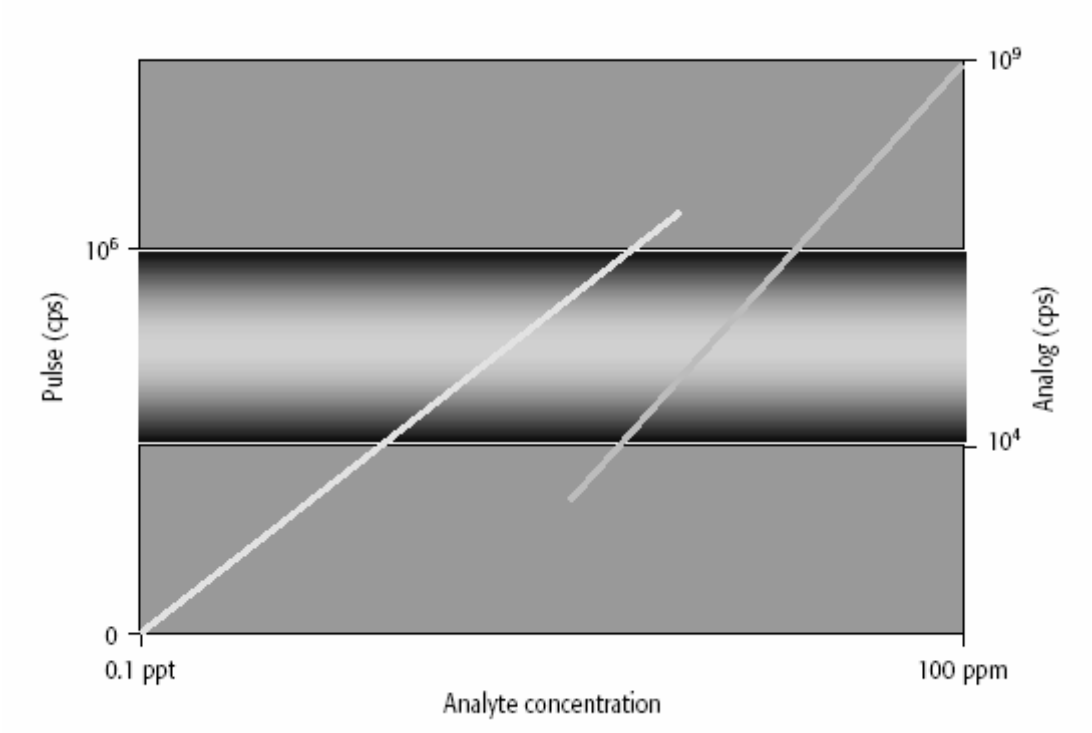

Figure 11. Calibration curves of pulse and analogue mode. [source: THOMAS 2002]

2.2.2 Setup of the MC-ICP-SFMS

The strontium isotope ratios of the otoliths and of the water samples were measured with a double-focusing sector field MC-ICP-MS instrument (Nu Plasma HR, Nu Instruments, Wrexham, Wales, UK).

A desolvating membrane nebuliser (DSN 100, Nu Instruments, Wrexham, Wales, UK) was used for sample introduction of water samples. The desolvating membrane nebuliser (DSN 100, Nu Instruments Ltd, North Wales, UK) reduces the aqueous matrix from the sample by evaporation of the water by heating and thus making the water molecules pass a membrane due to a difference in partial pressure. The operational parameters for strontium isotopic ratio analysis of water samples are given in chapter 2.7.1.

A laser ablation system (Lsx-200 Laser Ablation System, CETAC Technologies Inc., Omaha, Ne,USA) was used for the sampling and sample introduction of the otolith samples. The operational parameters for the strontium isotopic ratio analysis of the otolith samples are given in chapter 2.7.4.

The mass analyser consists of an electrostatic analyser and a magnetic sector field (Figure 12). In the electrostatic analyser the ions are focused with kinetic energy. Thus ions with a specific kinetic energy enter the magnetic field.

The ions are separated in the magnetic field by mass and kinetic energy. Thus ions with a specific mass to charge ratio reach a detector. The detection system consists of a set of 3 ion counters and 12 Faraday cups. Faraday cups were used for the strontium isotope ratio measurements. The positively charged ions reach the collector and are neutralised by electrons generated after passing a high-ohmic resistor. The ion current is measured by the voltage decrease across the resistor and is directly proportional to the number of ions and charges. [WATSON, 1985]

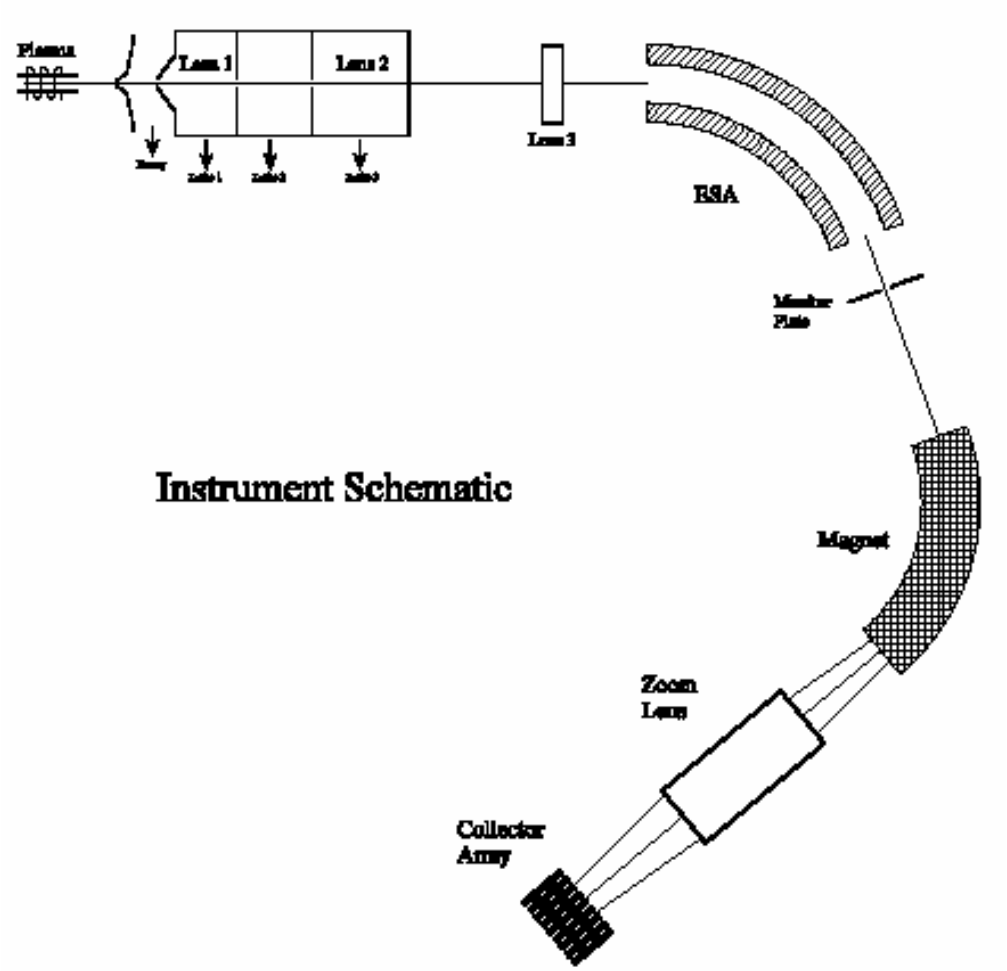

Figure 12. Scheme of inductively coupled plasma sector field mass spectrometer Plasma HR (Nu Instruments, Wrexham, Wales, UK)[source: NuInstuments, 2005]

2.2.3 Setup of the laser ablation

A UP-193 Laser Ablation System (New Wave Research Inc, Fremont, CA, USA) and a Lsx-200 Laser Ablation System (CETAC Technologies Inc., Omaha, Ne,USA) were used, for the sampling and sample introduction of the otolith samples for the multielement measurement and the strontium isotope ratios, respectively (see Figure 13).

Figure 13. UP-193 Laser Ablation System (New Wave Research Inc, Fremont, CA, USA) (left) [source: NEW WAVE RESEARCH, 2007] and a Lsx-200 Laser Ablation System (CETAC Technologies Inc., Omaha, Ne,USA) (right) [source: CETAC, 2007]

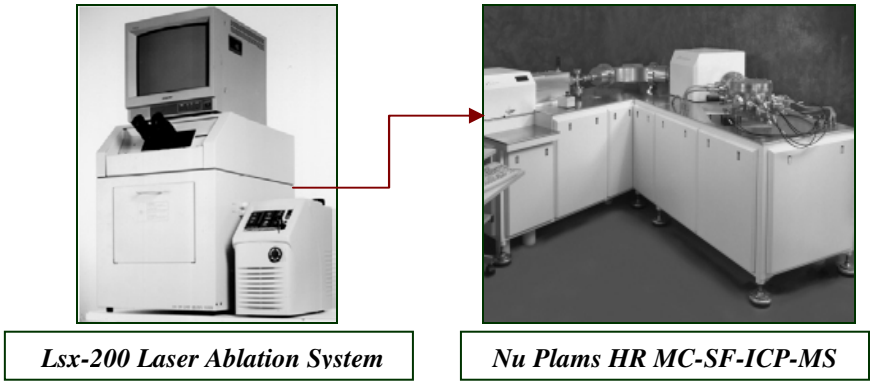

Figure 14. Coupling of Lsx-200 Laser Ablation System (CETAC Technologies Inc., Omaha, Ne,USA) (left) [source: CETAC, 2007]to inductively coupled plasma sector field mass spectrometer Plasma HR (Nu Instruments, Wrexham, Wales, UK)[source: Nu Instuments, 2008] for the Sr isotope ratio measurement of the otoliths.

The principles of a laser ablation system are shown in Figure 15 for the Lsx-200 Laser Ablation System (CETAC Technologies Inc., Omaha, Ne,USA):

Laser ablation is a vaporization process using a laser beam as primary energy source. A particle aerosol is generated when a laser beam of sufficient power density strikes the surface of a solid material caused by the interaction of laser photons with the solid material. A solid sample is put into an enclosed chamber and the laser beam is focused on the surface of the sample. A cloud of particles is produced when the laser is fired. These particles are swept from the sampling cell into the inductively coupled plasma by an argon gas flow. [CETAC, 2007] a Nd:YAG laser generates the laser beam both in the Lsx-200 Laser Ablation System

(CETAC Technologies Inc., Omaha, Ne,USA) and in the UP-193 Laser Ablation System (New Wave Research Inc, Fremont, CA, USA) using a neodymium yttrium aluminium garnet (Nd:YAG). [CETAC, 2007 and NEW WAVE RESEARCH, 2007]

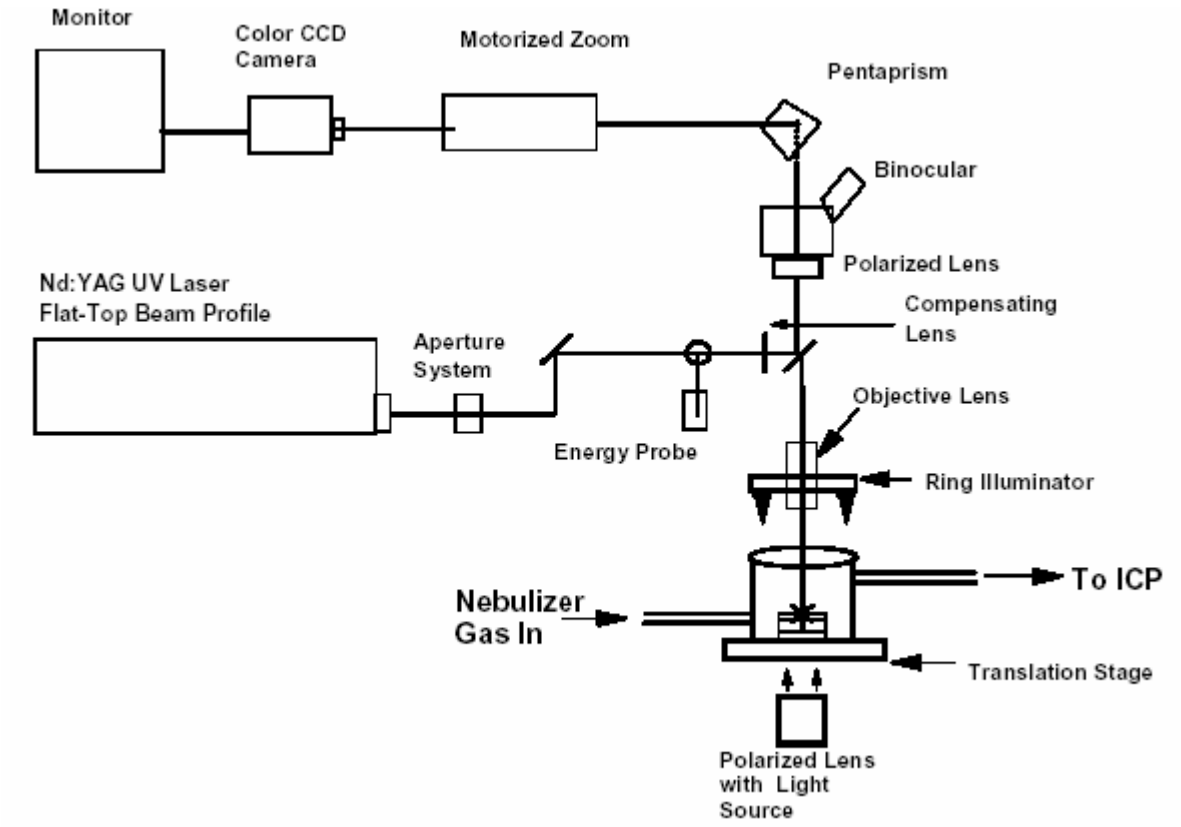

Figure 15. Scheme of Lsx-200 Laser Ablation System (CETAC Technologies Inc., Omaha, Ne,USA) [source: CETAC, 2007]

2.3 Sampling

2.3.1 Sampling of fish

Brown trout and rainbow were collected from five locations in Lower Austria in January 2007 (Figure 16). Two locations were rivers, three of the locations were fish farms (Table 2). All fish from Kleiner Kamp and Flüsslberger were brown trout. All fish from Weinzettl and Dolezal were rainbow trout. Both rainbow and brown trout were caught in the river Ois (Table 3). All fish were treated the same way regardless of their species. Both rivers have not been stocked with fish from other sources for about 20 years. Therefore the fish in these rivers might have spent their entire life within the same environment. The river Ois and the fish farms Weinzettl, Flüsslberger and Dolezal lie within the calcareous part of Lower Austria, the river Kleiner Kamp lies within the siliceous part of Lower Austria. Sampling of fish at rivers

was done by electric fishing and at the pools of the fish farms with dip nets. Electro fishing means that fish are stunned by a direct current which is applied to the water. The paralysed fish were subsequently collected from the surface with a dip net (Figure 17). After capture all fish were stroke death with a club and transported to the laboratory on dry ice and subsequently deep frozen.

Figure 16. Sampling locations for brown trout and rainbow trout in LowerAustria: red arrows indicate rivers; blue arrows indicate hatcheries (http://www.viamichelin.de/ [2007-03-04])

Table 2. Description of the sampling locations.

Identification	***Type of location***	***name***	***address***
Füsslberger	Fish farm	Zucht Anton Füsslberger	Altenreith 17, 3292 Gaming
Dolezal	Fish farm	Zucht Thomas Dolezal	Oberradlberg, 3105 St. Pölten, Austria
Weinzettl	Fish farm	Zucht Josef Weinzettl	Jungherrntalstraße 23, 3180 Lilienfeld, Austria
Ois	river	Ois	Ois near 3293 Lunz am See, Austria
Kleiner Kamp	river	Kleiner Kamp	Kleiner Kamp near 3633 Klein-Siegharts, Austria

Table 3. Number, size and weight of fish from all five sampling locations. "Pool" stands for the bond where the breeders kept the sampled fish. "Hatchery" stands for the tank where the fish spend the first time of their live after they hatch from the eggs.

Location	***fish from***	***Total number of fish (number of brown trouts)***	***Fish size in mm***	***Fish weight in g***
Füsslberger	pool	17 (17)	218 - 280	119,8 - 249,8
Füsslberger	hatchery	-		
Dolezal	pool	15 (0)	223 - 315	144,2 - 380,5
Dolezal	hatchery	-		
Weinzettl	pool	15 (0)	200 - 320	103,9 - 494,5
Weinzettl	hatchery	-		
Ois	river	22 (14)	80 - 310	5,1 - 332,6
Kleiner Kamp	river	9 (9)	78 - 277	4,5 - 139,2

Figure 17. Monika Sturm with electro-fishing equipment.

2.3.2 Sampling of the water samples

Water samples (3*100 ml) were taken at each location and the temperature, conductivity and pH of the water were measured. All three samples were taken simultaneously with a special

sampling device (KÖHA sampling device) which allows to lower up to 12 open bottles into the water at once (Figure 18). additional water samples were taken in case of the breeders from the tanks were the juvenile fish were kept after hatching from the eggs before they were moved to the pools where the fish were caught (Table 4). After hatching the fish larvae spent up to three months till a length of 3-5 cm in the hatchery tanks. Then the fish were put in the pools where they lived until they were captured for analysis. All water samples were collected in acid washed bottles and deep frozen until analysis.

Figure 18. Taking water samples with the KÖHA sampling device at Lanzenberger's Hatchery.

Table 4. Temperature, pH and conductivity of the water samples from all sampling locations.

Location	***Water samples from***	***Temperature***	***pH***	***Conductivity***
Füsslberger	pool	5,6	8,04	276
Füsslberger	hatchery	7,1	7,96	291
Dolezal	pool	10,2	7,66	637
Dolezal	hatchery	11,2	7,5	722
Weinzettl	pool	5,6	8,33	291
Weinzettl	hatchery	9,2	7,63	460
Ois	river	5,1	8,2	182,8
Kleiner Kamp	river	0,5	7,3	48,7

2.4 Sample preparation

2.4.1 Sample preparation of otoliths

The deep frozen fish were defrosted in warm water. The total length (from the end of the tail fin to the tip of the nose) and weight of each fish was measured. (Table 3). Naturally, size and weight differed most in the rivers, since rivers are inhabited by fish of different age. Since the fish from the breeders came from the same pool, all fish were of the same age and thus weight and size did not differ much. Additionally we tried to figure out the fish's sex, but since the reproductive organs in small, young fish and in bred fish were underdeveloped we were not able to determine the sex of most fish. Additionally, both sexes of trout look quite similar and even after cutting the fish's belly in order to examine the inner organs it is not easy to differentiate between the sexes. The fish from the breeders probably have underdeveloped sexual organs because they do not experience any environmental changes (except changes caused by weather and seasons) since they stay in the same pool all of their lives and are not able to migrate. Moreover, they feed differently than in nature and there is no variation in their feeding throughout the year unlike in nature. This inability to follow their natural rhythm of life, might be the cause for this underdevelopment.

2.4.1.1 Otolith removal

Otoliths were sampled from all fish. First the head of the fish was cut open with chirurgical scissors in order to remove the saggital otoliths. By putting one blade of the scissors inside the opened mouth of the fish the scull was split between the eyes through the middle of the brain. It is of vital importance that the skull is not cut skew, because one of the otolith containing vessels might be damaged. This damage can lead to the loss of an otolith because it can be damaged by the blade or slip out of the vessel and get lost in the mixture of blood and tissue. The latter of these two problems occurs quite frequently especially in smaller fish. After cutting the head into halves the brain was removed by tweezers and the vessels which contain the otoliths were located. These vessels are located left and right almost at the torsal end of the brain. If the otolith had not slipped out of its vessel, it can be retrieved from the vessel with the help of tweezers. Afterwards the otoliths were cleaned from adherent tissue with distilled water, air-dried and stored in plastic tubes. Elemental fingerprints are suggested to be consistent between right and left otoliths (Campana et al., 2000), therefore only one otolith per fish was analysed.

2.4.1.2 Otolith grinding

In order to expose the core and the growth zones of an otolith it must be grinded to the plane which contains the core zone. Lapping films were used for grinding which are manufactured in order to be used for fibre optic connectors (3M™ Lapping Film, 261X Sheets, 3M, St. Paul, Mn, USA). Traditionally also oil shale is used to grind otoliths for age estimation of fish, but this natural stone lacks a defined grain size and might pollute the otolith surface. The lapping films had a grain size of 30 µm and 5 µm for grinding and 1,0 µm and 0,3 µm for polishing. The otolith was placed on the lapping film with its concave side pointing to the lapping film. Then a piece of cork was placed upon the otolith to hold it while grinding. The otolith is moved upon the lapping film in small circles. It is of vital importance not to apply to much pressure, because otoliths break easily. When starting to grind an otolith it can be advisable to wet the otolith with distilled water while grinding to prevent the otolith from slivering. From time to time the progress of grinding was checked under a light microscope with 25 and 50-fold magnification. The ring structure of the otolith can easily be seen when the grinded otolith is placed into a droplet of water. The core should be clearly visible without water after polishing. The last part of grinding and the polishing process were performed dry. It usually takes 45 to 70 minutes to grind one otolith. Some otoliths tend to break more easily because they have cracks from the beginning. Otoliths from breeders' fish seem to be less stable. It happens quite often that almost completely finished otoliths break right through or next to the core. It is also advisable for otoliths with cracks to do most of the grinding with the 5 µm lapping film and to grind only the very beginning with the 30 µm lapping film.

The core and the growth zones are usually better visible in fish from natural rivers than from breeders, because they encounter different food and environmental conditions. After grinding and polishing the otoliths are rinsed with subboiled water, sonifcated for 5 minutes in subboiled water and rinsed again, air-dried, and stored in plastic bags.

The otoliths were mounted on glass slides for the laser ablation using a solvent-free, crystal-clear multi-purpose adhesive called "UHU Vielzweckkleber flinke Flasche ohne Lösungsmittel"(UHU GmbH & Co. KG, Bühl/Baden, Germany). It is of vital importance that the polished surface of the otolith is parallel to the slide for the laser ablation.

2.4.2 Sample preparation of eye lenses

Eye lenses were sampled from some fish, as well. The eye lenses of the defrosted fish were removed from the eye using a scalpel. The eye lenses were rinsed with deionised water, air dried and stored in polyethylene tubes. Prior to examination the lenses were rinsed with subboiled water, sonicated in fresh subboiled water for 5 minutes , rinsed again and left to for air drying. The eye lenses were mounted on glass slides for laser ablation using a solvent-free, crystal-clear multi-purpose adhesive called "UHU Vielzweckkleber flinke Flasche ohne Lösungsmittel"(UHU GmbH & Co. KG, Bühl/Baden, Germany) similar to the otoliths.

2.4.3 Sample preparation of scales

A few scales were sampled from five fish per location. The scales were removed by scraping on the skin of the fish with the tweezers and transferred directly into paper envelopes without any cleaning steps. Since the scales had not been cleaned when the sample was taken the protective mucus from the fish surface still adhered to the scales. Thus, the scales had to be detached from each other in the process of cleaning, because they were stuck together by the dried mucus. Therefore the sample was covered with about 1 ml subboiled water in a acid cleaned vessel and the scales were divided gently with a pipette tip. The water was removed with the pipette and fresh water was added. The scales were sonicated for 5 minutes and resuspended in fresh water. Finally, the water was removed and the scales air dried on heating plate at about 40°C was used. The scales were mounted on glass slides for laser ablation using a solvent-free, crystal-clear multi-purpose adhesive called "UHU Vielzweckkleber flinke Flasche ohne Lösungsmittel" (UHU GmbH & Co. KG, Bühl/Baden, Germany) similar to the otoliths.

2.4.4 Sample preparation of the water samples

2.4.4.1 Standard preparation for the multi-element measurement of the water samples

Four multi element calibration standards were prepared. Data from previous water sample measurements gave the list of elements for further investigation. Four concentrations were chosen to cover the concentration range of each element (Table 5). The concentrations of strontium, magnesium and sodium in the standards were chosen 100 times lower than what

was expected in the water samples, since the water samples were diluted 1:100 for the measurement of these elements. The standards were prepared gravimetrically from 10^6 ng g^{-1} single element stock solutions (Merck, Darmstadt, Germany) and 1 % HNO_3 made of concentrated subboiled HNO_3 and subboiled water. Finally, 10 ng $g^{-1}$of an indium standard solution with a concentration of 110 ng g^{-1} was added as internal standard to a final concentration of 10 ng g^{-1} to the water samples, the standards and the blank solution.

Table 5. Elements and their concentrations in the standard solutions and the measured isotopes for the multi-element measurement of the water samples.

Measured elements	*Measured isotopes*	*Concentration in standard A in ng g^{-1}*	*Concentration in standard B in ng g^{-1}*	*Concentration in standard C in ng g^{-1}*	*Concentration in standard D in ng g^{-1}*
Li	6; 7	0,1	0,5	1	2
Be	9	0,5	1	2,5	5
B	19; 11	2	10	20	30
Na	23	10	50	150	200
Mg	24;25	100	150	250	300
Al	27	2	10	20	30
Ca	42; 43; 44	200	400	700	1000
Ti	47; 49	5	50	75	100
V	51	0,1	0,5	1	2
Cr	52; 53	0,5	1	2,5	5
Mn	55	2	10	20	30
Fe	57	2	10	20	30
Co	59	0,01	0,05	0,1	0,2
Ni	60; 62	0,5	1	2,5	5
Cu	63; 65	0,1	0,5	1	2
Zn	64; 66	0,5	1	2,5	5
As	75	0,1	0,5	1	2
Se	77 ; 82	0,5	1	2,5	5
Rb	85	0,5	1	2,5	5
Sr	86; 88	50	500	750	1000
Zr	90; 91	0,01	0,05	0,1	0,2
Mo	95; 97	0,1	0,5	1	2
Sn	118; 120	0,01	0,05	0,1	0,2
Sb	121	0,01	0,05	0,1	0,2
Ba	135; 137	5	50	75	100
W	182; 183	0,01	0,05	0,1	0,2
Au	197	0,1	0,5	1	2
Pb	208	0,1	0,5	1	2
U	239	0,5	1	2,5	5

2.4.4.2 Preparation of the water samples for multi-element measurement

The deep frozen water samples were defrosted in a water bath at 50°C and diluted 1:100 with HNO_3 (1% w/w) for the measurement of strontium, magnesium and sodium. The concentration of the other elements was measured in the undiluted water samples. An indium

standard solution with a concentration of 110 ng g^{-1} was added as internal standard to a final concentration of 10 ng g^{-1} in all samples.

2.4.4.3 Preparation of the water samples for the strontium isotope measurement

The deep frozen water samples were defrosted in a water bath at 50°C. Then they were diluted to a Sr concentration of 10 ng/g with HNO_3 (1% w/w) and filtered via a cellulose acetate filter membrane unites (Minisart® 0.45 micron syringe filter units, Minisart, Sartorius, Göttingen, Germany) with 0.45 µm pores in order to remove possible particles. Each filter unit was cleaned with 5 ml HNO_3 (1% w/w) and used for the three parallel samples from one sampling location. 5 ml HNO_3 (1% w/w) were passed through the filter for cleaning.

2.5 Solid $CaCO_3$ standard for the strontium isotope measurement by LA-ICP-MS

Since no solid $CaCO_3$ standard with a known strontium isotope ratio was available, a solid $CaCO_3$ standard had to be prepared. The $^{87}Sr/^{86}Sr$ ratio of the solid $CaCO_3$ standard was measured for quality control by laser ablation ICP-MS as well as by liquid based ICP-MS of a fraction of the solid $CaCO_3$ standard, which had been dissolved and separated.

2.5.1 Preparation of the solid $CaCO_3$ standard

An estimated strontium concentration in otoliths was determined from data of two digested otoliths. The strontium content was 65 ng/g and 210 ng g^{-1}, respectively. Therefore a concentration of 150 ng g^{-1} was chosen for the solid standard. A SRM 987 solution with a strontium concentration of 5365 ng g^{-1} was diluted 1:10 in subboiled water. It is of vital importance that the subboiled water is used for the dilution instead of HNO_3 (1% w/w), because the acid would lead t a dissolution of $CaCO_3$ (equation (1)).

$$CaCO_3 + 2H^+ \rightarrow Ca^{2+} + CO_2 + H_2O \quad (1)$$

0.14 g of this solution were mixed with 0.5 g $CaCO_3$ powder. This slurry was dried in a drying chamber (WTB-Binder, Tuttlingen, Germany) at 100°C to constant weight. The $CaCO_3$ powder was pressed into a pellet with a pressure of ten tons for five minutes with a laboratory compactor (Manual Hydraulic Press 15 tons maximum load, Specac Inc, RI, USA). The pellet had a diameter of about 7 mm and a thickness of about 1 mm. Even if the $CaCO_3$ pellets tend to break when being removed from the compacter, the pellet fragments can also be used further. The pellets were sintered in a muffle type furnace at the Institute of Chemical Technologies and Analytics at the University of Technology, Vienna. A sintering temperature of 500°C was chosen, since $CaCO_3$ reacts at a temperature of 550°C according to equation (2).

$$CaCO3 \rightarrow CaO + CO2 \quad (2)$$

The temperature was increased at a speed of 300°C per hour until 500°C were reached. The pellets were exposed to 500°C for one hour. The strontium isotope ratio of the strontium spiked $CaCO_3$ pellet was determined in the laser ablation experiment (see chapter 2.7.2). Additionally, a part of the pellet was digested, the strontium was separated from the matrix and the isotope ratio was measured. These isotope ratios were used for quality control to test whether matrix effects caused by the $CaCO_3$ matrix influence the strontium isotope ratio measurement of otoliths via laser ablation ICP-MS (see chapter 2.7.4).

2.5.2 Preparation of the solid $CaCO_3$ standard for the liquid based ICP-MS

2.5.2.1 Digestion of the solid standard for the strontium isotope measurement

About 0.1 g $CaCO_3$ pellet was dissolved in 7.5 g HNO3 (1% w/w). Since $CaCO_3$ dissolves in acidic solutions (see equation (3)), no microwave digestion was necessary.

$$CaCO_3 + 2H^+ \rightarrow Ca^{2+} + CO_2 + H_2O \quad (3)$$

The sample volume for the strontium matrix separation the sample was reduced to 2 ml on a heating plate at 150°C.

2.5.2.2 Strontium matrix separation

In order to separate the strontium from matrix elements such as rubidium a strontium-specific cation exchange resin (EIChroM Industries Inc., Darien, IL, USA) with a particle size of 100 to150 µm was used. This resin consists of crown ether (bis-t-butyl-cis-dicyclohexano-18-crown-6) absorbed on an inert substrate [EIChrom, 2007]. The dry resin was conditioned according to the instructions given by EIChrom Industries, Inc.,Darien, IL, USA. The dry resin was mixed with HNO_3 (1% w/w). Ideally, the resin is conditioned for several hours (minimum 30 minutes). Then the supernatant was removed and fresh HNO_3 (1% w/w) was added. The resin can be used for up to four separations. The used resin must be cleaned before being used again. Therefore the resin is suspended in HNO_3 (1% w/w) or subboiled water and stirred for two minutes. This procedure is repeated three times. The resin is stored in HNO_3 (1% w/w) at -8°C. For the separation a separating procedure for bone samples [SCHULTHEIS, 2003] in an optimized form [BRUNNER, 2007] was used:

The columns for the separation were cleaned with HNO_3 (10% w/w), followed by HNO_3 (1% w/w) and rinsed with subboiled water. A polyethylene frit (Separtis GmbH, Grenzach-Wyhlen, Germany) with a pore size of 10 µm was placed on the bottom of each column. The resin slurry was pipetted into the columns to an end volume of 0.5 to 1 ml settled resin. Then the resin was washed with 15 ml HNO_3 (1% w/w) and 15 ml subboiled water. In order to condition the resin for the strontium uptake a total of 1.5 ml HNO_3 (8 molar; made from 54 ml double subboiled HNO_3 + 42 ml subboiled water) was used per column. Next the sample was put on the resin drop by drop in order to make sure that the dwell time of the sample solution and the contact with the resin are sufficient so that the strontium is bound to the resin. Then the matrix components which had not bound to the resin were washed off the column by 1.5 ml HNO_3 (8 molar). The strontium was eluted from the column into an acid washed tube with 1.5 ml subboiled water.

2.6 Measurement of the multi-elemental pattern

2.6.1 Multi-element measurement of the otoliths

The multi-element pattern of the otoliths were measured with a combination of a quadrupole ICP-MS instrument (ELAN DRC-e, Perkin Elmer, Ontario, Canada) and a laser ablation system (UP-193 Laser Ablation System, New Wave Research Inc, Fremont, CA, USA) using

the operational parameters given in Table 6 and Table 7. The investigated elements are shown in Table 24. In total 20 otoliths were measured (i.e. four otoliths per location). A line from otolith rim to otolith rim across the otolith core was measured per otolith. In order to clean the surface the lines were pre-ablated prior to the measurement. A gas blank was measured prior to each ablation for blank correction.

Table 6. Operational parameters of the quadrupole ICP-MS instrument (ELAN DRC-e, Perkin Elmer, Ontario, Canada) for the multielement measurement of the otoliths by LA-ICP-MS.

ELAN DRC-e	*value*
Nebulizer Gas Flow [NEB]	1.09 L min^{-1}
Auxiliary Gas Flow	1.85 L min^{-1}
Plasma Gas Flow	15 L min^{-1}
Lens Voltage	11.5 V
ICP RF Power	1300 W
Analog Stage Voltage	-1950 V
Pulse Stage Voltage	1200 V
Quadrupole Rod Offset Std [QRO]	-3.5 V
Cell Rod Offset Std [CRO]	-14 V
Discriminator Threshold	79 mV
Cell Path Voltage Std [CPV]	-33 V
RPa N/A	0
RPq N/A	0.25
Cell Gas A	0 ml min^{-1}
DRC Mode NEB	0.9 L min^{-1}
DRC Mode QRO	-6 V
DRC Mode CRO	-1 V
DRC Mode CPV	-15 V
Readings per replicate	150 – 350 (depending on line length)

Table 7. Operational parameters of the laser ablation system (UP-193 Laser Ablation System, New Wave Research Inc, Fremont, CA, USA) for the multielement measurement of the otoliths by LA-ICP-MS.

UP-193 Laser Ablation System	*value*
Pre-ablation	
Spot size	120 µm
Scan speed	20 µm s^{-1}
Laser energy	30 %
Ablation	
Spot size	20 µm
Scan speed	5 µm s^{-1}
Laser energy	80 %

2.6.1.1 Data evaluation

Strontium isotopes of ten otoliths were measured by LA-ICP-MS in addition to the multi-element measurement. Element to ^{43}Ca ratios were calculated for the rim and core region which was used for the measurement of the strontium isotope ratio. The average of the

intensities of each element in these regions was calculated and the blank value was subtracted. An argon gas blank was measured for about 45 seconds prior to each laser ablation and an average blank value was calculated. This value was considered above the detection limit when the blank corrected value exceeded the standard deviation of the blank by three times. Subsequently element to ^{43}Ca ratios were calculated for the three elements (strontium and sodium) which were above the detection limit in the core and the rim region of these otoliths. The combined standard uncertainty was determined with GUM workbench pro.

The multi-element lines across the otoliths were additionally evaluated graphically by laying the graphs for the element to ^{43}Ca ratios for sodium, strontium and magnesium over the image of the grinded otolith. In order to calculate these element to ^{43}Ca ratios each single value of the measurement was blank corrected as described above and divided by the blank corrected ^{43}Ca value that was measured at the same time.

2.6.1.2 Uncertainty evaluation

.

Both strontium isotope ratio and the multi-element pattern were measured in ten otoliths. ^{23}Na/^{43}Ca and ^{88}Sr/^{43}Ca ratios were calculated for the core and rim regions of these otoliths. The combined standard uncertainties for these element to ^{43}Ca ratios were determined from the measured intensities and their standard deviation with GUM workbench pro using equation (4).

$$E/^{43}Ca = (av_E - bl_E)/(av_{43Ca} - bl_{43Ca}) \quad (4)$$

$E/^{43}Ca$ .....element (^{23}Na, and ^{88}Sr) to ^{43}Ca ratio
av_E.....average of the intensity of the element (^{23}Na and ^{88}Sr)
bl_E .....blank of the element (^{23}Na and ^{88}Sr)
av_{43Ca} .....average of ^{43}Ca
bl_{43Ca}.....blank of ^{43}Ca

2.6.2 Multi-element measurement of the eye lenses

The multi-element pattern of the eye lenses were measured similarly to the otolith multi-element patterns with a combination of a quadrupole ICP-MS instrument (ELAN DRC-e, Perkin Elmer, Ontario, Canada) and a laser ablation system (UP-193 Laser Ablation System,

New Wave Research Inc, Fremont, CA, USA) using the operational parameters given in Table 6 in chapter 2.6.1. The same elements were investigated for the otoliths and for the eye lenses (Table 24) and also the same operational parameters of the ELAN DRC-e instrument were used (Table 6). Three spots were ablated using operational parameters shown in Table 8. In total four eye lenses from four fish were ablated; two from the river Kleiner Kamp and two from the hatchery Weinzettl. A gas blank was measured prior to each ablation. The blank corrected intensities were considered above the limit of detection when they exceeded three times the standard deviation of the blank. The relative standard deviation of the uncorrected elemental signal was assumed to be similar to the relative standard deviation of the blank corrected value, which was applied in Figure 42.

Table 8. Operational parameters of the laser ablation system (UP-193 Laser Ablation System, New Wave Research Inc, Fremont, CA, USA) for the multielement measurement of the eye lenses by LA-ICP-MS.

UP-193 Laser Ablation System	*value*
Ablation	
Spot size	20 µm
Dwell time	60 s
Laser energy	80 %

2.6.3 Multi-element measurement of the scales

The multi-element pattern of the scales were measured similarly to the otolith multi-element patterns with a combination of a quadrupole ICP-MS instrument (ELAN DRC-e, Perkin Elmer, Ontario, Canada) and a laser ablation system (UP-193 Laser Ablation System, New Wave Research Inc, Fremont, CA, USA) using the operational parameters given in Table 6 in chapter 2.6.1. The same elements were investigated for the otoliths and for the scales (Table 24) and also the same operational parameters of the ELAN DRC-e instrument were used (Table 6). One line per sample was ablated using operational parameters shown in Table 9. In total four scales were ablated; two from the river Kleiner Kamp and two from the hatchery Weinzettl. A gas blank was measured prior to each ablation. When the blank corrected value exceeded standard deviation of the blank three times, this value was considered above the detection limit. Calcium, sodium, strontium, barium and magnesium were found to be above the detection limit when the average intensities of the whole line were concerned. The multi-element lines across the scales were evaluated graphically by laying the graphs for the element to ^{43}Ca ratios for sodium, strontium, barium and magnesium over the image of the ablated scale. In order to calculate these element to ^{43}Ca ratios each single value of the

measurement was blank corrected as described above and divided by the blank corrected ^{43}Ca value that was measured at the same time.

Table 9. Operational parameters of the laser ablation system (UP-193 Laser Ablation System, New Wave Research Inc, Fremont, CA, USA) for the multielement measurement of the scale samples by LA-ICP-MS.

UP-193 Laser Ablation System	*value*
Ablation	
Spot size	20 µm
Scan speed	5 µm s^{-1}
Laser energy	80 %

2.6.4 Multi-element measurement of the water samples

The water samples were measured with a quadrupole mass spectrometer (ELAN DRC II, Perkin Elmer, Ontario, Canada) using the internal standard method using the operational parameters given in Table 10. For each element one to three isotopes were measured (see chapter 2.3.2.

Table 10. Operational parameters of the quadrupol ICP-MS instrument (ELAN DRC II, Perkin Elmer, Ontario, Canada) for the multi-element measurement of the water samples.

ELAN DRC II	*value*
Nebulizer Gas Flow [NEB]	0.97 mL min-1
Auxiliary Gas Flow	0.9 mL min-1
Plasma Gas Flow	14.25 mL min-1
lens settings	11 V on Indium
signal intensity	Obtain a maximum with an oxide rate below 3% in mind
sample uptake rate	~ 100 µL min-1
sample cone	Nickel
skimmer cone	Nickel
Nebuliser	PFA-nebuliser
spray chamber	cyclonic spray chamber
Measurement	dual mode (pulse combined with analog mode)
number of sweeps	7
number of readings	1
number of replicates	10
measurement time	~ 3 min
flush delay	calibration (60 s), samples (35 s)
wash time	calibration (45 s), samples (120 s)
pump velocity (peristaltic pump)	20 rpm

2.6.4.1 Data evaluation

$^{88}Sr/^{43}Ca$ and $^{23}Na/^{43}Ca$ ratios of the water samples were calculated for the water samples as well as strontium and sodium concentrations in ng g^{-1}. The intensities of Sr and Na were blank corrected and than divided by the blank corrected intensities of the internal standard (^{115}In). Finally the element to ^{43}Ca ratios were calculated. An external four-point-calibration was used for quanitfication.

2.6.4.2 Uncertainty evaluation

The concentration and the combined standard uncertainty of Na and Sr in the sample was determined using GUM workbench pro taking in account the measured intensities as well as all weighing steps of the standard preparation and the sample preparation. Since two isotopes (^{86}Sr and ^{88}Sr) were measured in case of Sr the Sr concentration was determined for each isotope separately and than the average concentration was calculated. The ^{88}Sr $^{88}Sr/^{43}Ca$ and $^{23}Na/^{43}Ca$ ratios of the water samples and their combined standard uncertainty were also determined with the GUM work bench pro (see equation (4)).

2.7 Measurement of the strontium isotope ratio

2.7.1 Measurement of the strontium isotope ratio in the water samples

The strontium isotope ratios of the water samples were measured with a double-focusing sector field MC-ICP-MS instrument (Nu Plasma HR, Nu Instruments, Wrexham, Wales, UK) with a desolvating membrane nebuliser (DSN 100, Nu Instruments, Wrexham, Wales, UK) using the operational parameters given in Table 11. A SRM 987 solution with a strontium concentration of 5 ng g^{-1} served as quality control instrument. The Faraday collector set up is shown in Table 12 as well as the measured isotopes and their natural abundances. The "measure zero" method of the NU Plasma software was used for the blank correction using HNO_3 (1% w/w) as blank.

Table 11. Operational parameters of the double-focusing sector field MC-ICP-MS instrument (Nu Plasma HR, Nu Instruments, Wrexham, Wales, UK) with a desolvating membrane nebuliser (DSN 100, Nu Instruments, Wrexham, Wales, UK) for the strontium isotope measurement of the water samples.

Nu Plasma HR	*value*
RF power	1300 W
auxilliary gas flow rate	0.95 L min^{-1}
cool gas flow rate	13.0 L min^{-1}
lens settings	optimised for optimal sensitivity and peak shape
sample uptake rate	~ 40 µL min^{-1}
sample cone	nickel
skimmer cone	nickel
nebuliser	PFA-nebuliser
sampling mode	6 blocks of 10 measurements
measurement time	~ 10 min
mass analyser pressure	$5.88*10^{-09}$ mbar
detection system	Faraday collectors
background/baseline determination	HNO3 (1% w/w)
background signal	below 1 mV
wash time	180 s
axial mass/mass separation	86.09/0.5
DSN 100	*value*
nebuliser pressure	45.1 psi
DSN hot gas flow	0.32 L min^{-1}
DSN membrane gas flow	2.7 L min^{-1}
spray chamber temperature	111°C
DSN membrane temperature	121°C

Table 12. faraday collector set up of the double-focusing sector field MC-ICP-MS instrument (Nu Plasma HR, Nu Instruments, Wrexham, Wales, UK) for the strontium isotope measurement of the water samples including the measured isotopes and their natural abundances.

Farady cup	L5	L4	L3	L2	L1	Ax	H1	H2	H3	H4	H5	H6
Detected mass					85	86		87		88		
Isotope of interest					^{85}Rb	^{86}Sr		^{87}Sr		^{88}Sr		
Abundance in %					72.2	9.86		~7		82.6		

2.7.1.1 Mass bias and rubidium correction

The strontium isotope ratios were corrected for mass bias using the equation for the exponential mass fractionation law shown in equation (5) and (6).[ALBARÈDE et al, 2004].

$$IR_{87/86}=(I_{87sam}-I_{87bl})/(I_{86sam}-I_{86bl})*(mass_{87Sr}/mass_{86Sr})^{F} \quad (5)$$

$$F = (\log((abund_{86Sr}/abund_{88Sr})/((I_{86sam}-I_{86bl})/(I_{88sam}-I_{88bl})))/(mass_{86Sr}/mass_{88Sr}) \quad (6)$$

$IR_{87/86}$.....isotopic ratio of $^{87}Sr/^{86}Sr$ after mass bias correction in sample
I_{87sam} .....intensity at mass 87 in sample in V
I_{87bl} .....intensity at mass 87 in blank in V
I_{86sam} .....intensity at mass 86 in sample in V
I_{86bl}.....intensity at mass 86 in blank in V
$mass_{87Sr}$.....molar mass of ^{87}Sr in g/mol (m (^{87}Sr) = 86.9088793 ± 0.0000024 ; N. N. 2007)
$mass_{86Sr}$.....molar mass of ^{86}Sr in g/mol (m (^{86}Sr) = 85.9092624 ± 0.0000024; N. N. 2007)
F .....fractionation factor
$abund_{86Sr}$.....abundance ^{86}Sr in % (abundance (86Sr) = 9.8566 ± 0.0034; WISE and WATTERS 2007)
$abund_{88Sr}$.....abundance ^{88}Sr in % (abundance (88Sr) = 82.5845 ± 0.0066; WISE and WATTERS 2007)
I_{86sam} .....intensity at mass 86 in sample in V
I_{86bl}.....intensity at mass 86 in blank in V
I_{88sam} .....intensity at mass 88 in sample in V
I_{88bl}.....intensity at mass 88 in blank in V
$mass_{88Sr}$.....molar mass of ^{88}Sr in g/mol (m (^{88}Sr) = 87.9056143 ± 0.0000024; N. N. 2007)

Additionally, the naturally stable ratios of $^{87}Rb/^{85}Rb$ and $^{86}Sr/^{88}Sr$ were used to correct the ratio of $^{87}Sr/^{86}Sr$ for ^{87}Rb (see equation (7) to (10)). These corrections were made automatically by the Nu Plasma software.

$$I_{87Rb}=(abund_{87Rb}/abund_{85Rb})*(I_{85sam}- I_{85bl})/(mass_{87Rb}/mass_{85Rb})^{F} \quad (7)$$

$$F = (\log((abund_{86Sr}/abund_{88Sr})/((I_{86sam}-I_{86bl})/(I_{88sam}-I_{88bl})))/(mass_{86Sr}/mass_{88Sr}) \quad (8)$$

$$IR_{87Rb/86Sr}=I_{87Rb}/(I_{86sam}-I_{86bl}) \quad (9)$$

$$IR_{87Sr/86Sr}=IR_{87/86}-IR_{87Rb/86Sr} \quad (10)$$

I_{87Rb}.....intensity of ^{87}Rb in V
$abund_{87Rb}$ .....abundance ^{87}Rb in % (abundance (^{87}Rb)= 27.8346 (132); ROSMAN and TAYLOR 1997)
$abund_{85Rb}$ .....abundance ^{85}Rb in % (abundance (^{87}Rb)= 72.1654 (132); ; ROSMAN and TAYLOR 1997)

I_{85sam} .....intensity at mass 85 in sample in V

I_{85bl}.....intensity at mass 85 in blank in V

$mass_{87Rb}$.....molar mass of ^{87}Rb in g/mol (m (^{85}Rb) = 86.9091835 ± 0.0000027; N. N. 2007)

$mass_{85Rb}$.....molar mass of ^{85}Rb in g/mol (m (^{85}Rb) = 84.9117893 ± 0.0000025; N. N. 2007)

F .....fractionation factor

$aAbund_{86Sr}$.....abundance ^{86}Sr in % (abundance (86Sr) = 9.8566 ± 0.0034; WISE and WATTERS 2007)

$abund_{88Sr}$.....abundance ^{88}Sr in % (abundance (88Sr) = 82.5845 ± 0.0066; WISE and WATTERS 2007)

I_{86sam} .....intensity at mass 86 in sample in V

I_{86bl}.....intensity at mass 86 in blank in V

I_{88sam} .....intensity at mass 88 in sample in V

I_{88bl}.....intensity at mass 88 in blank in V

$mass_{86Sr}$.....molar mass of ^{86}Sr (m (^{86}Sr) = 85.9092624 ± 0.0000024; N. N. 2007)

$mass_{88Sr}$.....molar mass of ^{88}Sr (m (^{88}Sr) = 87.9056143 ± 0.0000024; N. N. 2007)

$IR_{87Rb/86Sr}$ .....isotopic ratio of $^{87}Rb/^{86}Sr$

$IR_{87/86}$.....isotopic ratio of $^{86}Sr/^{88}Sr$

$IR_{87Rb/86Sr}$ .....isotopic ratio of $^{86}Sr/^{88}Sr$

2.7.1.2 Uncertainty evaluation

The weight average of the strontium isotope ratios of the three parallel water samples and the weighted standard deviation was calculated in accordance with equation (11) to (13).

$$R_w = \Sigma (R_i * w_i) * (\Sigma w_i)^{-1} \quad (11)$$

$$w_i = stdev^{-2} \quad (12)$$

$$\sigma = (\Sigma w_i)^{-1/2} \quad (13)$$

R_w.....weighted average

R_i.....average

stdev.....standard deviation

σ .....weighted standard deviation

2.7.2 Measurement of the strontium isotope ratio in the digested solid $CaCO_3$ standard

For quality control the $^{87}Sr/^{86}Sr$ ratio of the solid $CaCO_3$ standard was determined by laser ablation ICP-MS as well as by liquid based ICP-MS of a fraction of the solid $CaCO_3$ standard, which had been dissolved and strontium matrix separated (see chapter 2.5). The influence of matrix effects and mass bias on the laser ablation measurement was investigated in this way. This measurement was performed with a double-focusing sector field MC-ICP-MS instrument (Nu Plasma HR, Nu Instruments, Wrexham, Wales, UK) with a desolvating membrane nebuliser (DSN 100, Nu Instruments, UK).

First the intensities of ^{88}Sr in different dilutions of the digested sample were measured in order to find a concentration with a intensity of ^{88}Sr between 3 and 8 V. The sample was diluted with HNO_3 (1% w/w). Finally the strontium isotope ratio was measured using the operational parameter shown in Table 13. The Faraday collector as well as the mass bias and rubidium correction were the same as shown in chapter 2.7.3. The uncertainty for the isotope ratio was as well as the mass bias and rubidium correction calculated by the Nu Plasma HR software.

Table 13. Operational parameters of the double-focusing sector field MC-ICP-MS instrument (Nu Plasma HR, Nu Instruments, Wrexham, Wales, UK) and desolvating membrane nebuliser (DSN 100, Nu Instruments, UK) for the strontium isotope measurement of the dissolved and strontium matrix separated solid $CaCO_3$ standard.

Nu Plasma HR	*value*
RF power	1300 W
auxiliary gas flow rate	0.95 L min-1
cool gas flow rate	13.0 L min-1
lens settings	optimised for optimal sensitivity and peak shape
sample uptake rate	~ 40 µL min^{-1}
sample cone	nickel
skimmer cone	nickel
Nebuliser	PFA-nebuliser
sampling mode	6 blocks of 10 measurements
measurement time	~ 10 min
mass analyser pressure	$5*10^{-9}$ mbar
detection system	Faraday collectors
background/baseline determination	HNO3 (1% w/w)
wash time	300 s
axial mass/mass separation	86.09/0.5

DSN:	*DSN:*
nebuliser pressure	31.5 psi
DSN hot gas flow	0.3 L min^{-1}
DSN membrane gas flow	3.12 L min^{-1}
spray chamber temperature	115°C
DSN membrane temperature	121°C

2.7.3 Measurement of the strontium isotope ratio in the solid $CaCO_3$ standard

The strontium isotope ratio in the solid $CaCO_3$ standard was measured with a double-focusing sector field MC-ICP-MS instrument (Nu Plasma HR, Nu Instruments, Wrexham, Wales, UK) as described in the chapter 2.7.4.

2.7.4 Measurement of the strontium isotope ratio in otoliths

The strontium isotope ratios of the otoliths were measured with a combination of a double-focusing sector field MC-ICP-MS instrument (Nu Plasma HR, Nu Instruments, Wrexham, Wales, UK) and a laser ablation system (Lsx-200 Laser Ablation System, CETAC Technologies Inc., Omaha, Ne,USA) using the operational parameters given in Table 14. In total 10 otoliths (two per sampling location) were measured. Six spots were ablated in the core region of each otolith and six to eleven spots were ablated in the region of the otolith rim depending on the otolith size and the intensity of the strontium signal in order to ensure that there are at least six spots. In this measurement all spots in the core regions could be evaluated because the strontium content is higher (as was also shown in the multi-element measurement) in the otolith cores than in the otolith rims. For this reason it was also necessary to use spot size 7 for the otolith rims instead spot size 5, which was used for the core regions of the otoliths. The average diameter of spot size 5 and 7 was 173 ± 18 µm and 312 ± 35 µm , respectively. These spot sizes were measured with the digital imaging system KS 300 3.0 (Carl Zeiss MicroImaging GmbH, Göttingen, Germany) in combination with a light microscope (Olympus BX 50, Olympus Europa GmbH, Hamburg, Germany), a camera (Sony Power HAD 3ccd Color Video Camera, Sony Corporation, Tokyo, Japan) and a camera adaptor (Sony Camera Adaptor CMA-D2, Sony Corporation, Tokyo, Japan). A gas blank was measured prior to each ablation. The Faraday collector set up is shown in Table 15 as well as the measured isotopes and their natural abundances.

Table 14. Operational parameters of the double-focusing sector field MC-ICP-MS instrument (Nu Plasma HR, Nu Instruments, Wrexham, Wales, UK) and the laser ablation system (Lsx-200 Laser Ablation System, CETAC Technologies Inc., Omaha, Ne, USA) for the multi-element measurement of the otoliths by LA-ICP-MS.

Nu Plasma HR	*value*
RF power	1300 W
auxilliary gas flow rate	0.95 mL min^{-1}
cool gas flow rate	13.0 mL min^{-1}
lens settings	optimised for optimal sensitivity and peak shape
sample cone	nickel
skimmer cone	nickel
mass analyser pressure	$5.17*10^{-9}$ mbar
detection system	Faraday collectors
background/baseline determination	Argon gas
axial mass/mass separation	85.98
Lsx-200 Laser Ablation System	*value*
Energy level	20
Soptsize	5 and 7
Repetition rate	20 Hz
Burst count	1200

Table 15. faraday collector set up of the double-focusing sector field MC-ICP-MS instrument (Nu Plasma HR, Nu Instruments, Wrexham, Wales, UK) for the strontium isotope measurement of the otoliths including the measured isotopes and their natural abundances.

Faraday cup	L5	L4	L3	L2	L1	Ax	H1	H2	H3	H4	H5	H6
Detected mass					85	86		87		88		
Isotope of interest					^{85}Rb	^{86}Sr		^{87}Sr		^{88}Sr		
Abundance in %					72.2	9.86		~7		82.6		

2.7.4.1 Data analysis

About 60 seconds of the gas blank prior to the ablations in one otolith region, e.g. core or rim, were used for blank correction of the ablations made in this region of the otolith. The blank corrected values for ^{88}Sr, ^{87}Sr, ^{86}Sr and ^{85}Rb were used for the mass bias and rubidium correction.

2.7.4.2 Rubidium correction

The naturally stable ratios of $^{87}Rb/^{85}Rb$ and $^{86}Sr/^{88}Sr$ were used to correct the ratio of $^{87}Sr/^{86}Sr$ for ^{87}Rb (see equation (14) to (17)). These corrections were made on a Microsoft Excel sheet for each data point.

$$I_{87Rb}=(abund_{87Rb}/abund_{85Rb})*(I_{85sam}- I_{85bl})/(mass_{87Rb}/mass_{85Rb})^{F} \quad (14)$$

$$F = (\log((abund_{86Sr}/abund_{88Sr})/((I_{86sam}-I_{86bl})/(I_{88sam}-I_{88bl})))/(mass_{86Sr}/mass_{88Sr}) \quad (15)$$

$$IR_{87Rb/86Sr}=I_{87Rb}/(I_{86sam}-I_{86bl}) \quad (16)$$

$$IR_{87Sr/86Sr}=IR_{87/86}-IR_{87Rb/86Sr} \quad (17)$$

I_{87Rb}.....intensity of ^{87}Rb in V

$abund_{87Rb}$ .....abundance ^{87}Rb in % (abundance (^{87}Rb)= 27.8346 (132); ROSMAN and TAYLOR 1997)

$abund_{85Rb}$ .....abundance ^{85}Rb in % (abundance (^{87}Rb)= 72.1654 (132); ; ROSMAN and TAYLOR 1997)

I_{85sam} .....intensity at mass 85 in sample in V

I_{85bl}.....intensity at mass 85 in blank in V

$mass_{87Rb}$.....molar mass of ^{87}Rb in g/mol (m (^{85}Rb) = 86.9091835 ± 0.0000027; N. N. 2007)

$mass_{85Rb}$.....molar mass of ^{85}Rb in g/mol (m (^{85}Rb) = 84.9117893 ± 0.0000025; N. N. 2007)

F .....fractionation factor

$abund_{86Sr}$.....abundance ^{86}Sr in % (abundance (86Sr) = 9.8566 ± 0.0034; WISE and WATTERS 2007)

$abund_{88Sr}$.....abundance ^{88}Sr in % (abundance (88Sr) = 82.5845 ± 0.0066; WISE and WATTERS 2007)

I_{86sam} .....intensity at mass 86 in sample in V

I_{86bl}.....intensity at mass 86 in blank in V

I_{88sam} .....intensity at mass 88 in sample in V

I_{88bl}.....intensity at mass 88 in blank in V

$mass_{86Sr}$.....molar mass of ^{86}Sr (m (^{86}Sr) = 85.9092624 ± 0.0000024; N. N. 2007)

$mass_{88Sr}$.....molar mass of ^{88}Sr (m (^{88}Sr) = 87.9056143 ± 0.0000024; N. N. 2007)

$IR_{87Rb/86Sr}$ .....isotopic ratio of $^{87}Rb/^{86}Sr$

$IR_{87/86}$.....isotopic ratio of $^{86}Sr/^{88}Sr$

$IR_{87Rb/86Sr}$ .....isotopic ratio of $^{86}Sr/^{88}Sr$

The $^{87}Sr/^{86}Sr$ ratio was plotted versus time and the stable part of the signal was utilized. This stable part was divided by three and the average of each of the thirds was build. Then these three average values were used to calculate the average of each otolith spot. For the otolith regions averages of the otolith spot values were calculated.

2.8 Imaging and measurement of lengths

The spot sizes and line lengths of the laser ablation of otoliths, scales and eye lenses as well as the otolith sizes were measured at the Museum of Natural History, Vienna, Austria. The digital imaging system KS 300 3.0 (Carl Zeiss MicroImaging GmbH, Göttingen, Germany) was used in combination with a light microscope (Olympus BX 50, Olympus Europa GmbH, Hamburg, Germany), a camera (Sony Power HAD 3ccd Color Video Camera, Sony Corporation, Tokyo, Japan) and a camera adaptor (Sony Camera Adaptor CMA-D2, Sony Corporation, Tokyo, Japan) as it is shown in Figure 19.

Figure 19. The digital imaging system KS 300 3.0 (Carl Zeiss MicroImaging GmbH, Göttingen, Germany) in combination with a light microscope (Olympus BX 50, Olympus Europa GmbH, Hamburg, Germany), a camera (Sony Power HAD 3ccd Color Video Camera, Sony Corporation, Tokyo, Japan) and a camera adaptor (Sony Camera Adaptor CMA-D2, Sony Corporation, Tokyo, Japan) at the Museum of Natural History, Vienna, Austria.

2.9 Statistical data evaluation

All statistical analyses of the water and otolith samples were conducted using SPSS® 15.0 except the nonparametric discriminant analysis using the DISCRIM procedure of SAS. Details about the statistical analysis are given in 3.1.3.5.

3 Results and Discussion

3.1 Otoliths and water samples

3.1.1 Sample nomenclature

Concerning the nomenclature of the water samples, the samples of the breeders are as demonstrated in these examples: D-H-1 is a water sample from the breeder Dolezal which was taken from the hatchery tank where the fish hatch from the egg and it was the first sample of three parallel water samples. D-P-2 is a water sample from the breeder Dolezal which was taken from the pool where the fish were caught and it was the second sample of three parallel water samples. O-R-1 is the first of three parallel water samples from the river Ois.

As to the nomenclature of the otoliths, the fish numbers from original protocols were kept. When the whole otolith is concerned, the otolith is named in the following way: for example D-40 indicates the otolith of fish number 40, which lived in Dolezal's fish farm.
When only part of the fish otolith is concerned the following nomenclature was used: The core region of fish from a fish farm was treated as the juvenile phase of the fish created under hatchery conditions. Thus, the core region of the 40th fish caught for this study from the breeder Dolezal is named D-H-40, whereas the otolith rim of the same fish is encoded as D-P-40 because it is supposed to correspond to the pool where the fish lived until sacrificed. Core and edge regions of fish from natural rivers were assigned to the juvenile (J) and adult (A) stage, respectively. Thus the core region of the 8th fish caught for this study from the river Ois is indicated by O-J-8. The otolith rim of the same fish is encoded as O-A-8.

3.1.2 Length parameters of the otoliths

Table 16 and Table 17 give an overview of the otoliths used for the multi-element plus strontium isotope measurement and only the multi-element measurement, respectively. The sections of the ablated lines used for the calculation of the element (sodium and strontium) ratios to ^{43}Ca are given in Table 18.

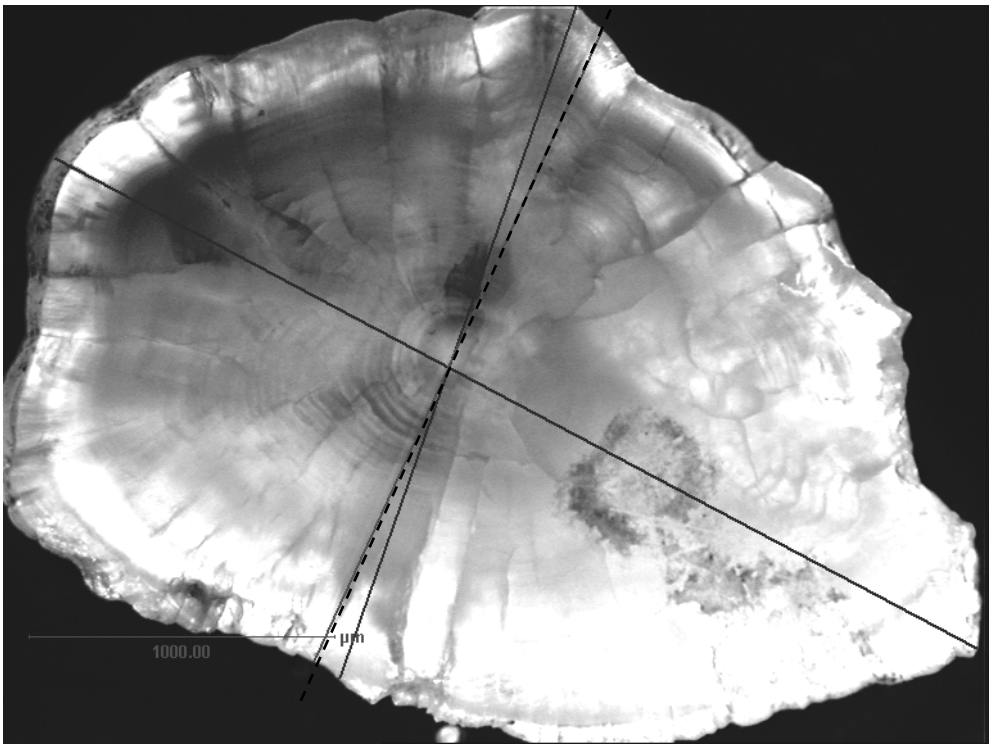

Figure 20. The measured length parameters of the otoliths: The width and the length of the otolith are indicated by solid lines and the laser ablated line is indicated by a dashed line.

Table 16. Length parameters of the otoliths used for the multi-element plus strontium isotope measurement

Sample ID	Sampling location	Otolith length in µm	Otolith width in µm	Length of ablated line in µm
D-40	Dolezal	3546	2268	2209
D-41	Dolezal	3931	2206	2278
K-73	Kleiner Kamp	1446	1050	1120
K-76	Kleiner Kamp	2524	1583	1611
FB-25	Füsslberger	3106	2084	2000
FB-27	Füsslberger	2917	1907	1880
FB-7	Ois	3615	2683	2760
O-8	Ois	3976	2271	2244
W-64	Weinzettl	3289	2165	2133
W-65	Weinzettl	3617	2272	2245

Table 17. Length parameters of the otoliths used for the multi-element measurement.

Sample ID	Sampling location	Otolith length in µm	Otolith width in µm	Length of ablated line in µm
D-42	Dolezal	3394	2327	2254
D-43	Dolezal	4279	2678	2622
K-74	Kleiner Kamp	1729	975	1005
K-77	Kleiner Kamp	1548	892	894
FB-34	Füsslberger	3566	2041	1903
FB-35	Füsslberger	2701	1979	2062
O-5	Ois	3341	2411	2421
O-11	Ois	1439	930	888
W-58	Weinzettl	1165	1603	1151
W-62	Weinzettl	2906	1864	1899

Table 18. Length parameters of the ablated lines of the otoliths used for the multi-element plus strontium isotope measurement.

Sample ID	total line length in µm	length of rim region in µm used for the calculation of the element to ^{43}Ca ratios	length from rim to begin of core region in µm	length of core region in µm used for the calculation of the element to ^{43}Ca ratios
D-42	2209	348	669	612
D-43	2278	349	640	649
K-74	1120	282	282	528
K-77	1611	294	522	489
FB-34	2000	532	819	447
FB-35	1880	419	669	535
O-5	2760	419	1232	620
O-11	2244	292	748	608
W-58	2133	411	827	539
W-62	2245	532	1124	539

3.1.3 Strontium isotope and multi-elemental pattern of water samples and otoliths

3.1.3.1 Quality control of the strontium isotope ratio measurements of the water samples

A SRM 987 solution with a strontium concentration of 5 ng g^{-1} served as quality control instrument for the strontium isotope ratios of the water samples and the dissolved solid $CaCO_3$ standard which were measured in May and September 2007, respectively (Figure 21.).

The SRM 987 has a certified value of the 87Sr/86Sr ratio of 0.71034 +/- 0.00026. The upper limit of the certified value is 0.71058 and lower limit is 0.71010. The accepted value for this standard reported in literature is 0.710245. [FAURE and MENSING, 2005] None of the measured standards was outside the range of the certified value.

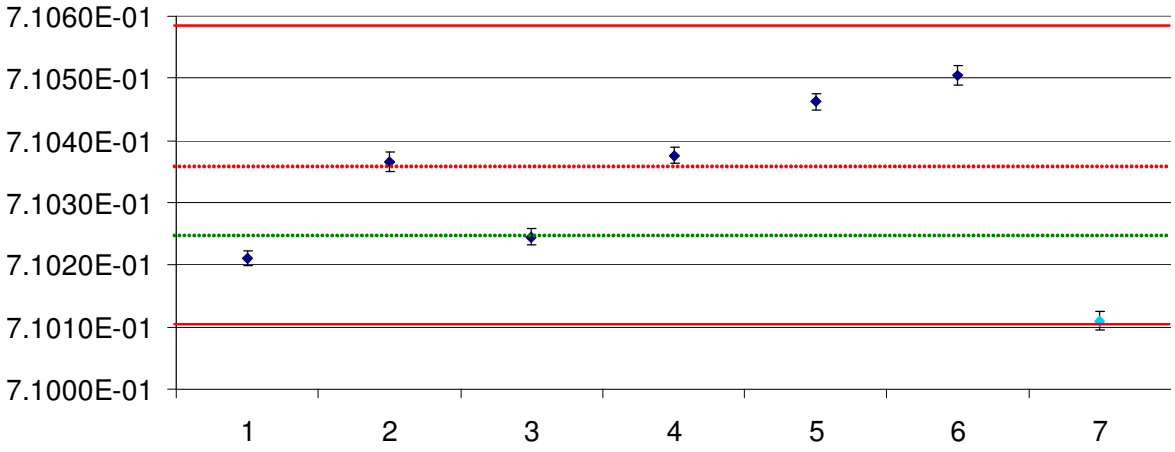

Figure 21. $^{87}Sr/^{86}Sr$ ratio in the SRM 987 measured as quality control after every fifth sample during the measurement of the $^{87}Sr/^{86}Sr$ ratio in the water samples and the dissolved solid $CaCO_3$ standard. The red dotted line represents the certified $^{87}Sr/^{86}Sr$ value of SRM 987, the red lines the range of the certified value of SRM 987. The dotted green line represents the accepted $^{87}Sr/^{86}Sr$ value of SRM 987. Data points 1 to 6 were measured during the measurement of the water samples; data point 7 was measured during the measurement of the dissolved solid standard. The date and time (0:00 stands for the first measurement of SRM 987 in the measurement series) of the measurement are given on the x–axis.

3.1.3.2 Quality control of the strontium isotope ratio measurements of the otoliths

The $^{87}Sr/^{86}Sr$ ratio of the solid $CaCO_3$ standard was determined by laser ablation ICP-MS as well as by liquid based ICP-MS for quality control. The influence of matrix effects and mass bias on the laser ablation measurement was investigated this way. Since there was no significant difference between both measurements, no correction factor was needed for the $^{87}Sr/^{86}Sr$ ratios of the otoliths (Table 19 and Figure 22).

Table 19. $^{87}Sr/^{86}Sr$ ratio of the solid $CaCO_3$ standard obtained by laser ablation ICP-MS and by liquid based ICP-MS.

	$^{87}Sr/^{86}Sr$ by LA- ICP-MS	*$^{87}Sr/^{86}Sr$ by liquid based ICP-MS*
$^{87}Sr/^{86}Sr$	0.70944	0.70962
Standard deviation	0.00028	0.00021
Relative standard deviation	0.040%	0.029%

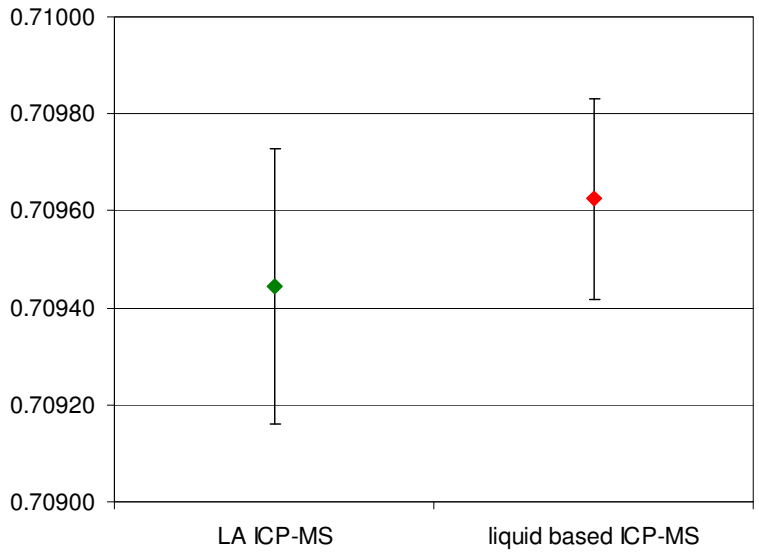

Figure 22. $^{87}Sr/^{86}Sr$ ratio of the solid $CaCO_3$ standard obtained by laser ablation ICP-MS and by liquid based ICP-MS.

3.1.3.3 Physical properties, strontium isotope ratios and multi-elemental patterns of water samples

Three water samples were taken at each location and the temperature, conductivity and pH of the water were measured (Table 20). In addition to samples from the water where the fish were caught, water samples were taken from the tanks were the juvenile fish were kept after hatching from the eggs were taken in case of the fish hatcheries. The fish larvae spent up to three months after hatching until it reached a length of 3-5 cm in the hatchery tanks. Then the fish were put in the pools where they lived until capture.

The concentrations of strontium and sodium of the water samples in ng g^{-1} with combined standard uncertainty (k=2) are given in Figure 23 and

Figure *24*, respectively, as well as in Table 21. The high combined standard uncertainty of ^{23}Na of the water samples from the fish farm Dolezal (D-H and D-P) originates from the standard deviation of the measured intensities. Suspended particles in the water might be the reason for the high standard deviations of the ^{23}Na intensities of these water samples. The calcium concentration is the most influent water property for elemental uptake in freshwater fishes and that therefore the element: Ca ratio is often more important for the uptake of elements in freshwater than the concentration of these elements [MAYER et al, 1994], $^{88}Sr/^{43}Ca$ and $^{23}Na/^{43}Ca$ ratios of the water samples were calculated. The $^{88}Sr/^{43}Ca$ and $^{23}Na/^{43}Ca$ ratios of the water samples with combined standard uncertainty (k=2) are given in

Figure 25 and Figure 26, respectively, as well as in Table 22. The $^{87}Sr/^{86}Sr$ of the water samples with combined standard uncertainty (k=2) are given in Table 23 and Figure 27.

Table 20. Temperature, pH and conductivity of the water samples from the sampling locations.

Sample ID	***Location***	***Water samples from***	***Temperature***	***pH***	***Conductivity***
FB-P	Füsslberger	pool	5,6	8,04	276
FB-H	Füsslberger	hatchery	7,1	7,96	291
D-P	Dolezal	pool	10,2	7,66	637
D-H	Dolezal	hatchery	11,2	7,5	722
W-P	Weinzettl	pool	5,6	8,33	291
W-H	Weinzettl	hatchery	9,2	7,63	460
O-R	Ois	river	5,1	8,2	182,8
K-R	Kleiner Kamp	river	0,5	7,3	48,7

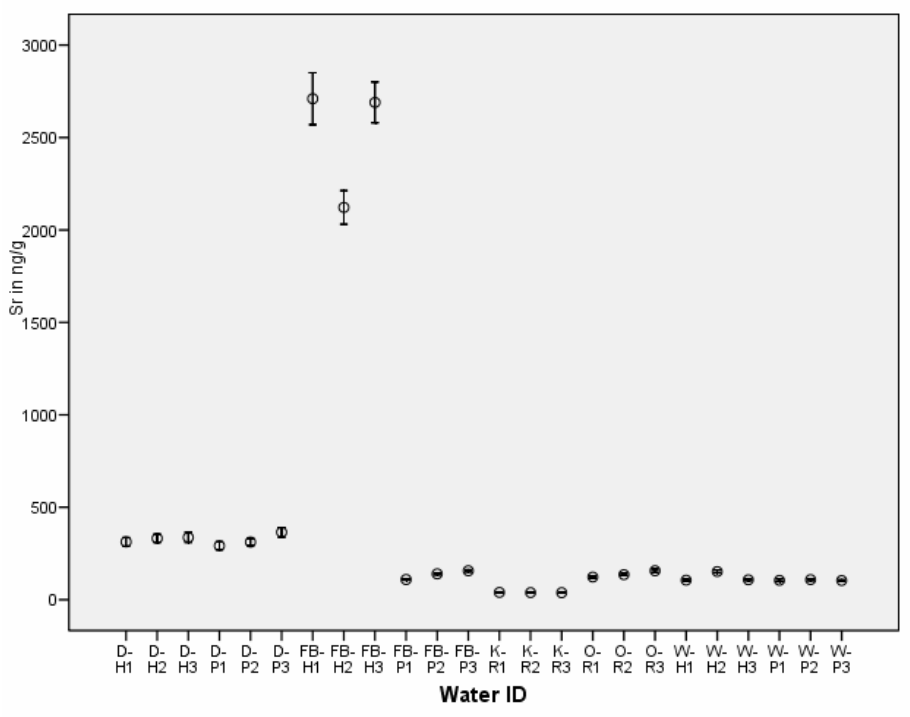

Figure 23.Strontium concentration of the water samples in ng/g with combined standard uncertainty (k=2)

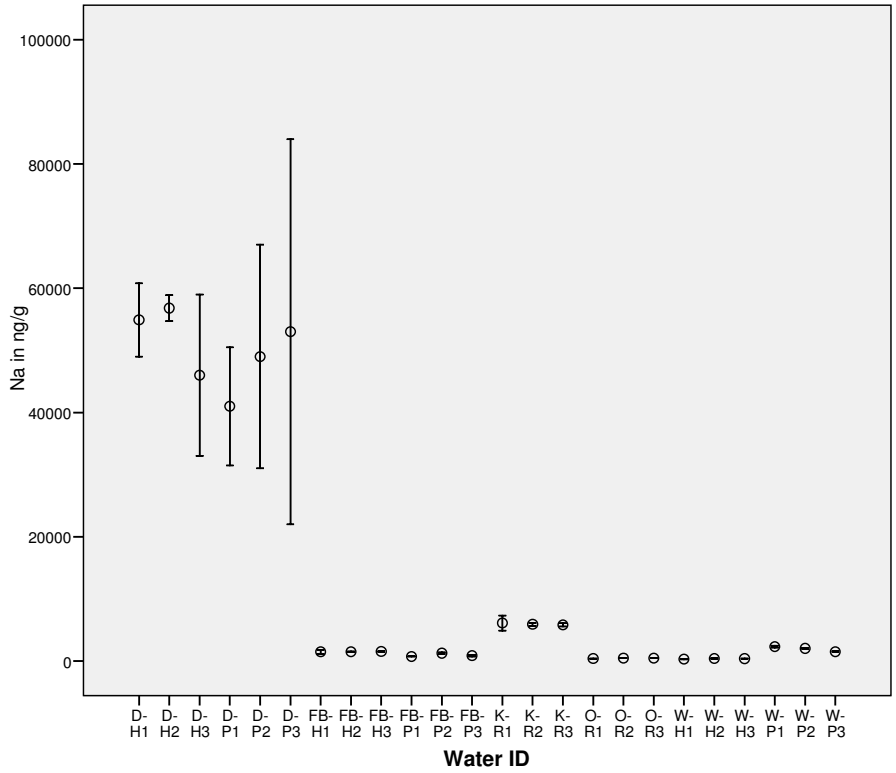

Figure 24.Natrium concentration of the water samples in ng/g with combined standard uncertainty (k=2)

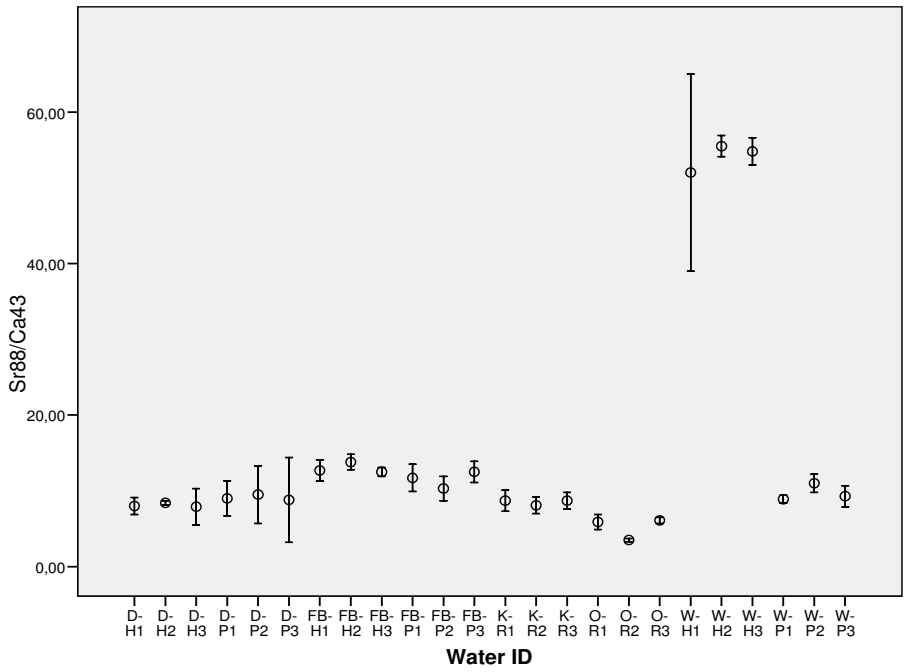

Figure 25. $^{88}Sr/^{43}Ca$ ratios of the water samples with combined standard uncertainty (k=2)

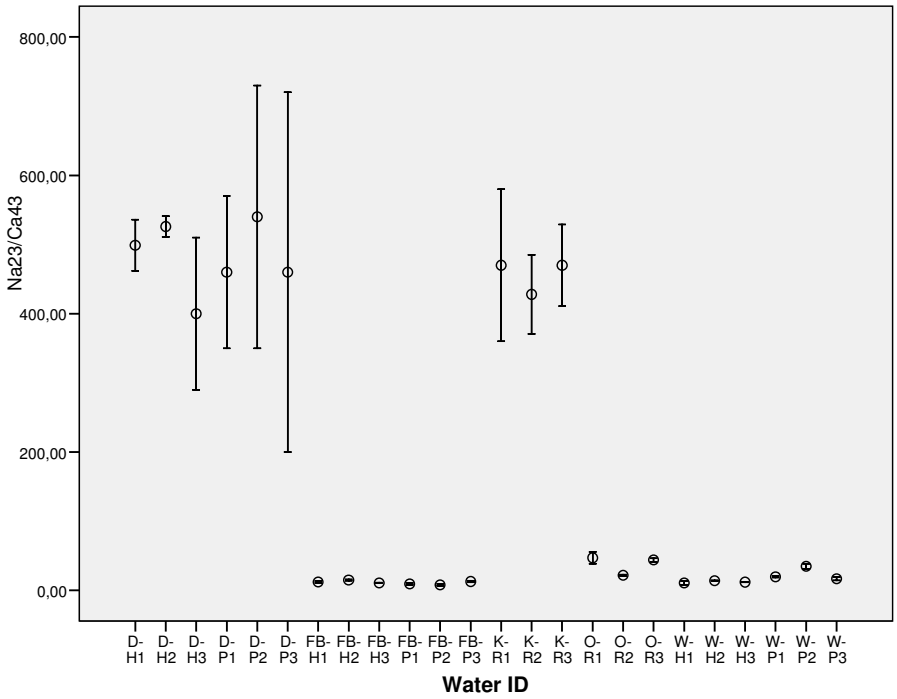

Figure 26. $^{23}Na/^{43}Ca$ ratios of the water samples with combined standard uncertainty (k=2)

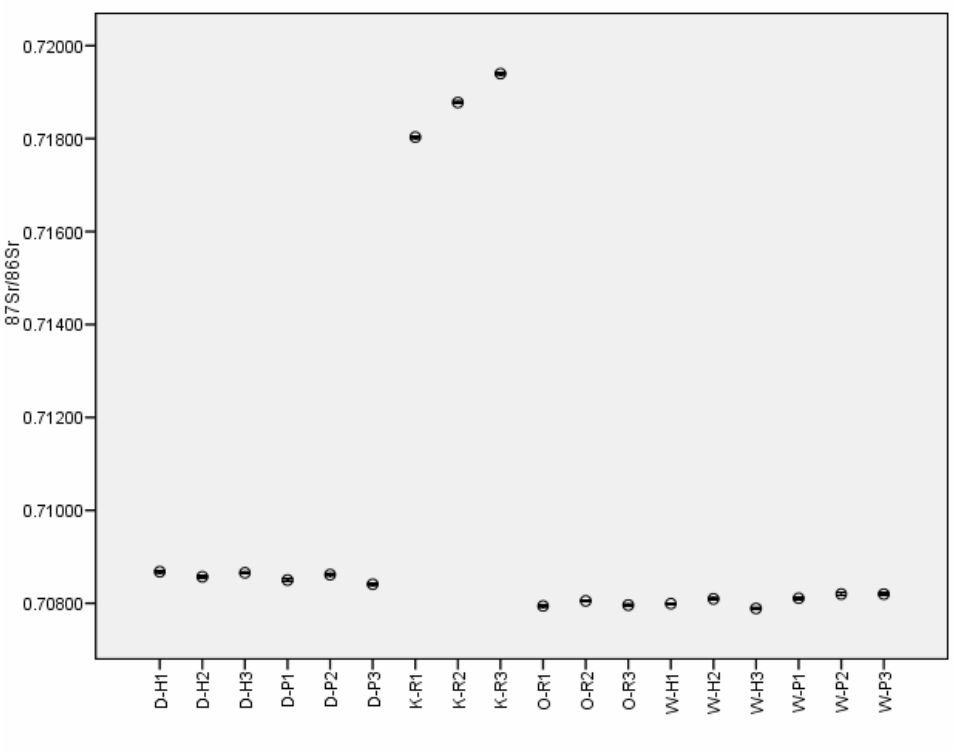

Figure 27. $^{87}Sr/^{86}Sr$ ratios of the water samples with standard deviation (k=1)

Table 21. Natrium and strontium concentration of the water samples in ng/g with combined standard uncertainty (k=2)

ID Wasser	Sr in ng/g	standard uncertainty (k=2) in ng/g	standard uncertainty (k=2) in %	Na in ng/g	standard uncertainty (k=2) in ng/g	standard uncertainty (k=2) in %
D-H1	313	24	7,8	54900	5900	11
D-H2	332	22	6,6	56800	2100	3,8
D-H3	337	27	8,1	46000	13000	28
D-P1	292	22	7,7	41000	9500	23
D-P2	312	19	6,2	49000	18000	36
D-P3	365	26	7,1	53000	31000	58
K-R1	39,6	1,5	3,9	6100	1200	20
K-R2	38,4	1,4	3,6	5890	220	3,7
K-R3	38,2	1,4	3,6	5790	250	4,4
FB-H1	122,8	4,9	4	387	31	7,9
FB-H2	135,7	5,9	4,3	463	21	4,6
FB-H3	156,9	8,5	5,4	447	20	4,5
FB-P1	105,8	4,4	4,1	284	27	9,5
FB-P2	152,1	7,4	4,9	385	57	15
FB-P3	107,9	4,1	3,8	372	32	8,6
O-R1	104,7	6,8	6,5	2300	140	6,1
O-R2	108,7	5,1	4,7	2013	84	4,2
O-R3	103,9	4,1	3,9	1480	77	5,2
W-H1	2710	140	5,1	1460	330	23
W-H2	2122	91	4,3	1464	49	3,4
W-H3	2690	110	4,2	1514	65	4,3
W-P1	109,3	3,9	3,6	724	29	4
W-P2	139,8	4,6	3,3	1250	110	8,9
W-P3	156,9	5,9	3,8	840	110	13

Table 22. ^{23}Na /^{43}Ca and ^{88}Sr/^{43}Ca ratios of the water samples with combined standard uncertainty (k=2)

ID Wasser	^{88}Sr /^{43}Ca	standard uncertainty (k=2)	standard uncertainty (k=2) in %	^{23}Na /^{43}Ca	standard uncertainty (k=2)	standard uncertainty (k=2) in %
D-H1	8	1,1	14	499	37	7,5
D-H2	8,4	0,3	3	526	15	2,8
D-H3	7,9	2,4	31	400	110	27
D-P1	9	2,3	26	460	110	24
D-P2	9,5	3,8	40	540	190	36
D-P3	8,8	5,6	64	460	260	57
K-R1	8,7	1,4	16	470	110	23
K-R2	8,1	1,1	14	428	57	13
K-R3	8,7	1,1	13	470	59	13
FB-H1	12,7	1,4	11	12,2	1,4	12
FB-H2	13,8	1	7,3	15,1	1	6,7
FB-H3	12,5	0,6	4,8	10,8	0,5	5
FB-P1	11,7	1,8	15	9,5	1,4	15
FB-P2	10,3	1,6	16	8	1,3	16
FB-P3	12,5	1,4	11	12,8	1,3	11
O-R1	5,9	1	17	47,1	8,4	18
O-R2	3,5	0,2	4,3	21,9	0,9	4
O-R3	6,1	0,4	6,3	44,1	2,6	6
W-H1	52	13	26	10,8	2,6	24
W-H2	55,5	1,4	2,5	14	0,4	2,7
W-H3	54,8	1,8	3,3	12	0,4	2,9
W-P1	8,9	0,5	5,7	19,7	1,1	5,4
W-P2	11	1,2	10	34,9	3,6	10
W-P3	9,3	1,4	15	17	2,3	14

Table 23. $^{87}Sr/^{86}Sr$ ratios of the water samples with standard deviation (k=1)

ID Wasser	$^{87}Sr/^{86}Sr$	standard deviation	Relative standard deviation in %
O-R1	0,70794	0,000017	0,002
O-R2	0,70805	0,000017	0,002
O-R3	0,70796	0,000016	0,002
K-R1	0,71803	0,000023	0,003
K-R2	0,71878	0,000021	0,003
K-R3	0,71940	0,000019	0,003
FB-P1	0,70855	0,000026	0,004
FB-P2	0,70833	0,000022	0,003
FB-P3	0,70850	0,000019	0,003
FB-H1	0,70848	0,000021	0,003
FB-H2	0,70817	0,000018	0,003
FB-H3	0,70808	0,000017	0,002
D-P1	0,70850	0,000029	0,004
D-P2	0,70862	0,000023	0,003
D-P3	0,70841	0,000018	0,002
D-H1	0,70868	0,00002	0,003
D-H2	0,70857	0,000018	0,002
D-H3	0,70866	0,000019	0,003
W-P1	0,70811	0,000023	0,003
W-P2	0,70820	0,000031	0,004
W-P3	0,70820	0,000021	0,003
W-H1	0,70799	0,000012	0,002
W-H2	0,70810	0,00002	0,003
W-H3	0,70789	0,000017	0,002

3.1.3.4 Strontium isotope and multi-elemental patterns of otoliths

Strontium isotopes were measured by LA-ICP-MS in ten otoliths additionally to the multi-element measurement as described in chapter 2.6.1. The detection limits in all otolith cores and rims element to ^{43}Ca ratios were calculated for the section of the ablated line in rim and core region which was used for the measurement of the strontium isotope ratio. Strontium and sodium were found to be above the detection limit in all core and the rim regions otoliths (Table 24). The $^{88}Sr/^{43}Ca$ and $^{23}Na/^{43}Ca$ ratios of the otolith samples with combined standard uncertainty (k=1) are given in Figure 28 and Figure 29, respectively, as well as in Table 26. The $^{87}Sr/^{86}Sr$ of the water samples with combined standard uncertainty (k=2) are given in Table 25 and Figure 30.

Table 24. Elements investigated in the LA-ICP-MS multi-element analysis of the otoliths.

Element	*Measured isotope*	*Above detection limit*	*Comment*
Li	7	no	
B	11	no	
Na	**23**	**yes**	**Above detection limit in otolith rim and core of all evaluated otoliths**
Mg	**24**	**yes**	**Above detection limit in otolith rim and core of some evaluated otoliths**
Al	27	no	
Ca	**42; 43**	**yes**	**^{43}Ca = internal standard**
Ti	46	no	
PO	47	no	
V	51	no	
Cr	52; 53	no	
Mn	55	no	
Fe	57	no	
Ni	58	no	
Co	59	no	
Ni	60; 62	no	
Cu	63; 65	no	
Zn	64; 66	no	
As	75	no	
Se	82	no	
Rb	85	no	
Sr	**88**	**yes**	**Above detection limit in otolith rim and core of all evaluated otoliths**
Zr	90	no	
Mo	98	no	
Sn	118; 120	no	
Sb	121; 123	no	
Ba	138	no	
Hg	200; 202	no	
Tl	205	no	
Pb	208	no	
U	238	no	

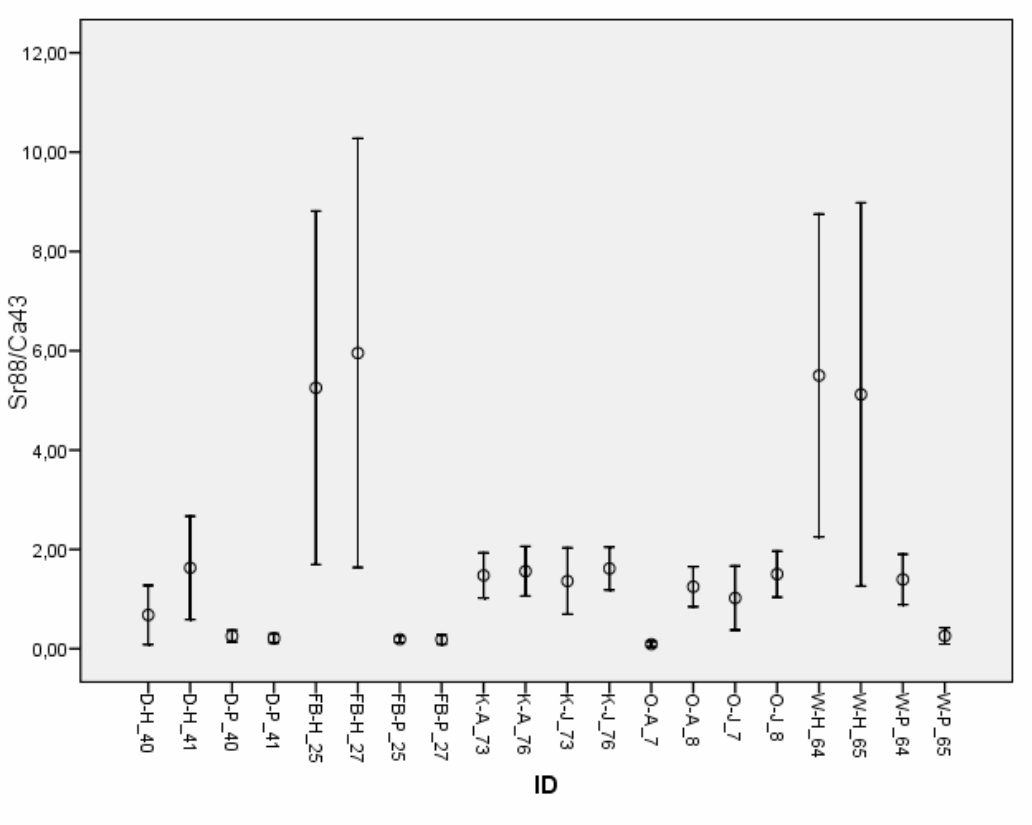

Figure 28. $^{88}Sr/^{43}Ca$ ratios of the otolith samples with combined standard uncertainty (k=1)

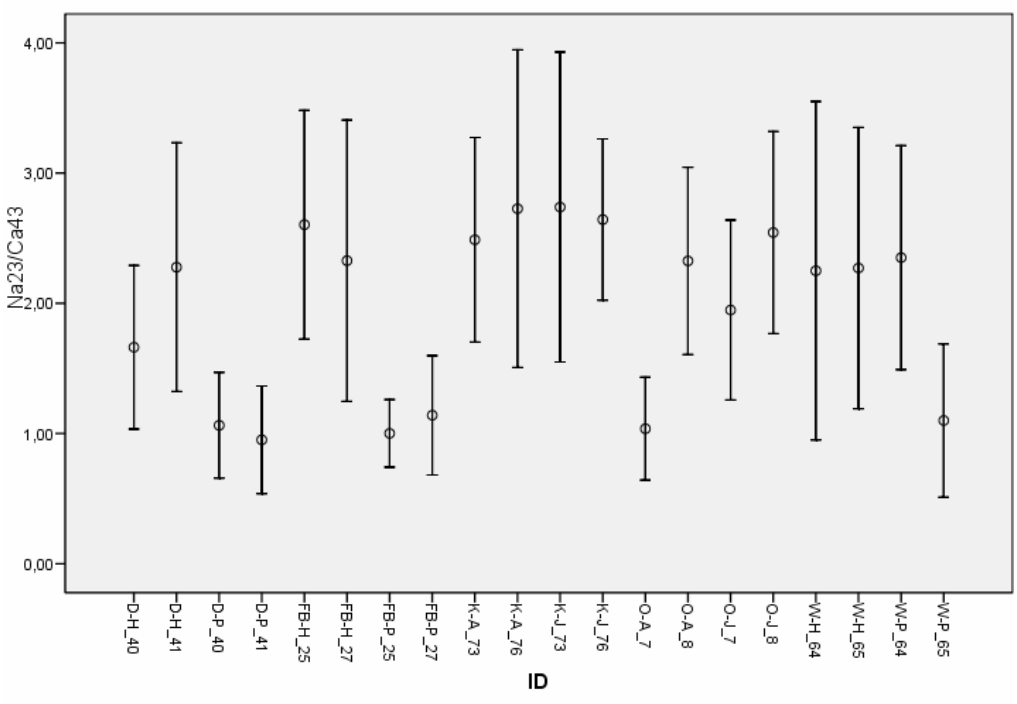

Figure 29. ^{23}Na /^{43}Ca ratios of the otolith samples with combined standard uncertainty (k=1)

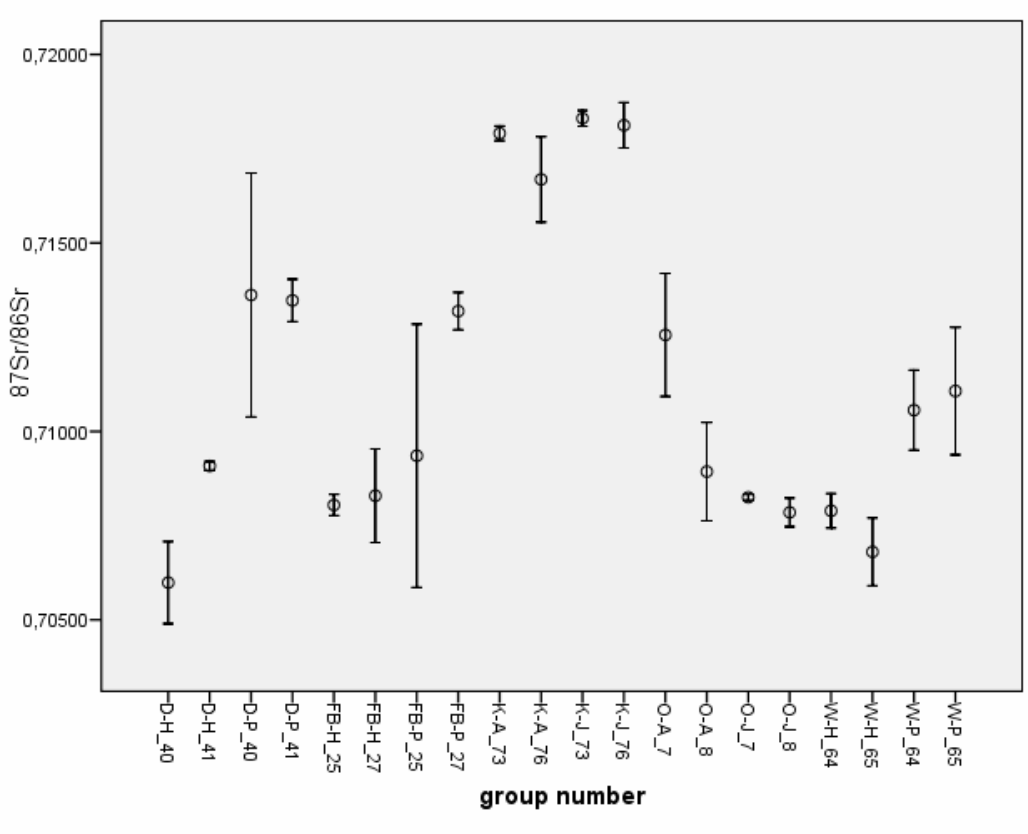

Figure 30. $^{87}Sr/^{86}Sr$ *ratios of the otolith samples with combined standard uncertainty (k=2)*

Table 25. $^{87}Sr/^{86}Sr$ *ratios of the otolith samples with combined standard uncertainty (k=1)*

ID Wasser	$^{87}Sr/^{86}Sr$	standard deviation	Relative standard deviation in %
D-H_40	0.70599	0.00109	0.154
D-H_41	0.70908	0.00012	0.017
D-P_40	0.71362	0.00324	0.454
D-P_41	0.71348	0.00056	0.079
K-J_73	0.71830	0.00021	0.029
K-J_76	0.71812	0.00060	0.084
K-A_73	0.71791	0.00020	0.027
K-A_76	0.71668	0.00113	0.158
FB-H_25	0.70805	0.00028	0.040
FB-H_27	0.70829	0.00124	0.175
FB-P_25	0.70935	0.00349	0.492
FB-P_27	0.71319	0.00050	0.070
O-J_7	0.70825	0.00008	0.012
O-J_8	0.70785	0.00038	0.053
O-A_7	0.71256	0.00163	0.229
O-A_8	0.70893	0.00131	0.184
W-H_64	0.70790	0.00046	0.064
W-H_65	0.70680	0.00090	0.127
W-P_64	0.71056	0.00106	0.149
W-P_65	0.71107	0.00169	0.238

Table 26. $^{23}Na/^{43}Ca$ and $^{88}Sr/^{43}Ca$ ratios of the otolith samples with combined standard uncertainty (k=1)

ID	$^{88}Sr/^{43}Ca$	standard uncertainty (k=1)	standard uncertainty (k=1) in %	$^{23}Na/^{43}Ca$	standard uncertainty (k=1)	standard uncertainty (k=1) in %
D-H_40	0,68	0,60	88	1,66	0,63	38
D-P_40	0,26	0,12	45	1,06	0,41	38
D-H_41	1,63	1,04	64	2,28	0,96	42
D-P_41	0,21	0,09	44	0,95	0,41	43
K-J_73	1,36	0,67	49	2,74	1,19	43
K-A_73	1,48	0,46	31	2,49	0,79	32
K-J_76	1,62	0,43	27	2,64	0,62	23
K-A_76	1,56	0,50	32	2,73	1,22	45
O-J_7	1,02	0,64	63	1,95	0,69	35
O-A_7	0,09	0,05	58	1,04	0,40	38
O-J_8	1,50	0,46	31	2,54	0,78	31
O-A_8	1,25	0,40	32	2,33	0,72	31
W-H_64	5,50	3,25	59	2,25	1,30	58
W-P_64	1,39	0,51	36	2,35	0,86	37
W-H_65	5,12	3,86	75	2,27	1,08	48
W-P_65	0,26	0,17	64	1,10	0,59	53
FB-H_25	5,25	3,56	68	2,60	0,88	34
FB-P_25	0,19	0,06	33	1,00	0,26	26
FB-H_27	5,95	4,32	73	2,33	1,08	46
FB-P_27	0,19	0,10	51	1,14	0,46	40

3.1.3.5 Statistical analysis of strontium isotopes and multi-elemental patterns of water samples and otolith cores and rims

The statistical analyses of the results of the water and otolith samples, except for the non-parametric discriminant analysis, were conducted using SPSS® 15.0. Figure 31 shows that the average vales of $^{88}Sr/^{43}Ca$ ratios of all otolith and water show a certain correlation except for the juvenile portions of the otoliths from the fish farm Flüsslberger (FB-H_25 and FB-H_27). This phenomenon was investigated and it was inquired that the fish farm Flüsslberger received juvenile fish from other sources. Figure 32 to Figure 34 illustrate the correlations of $^{88}Sr/^{43}Ca$, $^{23}Na/^{43}Ca$ and $^{87}Sr/^{86}Sr$ between water and otolith samples. Figure 33 shows the correlation of $^{88}Sr/^{43}Ca$ in the otolith samples to the Sr concentration in ng g^{-1} in the water samples. These correlations were further investigated using the Spearman rank test (see page 78), since the data cannot be not sufficiently described by linear regressions. Figure 32 and Figure 34 show the linear regressions of the otoliths and the water samples for $^{88}Sr/^{43}Ca$ and $^{23}Na/^{43}Ca$, respectively. Comparing the linear regression of $^{88}Sr/^{43}Ca$ of water and otoliths including and excluding fish from the fish farm Flüsslberger, it can be seen that the coefficient of determination changes from 0.370 to 0.756 (Figure 31 and Figure 32). Figure 34 shows that $^{23}Na/^{43}Ca$ ratios of otolith and water samples are not correlated as expected because sodium is physiologically regulated (see chapter 1.2.2.2). The $^{23}Na/^{43}Ca$ ratios were nonetheless used for the statistical data analysis since in spite of physiological regulation and

missing correlation to the ambient water, elements like Na might be useful for the discrimination of groups of fish. Figure 35 shows the linear regression of the otoliths and the water samples for $^{87}Sr/^{86}Sr$ coefficient of determination of 0.731.

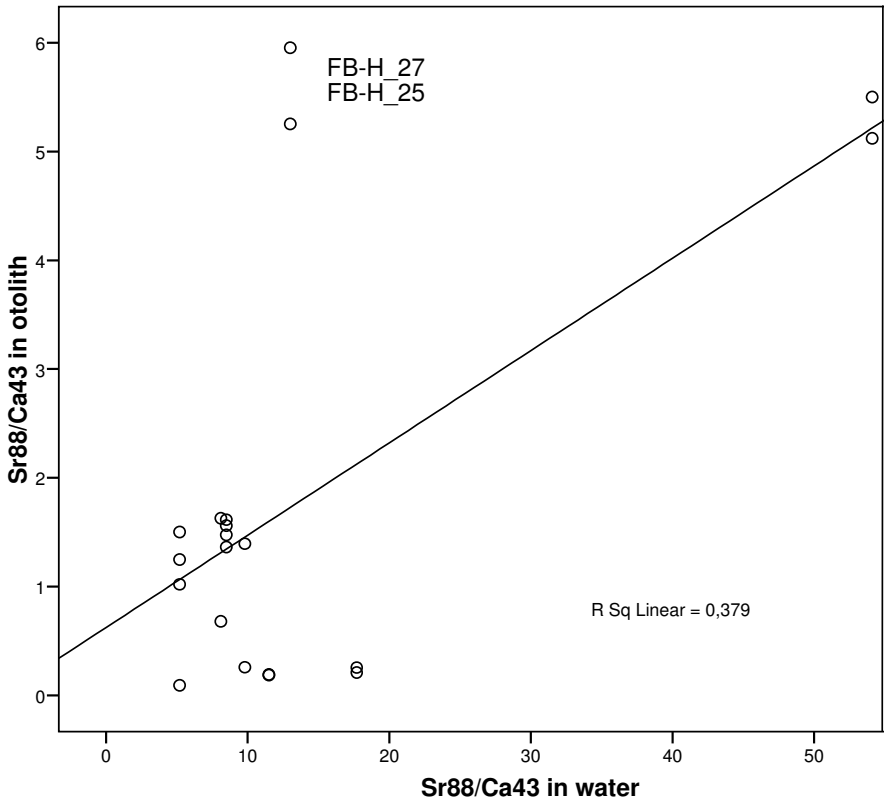

Figure 31.Linear regression of $^{88}Sr/^{43}Ca$ ratios of the otolith and the water samples including fish and water properties from fish farm Flüsslberger .

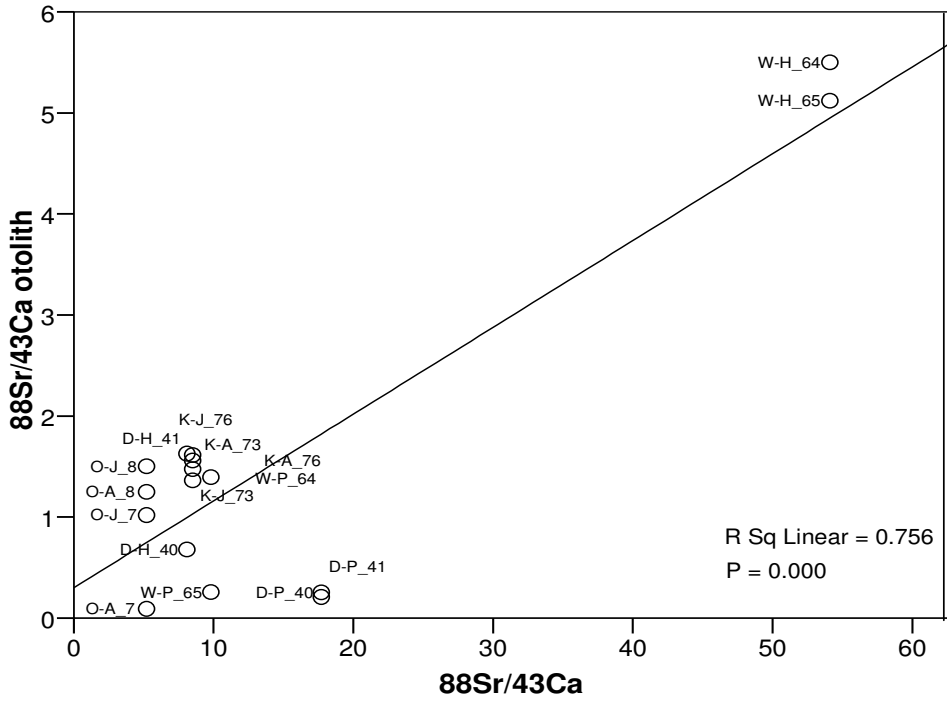

Figure 32.Linear regression of $^{88}Sr/^{43}Ca$ ratios of the otolith and the water samples.

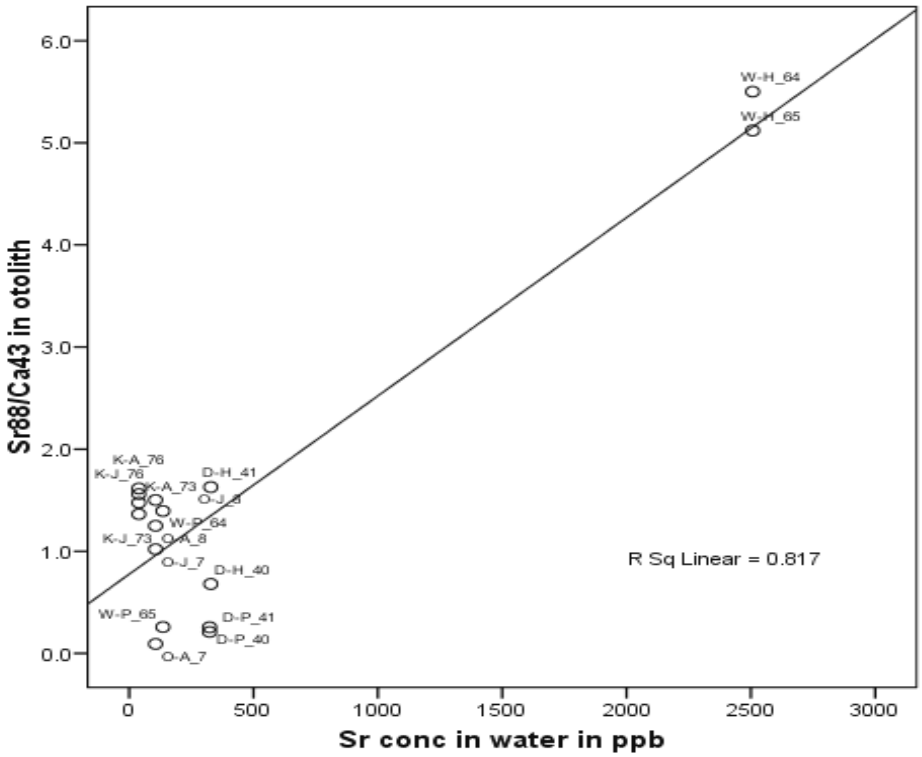

Figure 33. Linear regression of $^{88}Sr/^{43}Ca$ ratios of the otoliths versus the Sr concentration in the water samples including fish and water properties from fish farm Flüsslberger.

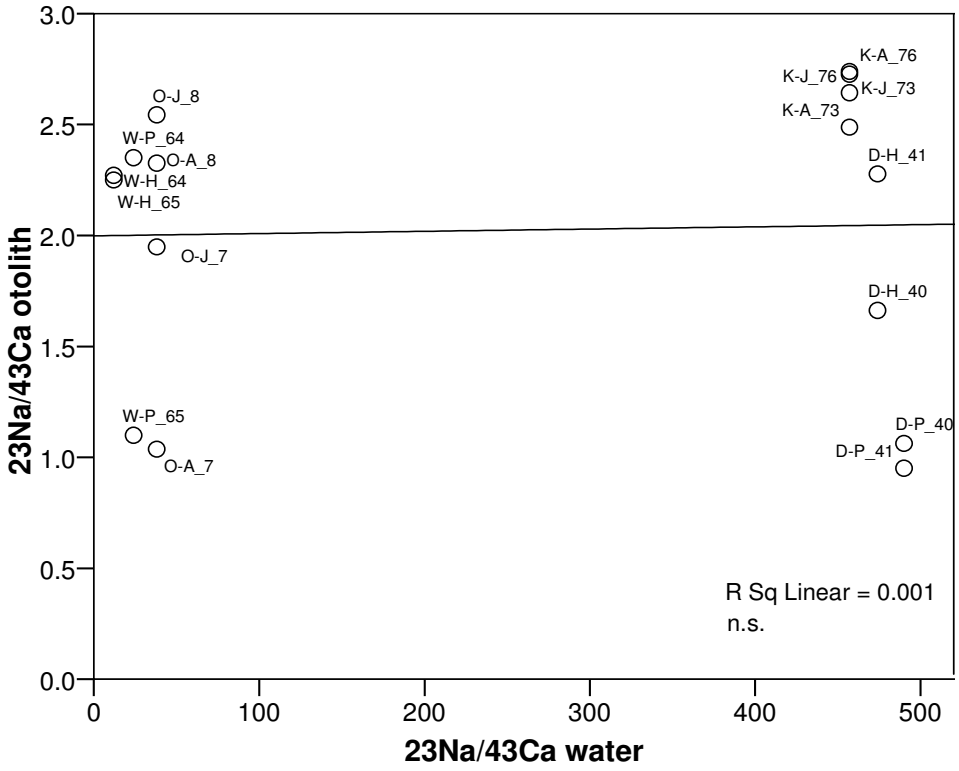

Figure 34.Linear regression of $^{23}Na/^{43}Ca$ ratios of the otolith and the water samples.

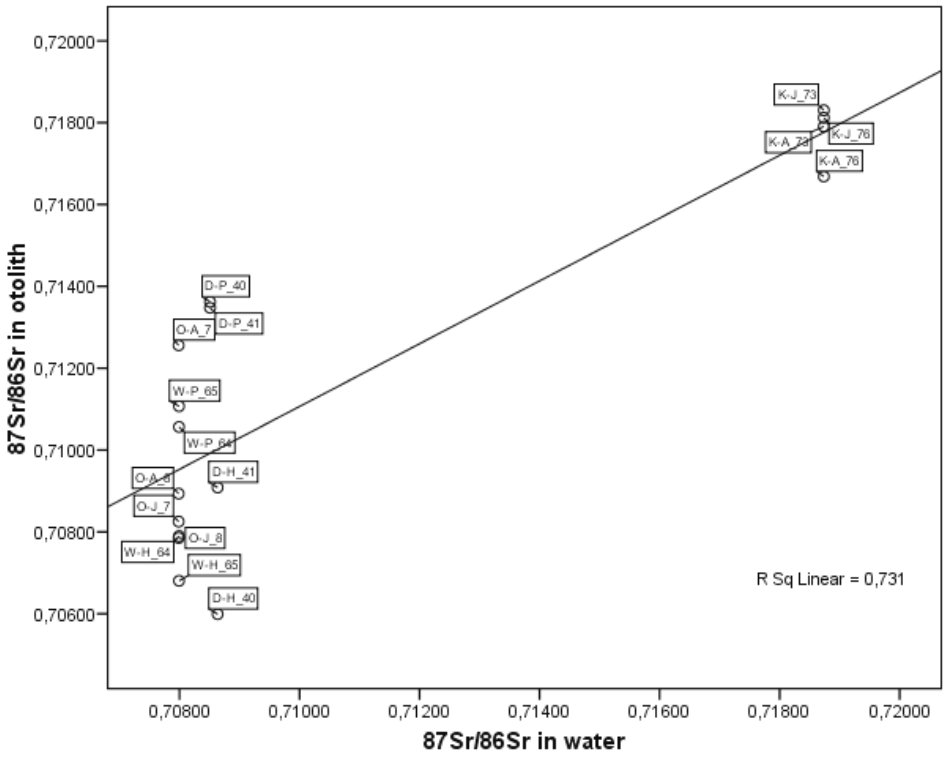

Figure 35.Linear regression of $^{87}Sr/^{86}Sr$ ratios of the otolith and the water samples.

It is quite obvious from Figure 35 that all sampling locations except the river Kleiner Kamp (K) have quite similar strontium isotope ratios, which is also reflected in the otolith chemistry. This observation reflects the geographical constitution of the samples, since the river Ois (O) and the fish farm Weinzettl (W) lie within the calcareous rock while the river Kleiner Kamp (K) lies within the siliceous part of Lower Austria. The fish farm Dolezal (D) lies in the calcareous gravel region (Figure 36).

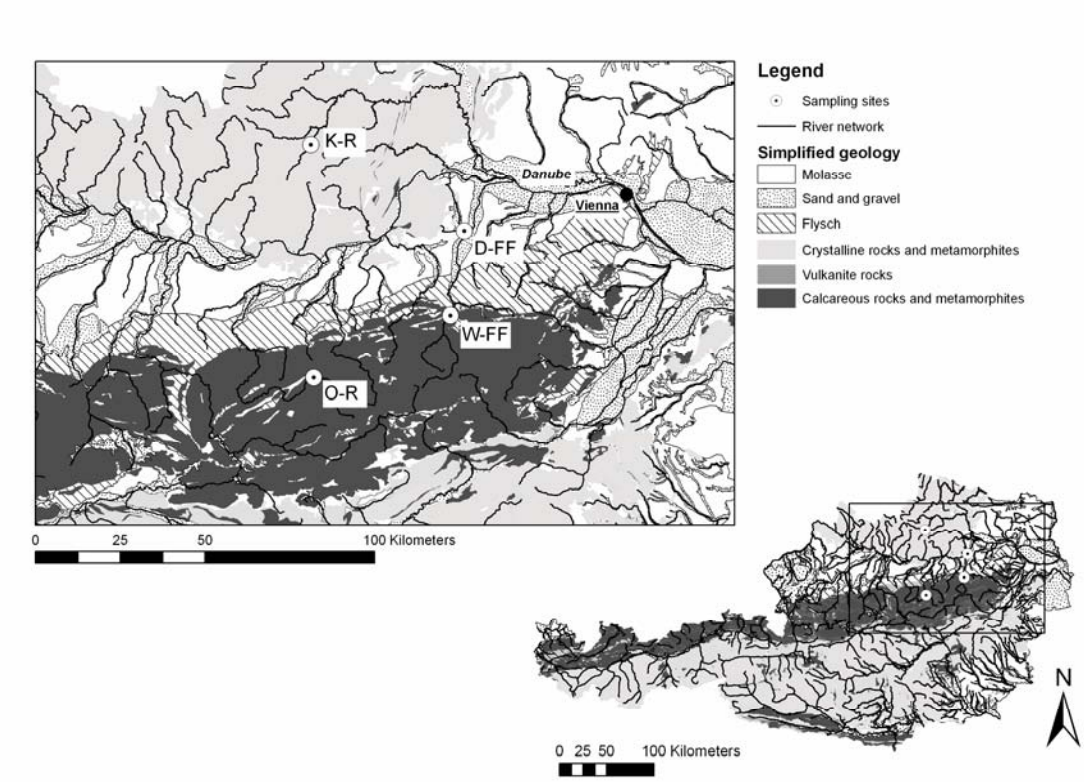

Figure 36. Geological image of Lower Austria including the four sampling locations used for the statistical data analysis (O-R, river Ois; K-R, river Kamp; W-FF, fish farm Weinzettl; D-FF, fish farm Dolezal).[source: ZITEK et al, 2008]

Generally, linear regressions describe the overall relationship between water chemistry and otolith chemistry although due to the small sample sizes, these analyses are of limited explanatory power. Therefore differences in water chemistry between sites were tested using the Kruskal–Wallis-test. When the Kruskal–Wallis-test was significant, Mann–Whitney-tests were used to identify pair-wise differences. All tests were carried out individually. As well as for the linear regression the average values regardless of their uncertainty were used. Statistical significance levels for this analysis were set at ≤ 0.1. Significant differences in water chemistry were found between sites for $^{88}Sr/^{43}Ca$ (Kruskal-Wallis, P=0.007), $^{23}Na/^{43}Ca$ (Kruskal-Wallis, P=0.012) and $^{87}Sr/^{86}Sr$ (Kruskal-Wallis, P=0.007) with most pair-wise comparisons being significant. The results of the pair-wise comparison by Mann–Whitney-tests are summarized in Table 27.

Correlations between $^{23}Na/^{43}Ca$, $^{88}Sr/^{43}Ca$ and $^{87}Sr/^{86}Sr$ of water and otolith samples were analyzed using Spearman rank correlation. $^{87}Sr/^{86}Sr$ in water showed a clear significant positive correlation with otolith chemistry (Spearman rank correlation, r_s=719, P=0.002). Additionally $^{88}Sr/^{43}Ca$ in otoliths was positively correlated to $^{23}Na/^{43}Ca$ in otoliths (Spearman rank correlation, r_s=629, P=0.009), and $^{87}Sr/^{86}Sr$ in water was positively correlated to $^{23}Na/^{43}Ca$ in water (Spearman rank correlation, r_s=707, P=0.002).

Table 27. The results of the pair-wise comparison by Mann–Whitney-tests with the statistical significance levels for this analysis were set at ≤0.1. Significant values results are indicated by 0.1.*

	$^{88}Sr/^{43}Ca$					
	D-H	D-P	W-H	W-P	O-R	K-R
D-H		0.1*	0.1*	0.1*	0.1*	-
D-P	0.1*		0.1*	-	0.1*	0.1*
W-H	0.1*	0.1*		0.1*	0.1*	0.1*
W-P	0.1*	-	0.1*		0.1*	0.1*
O-R	0.1*	0.1*	0.1*	0.1*		0.1*
K-R	0.1*	0.1*	0.1*	0.1*	0.1*	
	$^{23}Na/^{43}Ca$					
	D-H	D-P	W-H	W-P	O-R	K-R
D-H		-	0.1*	0.1*	0.1*	-
D-P	-		0.1*	0.1*	0.1*	-
W-H	0.1*	0.1*		0.1*	0.1*	0.1*
W-P	0.1*	0.1*	0.1*		0.1*	0.1*
O-R	0.1*	0.1*	0.1*	0.1*		0.1*
K-R	-	-	0.1*	0.1*	0.1*	
	$^{87}Sr/^{86}Sr$					
	D-H	D-P	W-H	W-P	O-R	K-R
D-H		-	0.1*	0.1*	0.1*	0.1*
D-P	-		0.1*	0.1*	0.1*	0.1*
W-H	0.1*	0.1*		0.1*	-	0.1*
W-P	0.1*	0.1*	0.1*		0.1*	0.1*
O-R	0.1*	0.1*	-	0.1*		0.1*
K-R	0.1*	0.1*	0.1*	0.1*	0.1*	

The water samples were grouped by cluster analysis based on the $^{23}Na/^{43}Ca$, $^{88}Sr/^{43}Ca$ and $^{87}Sr/^{86}Sr$. The nearest neighbor cluster analysis algorithm with squared Euclidian distance was used and the values were standardized to one before analyses. In a stepwise process all possible combinations of $^{23}Na/^{43}Ca$, $^{88}Sr/^{43}Ca$ and $^{87}Sr/^{86}Sr$ were used for cluster analysis. The results of the nearest neighbor cluster analysis are summarized in Table 28 showing that the number of clusters increases with the number of variables from two to four clusters. A similarity dendrogram for the nearest neighbor cluster analysis based on the $^{23}Na/^{43}Ca$, $^{88}Sr/^{43}Ca$ and $^{87}Sr/^{86}Sr$, which yielded four clusters, is shown in Figure 37.

Table 28. Results of the nearest neighbor cluster analysis of the water samples based on the $^{23}Na/^{43}Ca$, $^{88}Sr/^{43}Ca$ and $^{87}Sr/^{86}Sr$. The variables used for the clustering are in the first line. The numbers in line with the water ID indicate which water samples were placed in the same cluster. Calcareous gr., calcareous r. and crystalline r. stand for calcareous gravel, calcareous rocks and crystalline rocks.

Water ID	*geological unit*	$^{88}Sr/^{43}Ca$	$^{23}Na/^{43}Ca$	$^{87}Sr/^{86}Sr$	$^{88}Sr/^{43}Ca + ^{23}Na/^{43}Ca^{3}$	$^{88}Sr/^{43}Ca + ^{87}Sr/^{86}Sr$	$^{23}Na/^{43}Ca + ^{87}Sr/^{86}Sr$	$^{88}Sr/^{43}Ca + ^{23}Na/^{43}Ca + ^{87}Sr/^{86}Sr$
D-H1	calcareous gr.	2	1	2	3	3	2	3
D-H2	calcareous gr	2	1	2	3	3	2	3
D-H3	calcareous gr	2	1	2	3	3	2	3
D-P1	calcareous gr	2	1	2	3	3	2	3
D-P2	calcareous gr	2	1	2	3	3	2	3
D-P3	calcareous gr	2	1	2	3	3	2	3
W-H1	calcareous r.	1	2	2	1	2	3	2
W-H2	calcareous r.	1	2	2	1	2	3	2
W-H3	calcareous r.	1	2	2	1	2	3	2
W-P1	calcareous r.	2	2	2	2	3	3	4
W-P2	calcareous r.	2	2	2	2	3	3	4
W-P3	calcareous r.	2	2	2	2	3	3	4
O-R1	calcareous r.	2	2	2	2	3	3	4
O-R2	calcareous r.	2	2	2	2	3	3	4
O-R3	calcareous r.	2	2	2	2	3	3	4
K-R1	crystalline r.	2	1	1	3	1	1	1
K-R2	crystalline r.	2	1	1	3	1	1	1
K-R3	crystalline r.	2	1	1	3	1	1	1
Number of clusters		2	2	2	3	3	3	4

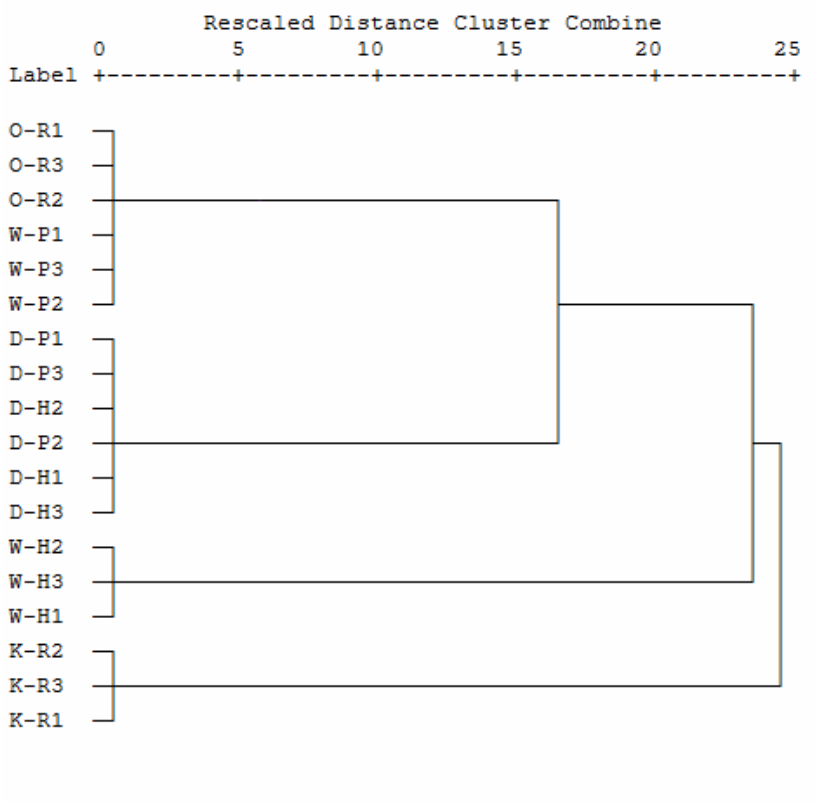

Figure 37. Similarity dendrograms for the nearest neighbor cluster analysis based on the $^{23}Na/^{43}Ca$, $^{88}Sr/^{43}Ca$ and $^{87}Sr/^{86}Sr$

Following the hypothesis that mainly the ambient water chemistry influences the otolith composition, a retrospective assignment of the otolith regions to the water clusters via non-parametric discriminant analysis was conducted. The cluster numbers were assigned to juvenile and adult life stages of the fish represented by different otolith regions, e.g. otolith core and rim. Based on this, a nonparametric discriminant analysis using the DISCRIM procedure of SAS [SAS, 2007] (kernel=Epanechnikov, radius=1) with group-specific probabilities was executed on the otolith data to achieve classification estimates for the clustered localities. The original and predicted cluster numbers as well as the total percentage of correctly classified otolith regions is given in Table 29. The retrospective assignment of otolith regions to water clusters via non-parametric discriminant analysis was of high accuracy since 100 % of the samples correctly classified except when 23Na/43Ca was used as single variable or in pair-wise combinations. Discrimination also yielded 100 % accuracy for the cluster using all three variables.

*Table 29. Results of the retrospective assignment of the otolith regions to the water clusters via a nonparametric discriminant analysis using the DISCRIM procedure of SAS [SAS, 2007]. Misclassified otolith regions are marked according to this example: 2**(1) means that the otolith region was wrongly assigned to cluster 2 instead of cluster 1.*

Otolith ID	$^{88}Sr/^{43}Ca$	$^{23}Na/^{43}Ca$	$^{87}Sr/^{86}Sr$	$^{88}Sr/^{43}Ca+$ $^{23}Na/^{43}Ca$	$^{88}Sr/^{43}Ca+$ $^{87}Sr/^{86}Sr$ [6]	$^{23}Na/^{43}Ca+$ $^{87}Sr/^{86}Sr$	$^{88}Sr/^{43}Ca+^{23}Na/^{43}Ca +$ $^{87}Sr/^{86}Sr$
D-H_40	2	2**(1)	2	3	3	2	3
D-H_41	2	2**(1)	2	3	3	3**(2)	3
D-P_40	2	1	2	3	3	2	3
D-P_41	2	1	2	3	3	2	3
W-H_64	1	2	2	1	2	3	2
W-H_65	1	2	2	1	2	3	2
W-P_64	2	2	2	2	3	3	4
W-P_65	2	1**(2)	2	**3(2)	3	3	4
O-J_7	2	2	2	2	3	3	4
O-J_8	2	2	2	2	3	3	4
O-A_7	2	1**(2)	2	2	3	2**(3)	4
O-A_8	2	2	2	2	3	3	4
K-J_73	2	1	1	3	1	1	1
K-J_76	2	1	1	3	1	1	1
K-A_73	2	1	1	2**(3)	1	1	1
K-A_76	2	2**(1)	1	3	1	1	1
Correctly classified (%)	100	68.8	100	87.5	100	87.5	100

3.1.3.6 Discussion of the statistical analysis of water and otolith samples

Clear differences were found when the fish experienced different environmental conditions during their live. However, fish living within the same geologic unit are hard to distinguish. Given a significant change of the geologic area as it can be found in rivers flowing along geologic borders like the Danube, it should be possible to determine the time of the migration of fish in right handed or left handed rivers branching from the main river. Generally, it can be assumed that since Austria‘s geology consists of several different geologic units, Austria‘s rivers and lakes might a high potential to be used in migration studies of fish using otolith micro chemistry. This potential is illustrated by the results of the multi-element measurements of water samples from several Austrian water bodies given in Figure 38. These measurements were carried out prior to this study. The sampling locations shown in Figure 38 are different from those where the fish were caught for this study. Figure 38 shows the content of several elements relative to the samples from Thaya Wohlfahrts for qualitative comparison. Since there are significant differences for some elements such as Sr, which are reflected in the fish otoliths, fish migration between these bodies of water can most probably be detected via otolith micro-chemistry.

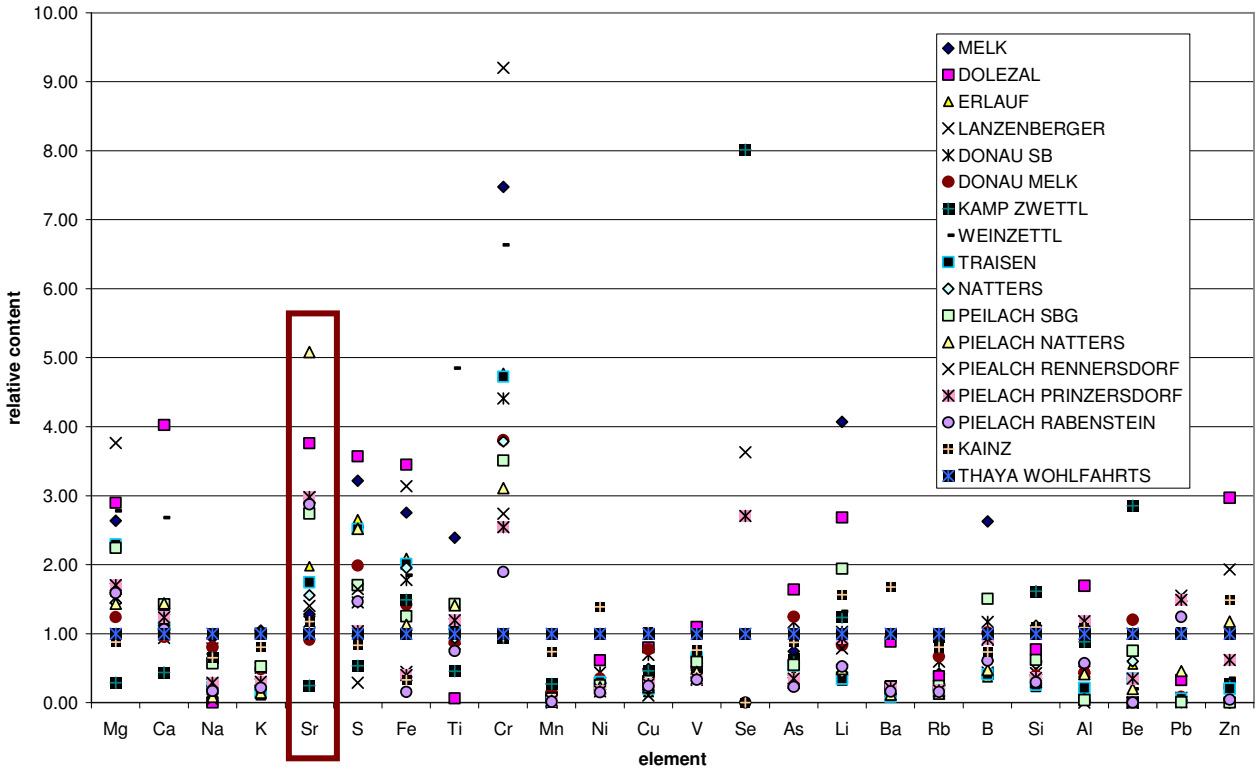

Figure 38. Multi-element measurements of several Austrian water bodies. The element content in the water is displayed as relative values to the values measured in Thaya Wohlfahrts.

3.1.4 Multi-elemental patterns of lines ablated across the otolith surface

$^{88}Sr/^{43}Ca$, $^{23}Na/^{43}Ca$ and $^{24}Mg/^{43}Ca$ data from laser transects were plotted as graphs for qualitative comparison. The graphs for two otoliths (W_62 from the fish farm Weinzettl and D_42 from the fish farm Dolezal) are shown in Figure 39 and Figure 40. Basically, these two figures show two distinct patterns: Some otoliths show an increase of $^{88}Sr/^{43}Ca$ in the core region like the otolith W_62 from the fish farm Weinzettl in Figure 39, in other otoliths this increase of $^{88}Sr/^{43}Ca$ is not observed like the otolith D_42 from the fish farm Dolezal shown in Figure 40. In otoliths with $^{88}Sr/^{43}Ca$ increase in the core region the height of the peak as well as its width varied considerably. Summing up, all four fish from the river Kleiner Kamp missed the $^{88}Sr/^{43}Ca$ peak in the core region, while all four fish from the fish farms Weinzettl and Flüsslberger, respectively, showed $^{88}Sr/^{43}Ca$ peaks in the core region. In the cases of the fish farm Dolezal and the river Ois, two and one of four otoliths, respectively, showed $^{88}Sr/^{43}Ca$ peaks in the core region. The increased strontium concentrations in the core might be due to physiological effects or due to influence of the environment the fish mother lived in before laying the eggs. The latter would also explain why not all fish hatched in the same environment show or lack these peaks.

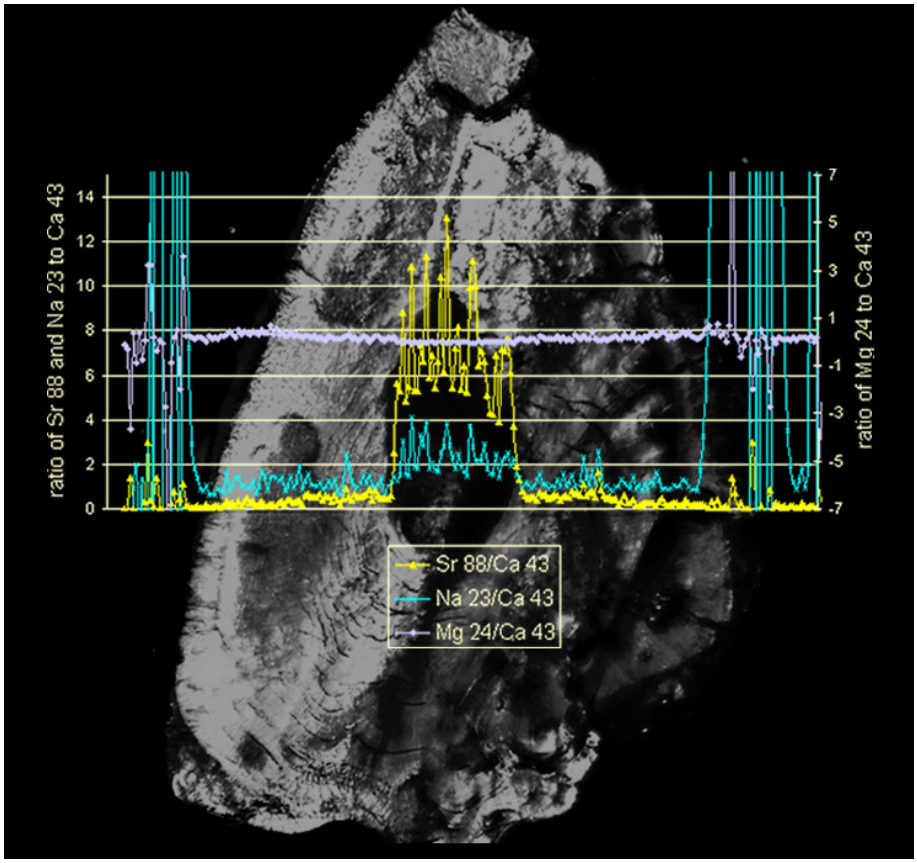

Figure 39. Line scan of otolith W_62 of a trout from the fish farm Weinzettl including the graphs for the $^{88}Sr/^{43}Ca$, $^{23}Na/^{43}Ca$ and $^{24}Mg/^{43}Ca$ displayed above the ablated line for quantitative comparison.

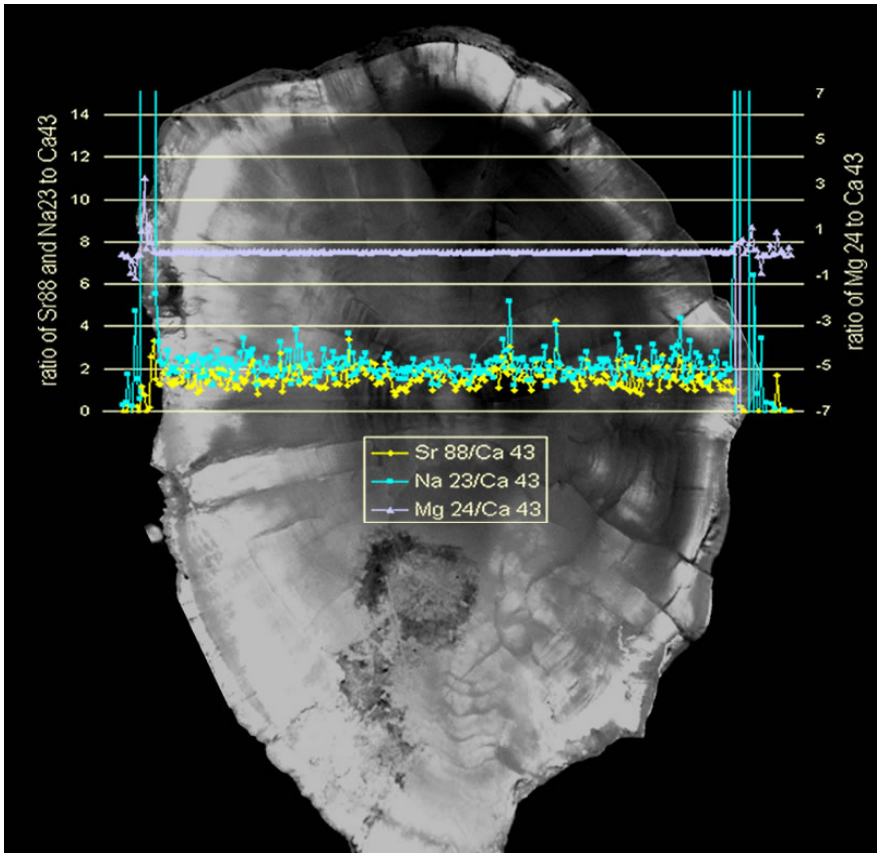

Figure 40. Line scan of otolith D_42 of a trout from the fish farm Dolezal including the graphs for the $^{88}Sr/^{43}Ca$, $^{23}Na/^{43}Ca$ [3] and $^{24}Mg/^{43}Ca$ displayed above the ablated line for quantitative comparison.

3.2 Eye lenses

Table 30 and Figure 41 give the diameters of the eye lenses. Four eye lenses of four fish, two from the river Kleiner Kamp and two of the Fish farm Weinzettl were used for the multi-element measurement by laser ablation ICP-MS. Three spots per eye lens were measured. The results are summarized in Table 31. The obvious surface contamination of one eye lens from the river Kleiner Kamp (L_K_73) underlines the need for straight forward cleaning protocols that ensure the complete removal of adhering tissue. Figure 42 shows the differences in the blank corrected intensities of Na in the eye lenses from two sampling locations illustrating the potential of the elemental composition of eye lenses to be used to distinguish groups of fish. In contrast to the eye lenses, the otolith rims from Kleiner Kamp and the fish farm Weinzettl do not show significant in their Na content (Figure 43).

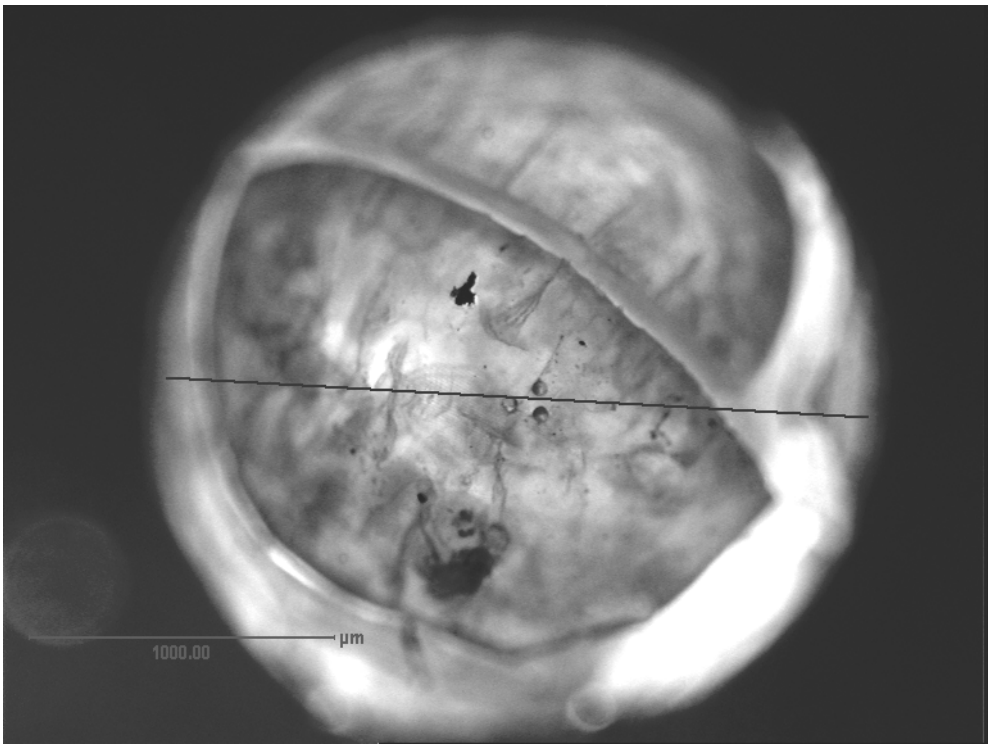

Figure 41. The measured diameter of the eye lens is indicated by a solid line.

Table 30. The diameters of the eye lenses used for the laser ablation.

Sample ID	Sampling location	Eye lens diameter in µm
L_W_65	Weinzettl	2629
L_W_64	Weinzettl	23366
L_K_76	Kleiner Kamp	1683
L_K_73	Kleiner Kamp	1255

Table 31. Elements investigated in the LA-ICP-MS multi-element analysis of the eye lenses.

Element	*Measured isotope*	*Above detection limit*	*Comment*
Li	7	no	
B	11	no	
Na	23	**yes**	**Above detection limit in all laser spots of all four eye lenses**
Mg	24	yes	Above detection limit in all laser spots of all four eye lenses except 1 spot (L_W_64_3); Peaks in beginning of ablations in lenses from river Kleiner Kamp (L_K_73 and L_K_76) probably due to surface contamination
Al	27	yes	Peaks in beginning of all ablations in 1 lens from river Kleiner Kamp (L_K_73) probably due to surface contamination
Ca	42; 43	yes	Peak in beginning of 1 ablation in 1 lens from river Kleiner Kamp (L_K_73) probably due to surface contamination
Ti	46	no	
PO	47	no	
V	51	no	
Cr	52; 53	no	
Mn	55	no	
Fe	57	no	
Ni	58	no	
Co	59	no	
Ni	60; 62	no	
Cu	63; 65	yes	
Zn	64; 66	yes	Peak in beginning of 1 ablation in 1 lens from river Kleiner Kamp (L_K_73) probably due to surface contamination
As	75	no	
Se	82	no	
Rb	85	no	
Sr	88	yes	Peak in beginning of 2 ablations in 1 lens from river Kleiner Kamp (L_K_73) probably due to surface contamination
Zr	90	no	
Mo	98	no	
Sn	118; 120	no	
Sb	121; 123	no	
Ba	138	yes	Peak in beginning of 1 ablation in 1 lens from river Kleiner Kamp (L_K_73) probably due to surface contamination
Hg	200; 202	no	
Tl	205	no	
Pb	208	yes	Peak in beginning of 1 ablation in 1 lens from river Kleiner Kamp (L_K_73) probably due to surface contamination
U	238	no	

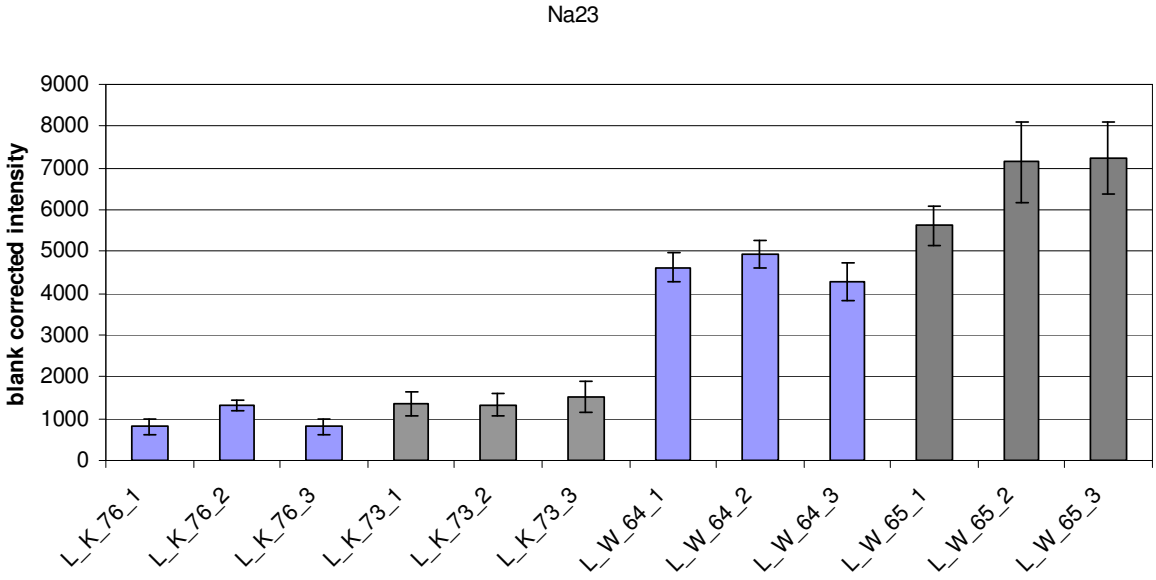

Figure 42. Blank corrected intensities of ^{23}Na of eye lenses sampled by laser ablation spots with standard deviation (k=1). Three spots per eye lens are shown.

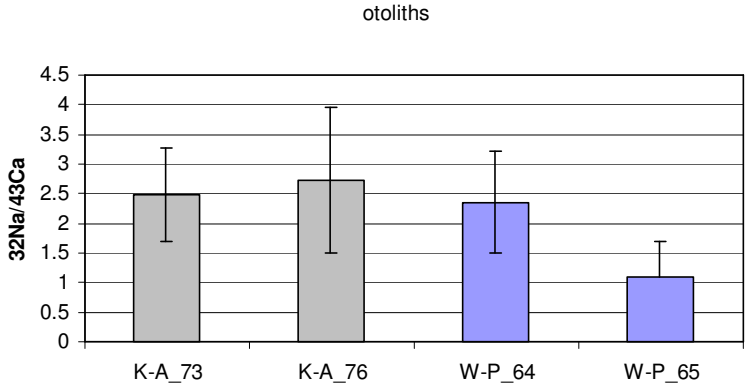

Figure 43. ^{23} Na/^{43}Ca ratios of otolith rims from fish from Kleiner Kamp and from the fish form Weinzettl with combined standard uncertainty (k=1).

3.3 Scales

Table 32 and Figure 44 show the length parameters the scales. Five scales from four different fish, two from the river Kleiner Kamp and two of the Fish farm Weinzettl, were used for the multi-element measurement by laser ablation ICP-MS. Lines across the scale surface were ablated as indicated in Figure 44. There are several difficulties in measuring multi-element lines on scales. Firstly, it must be assured that original scales and not substituted scales are sampled for the reconstruction of the live history of the fish. Since scales are the only protection of the fish against the environment, they are substituted quickly when they are lost by sampling or by accident. One scale from the fish farm Weinzettl measured in this study

(S_W_64) was a substituted scale. Figure 45 shows the difference between substituted and original scales: They can be distinguished by the rough centre of the substituted scale.

Secondly, it must be assured that the laser is focused on the scale surface while the material is ablated. Scales have a more ore less curved structure in addition to the fact that it is quite complicated to glue them horizontally on a glass slide for ablation. Scale S_K_73 was not interpretable probably because the laser could not be focused on the surface of the arched scale. On scale S_W_65 one line was pre-ablated before ablation resulting in no obvious differences to the ablations without pre-ablation.

Table 32. Length parameters of the scales used for the multi-element measurement

Sample ID	Sampling location	Scale length in µm	Scale width in µm	Length of ablated line(s) in µm
S_K_73	Kleiner Kamp	787	491	555
S_K _76	Kleiner Kamp	1207	675	1065
S_W_64	Weinzettl	2130	1740	2098
S_W_65	Weinzettl	2542	1837	1887; 1818; 1845
S2_W_65	Weinzettl	2513	1993	2005

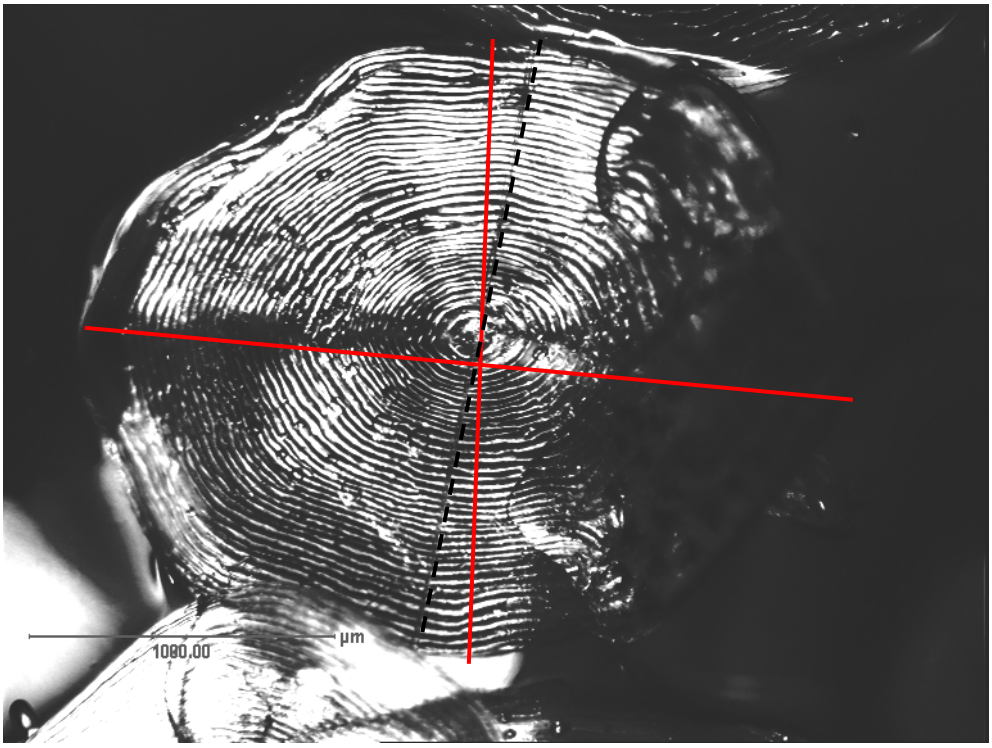

Figure 44. The measured length parameters of the scales: The width and the length of the otolith are indicated by solid red lines and the laser ablated line is indicated by a black dashed line.

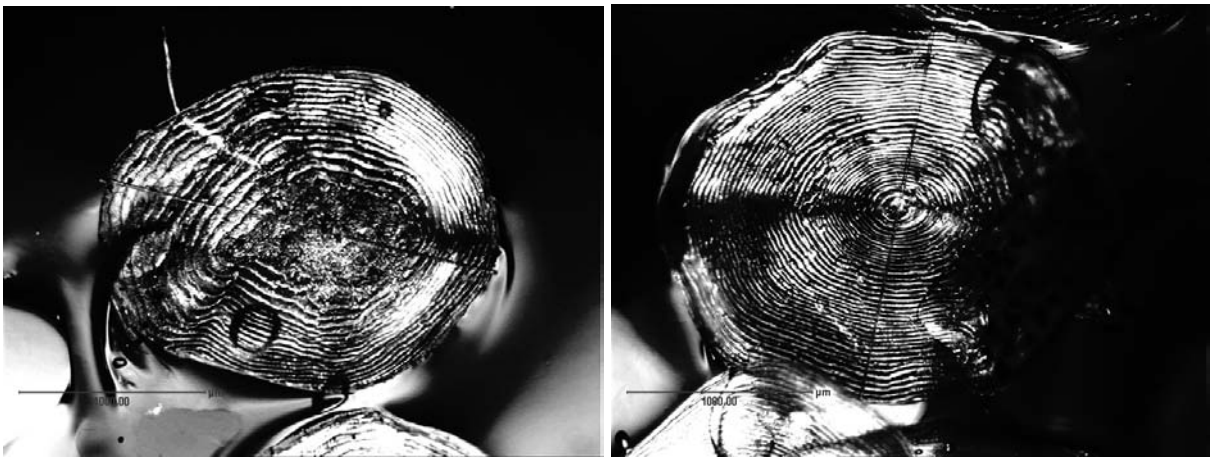

Figure 45 left: substituted scale (S_W_64) with laser ablated line; right: original scale (S2_W_65) with laser ablated line.

The measured elements and the outcome of the measurements are summarized in Table 33. Elements were considered above the detection limit when their blank corrected average intensity of the whole length of the ablated line exceeded three times the standard deviation of the blank. Figure 46 shows the line scan of scale S_W_65 from a trout from Weinzettl including the graphs for the $^{88}Sr/^{43}Ca$, $^{23}Na/^{43}Ca$, $^{24}Mg/^{43}Ca$ and $^{138}Ba/^{43}Ca$ displayed above the ablated line for qualitative observation. The difference of the graphs for the $^{88}Sr/^{43}Ca$, $^{23}Na/^{43}Ca$, $^{24}Mg/^{43}Ca$ and $^{138}Ba/^{43}Ca$ of an original and a substituted scale are displayed in Figure 47. The differences in the signal heights ($^{23}Na/^{43}Ca$ and $^{24}Mg/^{43}Ca$) and in the profile of the $^{23}Na/^{43}Ca$ signal underline the difference between original and substituted scales. Since the height of the strontium signal of the substituted scale corresponds to the signal at the rims of the original scale, it can be assumed that the substituted scale was built after the fish was put into the pool where the fish was caught. Apart from a slight increase of the $^{88}Sr/^{43}Ca$ in the centre of the scale, no pronounced changes in the elemental composition across the scale were observed. However, this increase in $^{88}Sr/^{43}Ca$ is less pronounced than the $^{88}Sr/^{43}Ca$ increase in the graphs of otoliths from the same fish farm (Figure 48). Therefore, the relationship between otoliths and scales needs further investigation.

Table 33. Elements investigated in the LA-ICP-MS multi-element analysis of the fish scales.

Element	*Measured isotope*	*Above detection limit*	*Comment*
Li	7	no	
B	11	no	
Na	23	**yes**	**Above detection limit in all ablated lines of the scales**
Mg	24	**yes**	**Above detection limit in all ablated lines of the scales**
Al	27	no	
Ca	42; 43	**yes**	**Above detection limit in all ablated lines of the scales**
Ti	46	no	
PO	47	no	
V	51	no	
Cr	52; 53	no	
Mn	55	**yes**	**Above detection limit in ablated lines of the scales from the fish farm Weinzettl (S2_W_65; S_W_64)**
Fe	57	no	
Ni	58	no	
Co	59	no	
Ni	60; 62	no	
Cu	63; 65	no	
Zn	64; 66	no	
As	75	no	
Se	82	no	
Rb	85	no	
Sr	88	**yes**	**Above detection limit in all ablated lines of the scales**
Zr	90	no	
Mo	98	no	
Sn	118; 120	no	
Sb	121; 123	no	
Ba	138	**yes**	**Above detection limit in all ablated lines of the scales**
Hg	200; 202	no	
Tl	205	no	
Pb	208	no	
U	238	no	

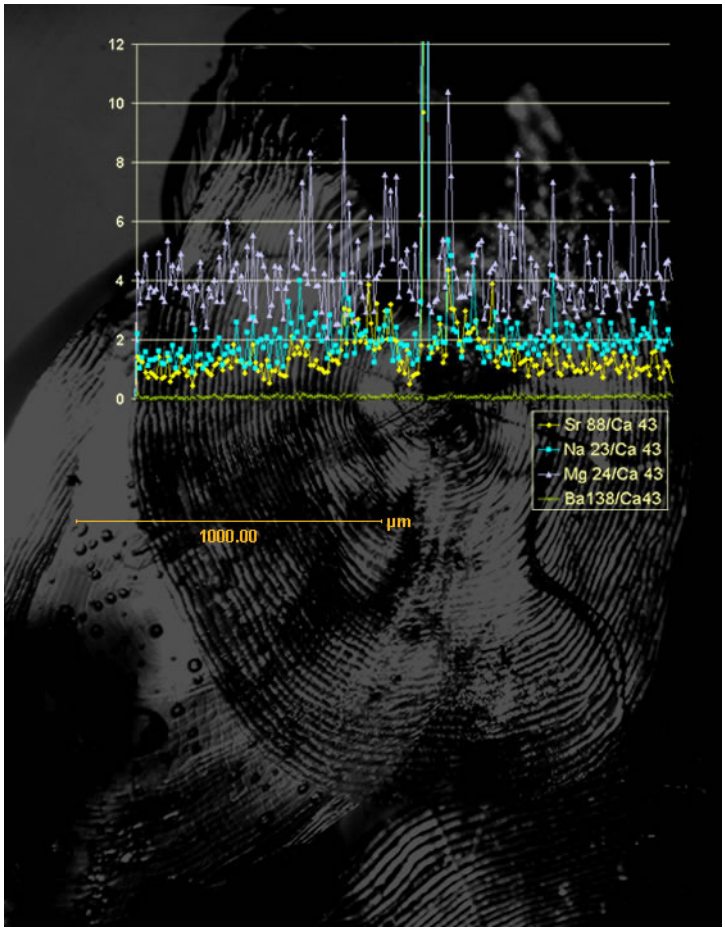

Figure 46. Line scan of scale S_W_65 from a trout from Weinzettl including the graphs for $^{88}Sr/^{43}Ca$, $^{23}Na/^{43}Ca$, $^{24}Mg/^{43}Ca$ and $^{138}Ba/^{43}Ca$ above the ablated line.

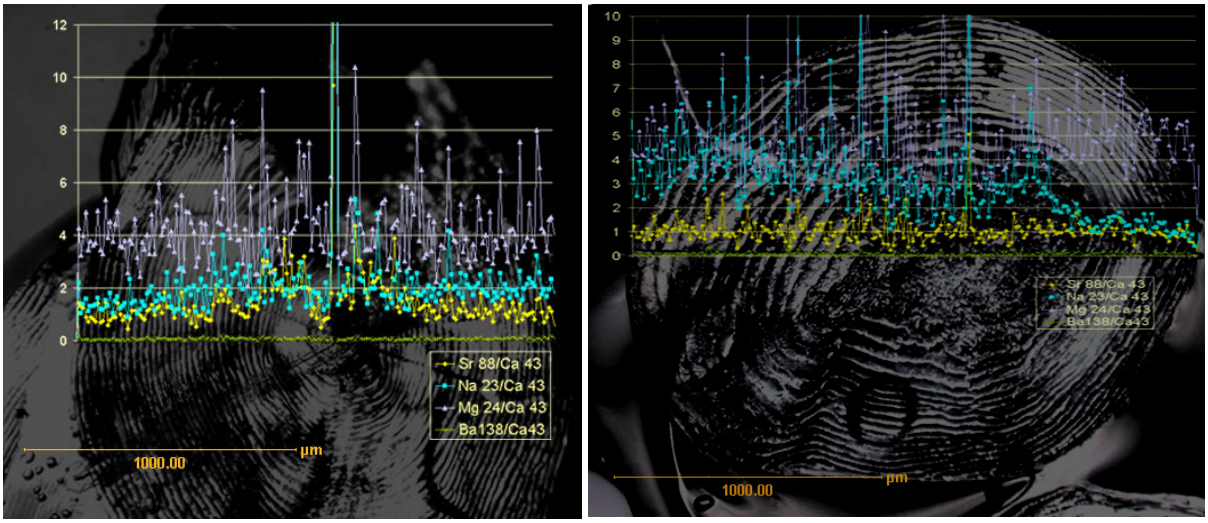

Figure 47. Line scans of two scales of a trout from Weinzettl including the graphs for $^{88}Sr/^{43}Ca$, $^{23}Na/^{43}Ca$, $^{24}Mg/^{43}Ca$ and $^{138}Ba/^{43}Ca$ displayed above the ablated line. Left: substituted scale (S_W_64) with laser ablated line; right: original scale (S2_W_65) with laser ablated line.

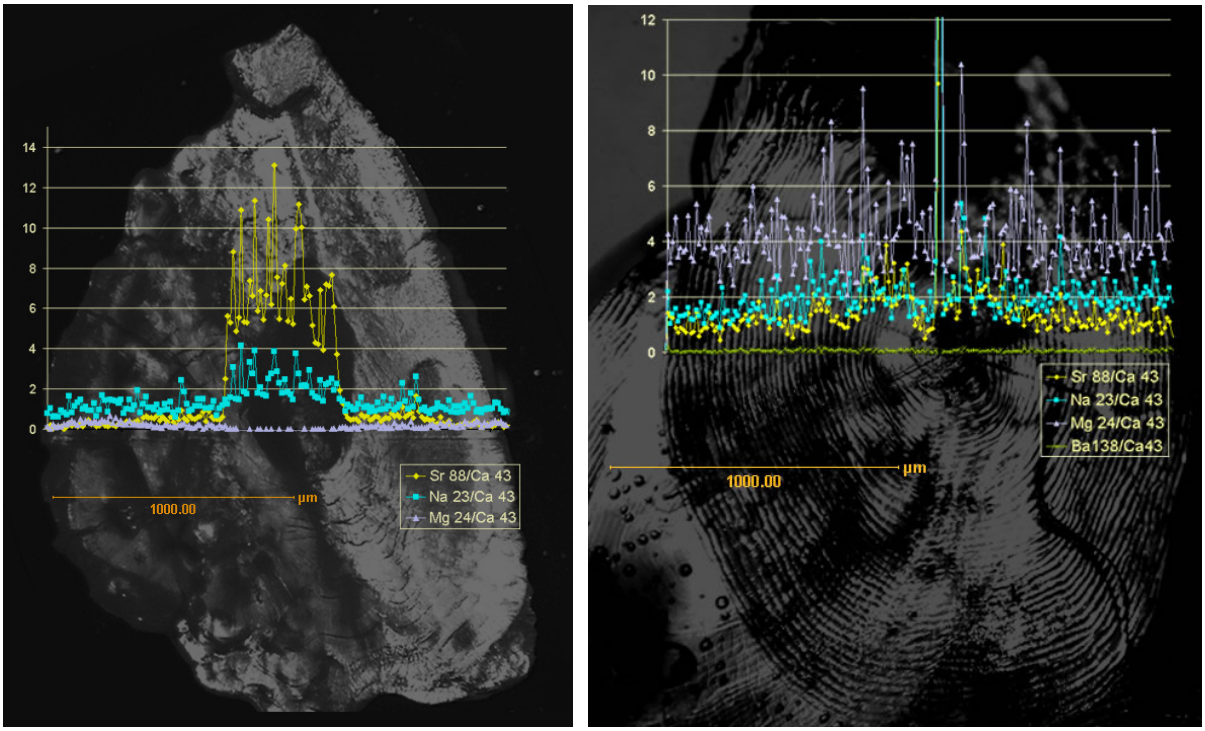

Figure 48 Line scans of one otolith and one scale of fish from Weinzettl including the graphs for the $^{88}Sr/^{43}Ca$, $^{23}Na/^{43}Ca$, $^{24}Mg/^{43}Ca$ and $^{138}Ba/^{43}Ca$ (in case of the scale) displayed above the ablated line. Left: otolith (W_62) with laser ablated line; right: scale (S2_W_65) with laser ablated line.

4 Summary and conclusion

This study showed that a combination of elemental patterns and isotope ratios can successfully be applied for the retrospective assignment of rainbow trout and brown trout in Austrian water bodies considering Austria's diverse geology, although fish from the same geological unit are more difficult to distinguish. Thus in rivers flowing along geologic borders like the Danube, it should be possible to determine the time of the migration of fish in right handed or left handed rivers branching from the main river. Generally, it can be assumed that since Austria's geology consists of several different geologic units, Austria's rivers and lakes might a high potential to be distinguishable in migration studies of fish using otolith micro chemistry. From all combinations of $^{88}Sr/^{43}Ca$, $^{23}Na/^{43}Ca$ and $^{87}Sr/^{86}Sr$ in the water samples the combination of all three values proofed to be the best description of the environment of the fish, since it allowed a retrospective assignment of fish via otolith chemistry to the four identified water clusters with 100% accuracy. Fish from different geological units (crystalline rocks and calcareous rocks) were separated by $^{87}Sr/^{86}Sr$ ratios. It is assumed that $^{87}Sr/^{86}Sr$ in natural habitats varies because of the underlying geology. In spite of the fact that the Na concentration in otoliths is physiologically controlled, which resulted in a poor correlation of $^{23}Na/^{43}Ca$ in water and otolith samples, $^{23}Na/^{43}Ca$ contributed positively to the retrospective assignment of the fish to the water clusters. This suggests that physiologically regulated elements can be used as well to distinguish groups of fish.

Speaking of the temporal resolution as a result of the laser ablation experiments of the otoliths, there might be potential to improve the spot size of the laser beam and thus the spatial resolution since the spot sizes of the lines for the multi-element measurement (20 µm) the strontium isotope ratio (173 ± 18 µm and 312 ± 35 µm) were quite large in comparison to other studies. For example [CAMPANA et al, 1994] used a spot size of 30 µm for the examination of $^{87}Sr/^{86}Sr$ of a marine fish species for the calculation of $^{87}Sr/^{86}Sr$ ratios, it must be considered, however, that the strontium concentrations in sea water are about 100 times higher than in fresh water and the large spot sizes in the present study were chosen in order to get a evaluable signal. Another observation that should be investigated in more detail in future are the strontium peaks found in several otoliths in the core region of the line scans. They might occur due to physiological changes during the growth of the fish and influences of the mother's environment prior to laying of the eggs. It was also shown that several elements can be detected in eye lenses and scales. Considerable differences in the sodium content in the

surface of eye lenses of fish from two different locations could be observed. Further attention should therefore be paid to alternative tissues to otoliths that can also be used as natural tag like scales, eye lenses and fin rays. Especially non lethal alternatives to otoliths like scales and fin rays are needed for migration studies and population discrimination of endangered fish species.

5 References

ABLE K. W. and LAMONACA J. C. (2006): Scale formation in selected western North Atlantic Flatfishes. Journal of Fish Biology (2006) 68, 1679–1692

ALBARÈDE F. et al (2004): Precise and accurate isotopic measurements using multiple-collector ICPMS; Geochimica et Cosmochimica Acta, Volume 68, pages 2725-2744

ARAI T. and HIRATA T. (2006): Determination of trace elements in otoliths of chum salmon Oncorhynchus keta by laser ablation-ICP-mass spectrometry. FISHERIES SCIENCE 2006; 72: 977–984

ARAI T., HIRATA T. and TAKAGI Y. (2007): Application of laser ablation ICPMS to trace the environmental history of chum salmon Oncorhynchus keta. Marine Environmental Research 63 (2007) 55–66

ARAI T., OHJI M. and HIRATA T. (2007): Trace Metal Deposition in Teleost Fish Otolith as an Environmental Indicator. Water Air Soil Pollute (2007) 179:255–263

ASANO M. and MUGIYA Y. (1993): Biochemical and calcium-binding properties of water-soluble proteins isolated from otoliths of the tilapia, Oreochromis niloticus. Comp. Biochem. Physiol.104B:201-205

ASHFORD J. and JONES C. (2007): Oxygen and carbon stable isotopes in otoliths record spatial isolation of Patagonian tooth fish (Dissostichus eleginoides). Geochimica et Cosmochimica Acta 71 (2007) 87–94

ASHFORD J. R., ARKHIPKIN A. I. and JONES C. M. (2006): Can the chemistry of otolith nuclei determine population structure of Patagonian tooth fish Dissostichus eleginoides? Journal of Fish Biology (2006) 69, 708–721

AUGLEY J., HUXHAM M., FERNANDES T. F., LYNDON A. R., BURY S. (2007): Carbon stable isotopes in estuarine sediments and their utility as migration markers for nursery studies in the Firth of Forth and Forth Estuary, Scotland. Estuarine, Coastal and Shelf Science xx (2007) 1-9

BOULYGA Sergei (2006): ELAN schematic in lecture: Advanced analytical techniques for elemental trace and isotope analysis; University of Natural Resources and Applied Life Sciences, Vienna

BROPHY D., DANILOWICZ B. S. and JEFFRIES T. E. (2003a): The detection of elements in larval otoliths from Atlantic herring using laser ablation ICP-MS. Journal of Fish Biology (2003) 63: 990-1007

BROPHY D., JEFFERIES T. E. and DANILOWICZ B. S. (2003): Elevated manganese concentrations at the cores of clupeid otoliths: possible environmental, physiological, or structural origins. Marine Biology (2004) 144: 779–786

BROWN J. (2006): Classification of juvenile flatfishes to estuarine and coastal habitats based on the elemental composition of otoliths. Estuarine, Coastal and Shelf Science 66 (2006) 594-611

BRÜGGEMANN-LEDOLTER M., J. RUTHNER, EGGER H., KRENMAYR H.G., MANDL G.W., MATURA A., NOWOTNY A., PASCHER G., PESTAL G., PISTOTNIK J., ROCKENSCHAUB M. und SCHNABEL W.(1999): Geologische Übersichtskarte der Republik Österreich. Geologischen Bundesanstalt Wien. Available online: http://www.geologie.ac.at/, date: 08-01-06

BRUNNER M. (2007): Master thesis: Determination of geographical origin of agricultural products via isotopic and elemental analyses by Inductively coupled plasma mass spectrometry (ICP-MS) on the example of Asparagus officinalis, University of Natural Resources and Applied Life Sciences, Vienna, pages 44-45

CAMPANA S. E. and JONES C. M. (1998): Radiocarbon from nuclear testing applied to age validation of black drum, Pogonias cromis. Fish. Bull. 96:185-192

CAMPANA S. E., CHOUINARD G. A., HANSON J. M., FREHET A. and BRATTEY J. (2000): Otolith elemental fingerprints as biological tracers of fish stocks. Fisheries Research 46 (2000): 343-357

CAMPANA S. E., CHOUINARD G. A., HANSON M., FRECHET A. and BRATTEY J. (1999a): Otolith elemental fingerprints as biological tracers of fish stocks. Fish. Res.

CAMPANA S. E., FOWLER A. J., JONES C. M. (1994): Otolith elemental fingerprinting for stock identification of Atlantic cod (Gadus morhua) using laser ablation ICPMS. Can. J. Fish. Aquat. Sci. 51:1942-1950

CAMPANA S. E., FOWLER A. L. and JONES C. M. (1994): Otolith elemental fingerprinting for stock identification of Atlantic cod (Gadus morhua) using Laser Ablation ICPMS. Canadian Journal of Fisheries and Aquatic Sciences 51: 1942-1950.

CAMPANA, S. E. and J.D. NEILSON (1985): Microstructure of fish otoliths. Can. J. Fish. Aquat. Sci. 42:1014-1032

CAMPANA, S. E., G. A. Chouinard, J. M. Hanson, A. Frechet and J. Brattey (2000). Otolith elemental fingerprints as biological tracers of fish stocks. Fisheries Research 46: 343-357.

CAMPANA, S.E. (1999): Chemistry and composition of fish otoliths: pathways, mechanisms and applications. Mar. Ecol. Prog. Ser. 188:263-297

CAMPANA, S.E. and W.-N. TZENG. (2000) Editorial – Section 4: Otolith Composition. Fish. Res. 46:287-288.

CAPO R., STEWARD B. W. and CHADWICK O. A. (1998): Strontium isotopes as tracers of ecosystem processes: theory and methods. Geoderma 82 (1998) 197-225

CARLSTRÖM D. (1963): A crystallographic study of vertebrate otoliths. Biol. Bull. 124:441-463

CETAC (2007): Service manual. Available online: http://www.cetac.com/, date: 08-01-22

CHITTARO P. M., GAGNON J. and FRYER B. J. (2006a): The differentiation of Stegastes partitus populations using lapillar and sagittal otolith chemistry. Journal of Fish Biology (2006) 68, 1909–1917

CHITTARO P. M., USSEGLIO P., FRYER B. J. and SALE P. F. (2006): Spatial variation in otolith chemistry of Lutjanus apodus at Turneffe Atoll, Belize. Estuarine, Coastal and Shelf Science 67 (2006) 673-680

CLARKE A. D., TELMER K. H., MARK SHRIMPTON J. (2007): Elemental analysis of otoliths, fin rays and scales: a comparison of bony structures to provide population and life-history information for the Arctic grayling (Thymallus arcticus). Ecology of Freshwater Fish 2007

CLARKE A., TELMER K. H., MARK SHRIMPTON J. (2007): Elemental analysis of otoliths, fin rays and scales: a comparison of bony structures to provide population and life-history information for the Arctic grayling (Thymallus arcticus). Ecology of Freshwater Fish 2007.

CROOK D. A., MACDONALD J. I., O'CONNOR J. P. and BARRY B. (2006): Use of otolith chemistry to examine patterns of diadromy in the threatened Australian grayling Prototroctes maraena. Journal of Fish Biology (2006) 69, 1330–1344

DEAN John R. (1997): Atomic absorption and plasma spectroscopy; pages 117-128

DOVE S. G. (1999): Ontological changes in the crystallin composition of the eye lenses of the territorial damselfish Parma microlepisand their possible effects on trace-metal accumulation. Marine Biology (1999) 134: 653-663

DOVE S. G. and KINGSFORD M. J. (1998); Use of otoliths and eye lenses for measuring trace-metal incorporation in fishes: a biogeographic study. Marine Biology (1998) 130: 377–387

EDMONDS J. S., CAPUTI N., MORAN M. J., FLETCHER W. J., MORITA M. (1995): Population discrimination by variation in concentrations of minor and trace elements in sagittae of two Western Australian teleosts. In: Secor DH, Dean JM, Campana SE (eds) Recent Developments in Fish Otolith Research.University of South Carolina Press., Columbia, SC p 655-670

EDMONDS J. S., CAPUTI N., MORITA M. (1991): Stock discrimination by trace-element analysis of otoliths of orange roughy (Hoplostethus atlanticus), a deep-water marine teleost. Aust. J. Mar. Freshwater Res. 42:383-389

EIChrom (2007): product description of Sr spec Resin: http://www.eichrom.com/products/info/sr_resin.cfm, date: 2007-10-23

ELSDON T. S. and GILLANDERS B. M. (2006): Identifying migratory contingents of fish by combining otolith Sr:Ca with temporal collections of ambient Sr:Ca concentrations. Journal of Fish Biology (2006) 69, 643–657

ELSDON T. S. and GILLANDERS B. M. (2006a): Temporal variability in strontium, calcium, barium, and manganese in estuaries: Implications for reconstructing environmental histories of fish from chemicals in calcified structures. Estuarine, Coastal and Shelf Science 66 (2006) 147-156

FALINI G., ALBECK S., WEINER S., ADDADI L. (1996): Control of aragonite or calcite polymorphism by mollusk shell macromolecules. Science 271:67-69

FARRELL J. and CAMPANA S. E. (1996): Regulation of calcium and strontium deposition on the otoliths of juvenile tilapia, Oreochromis niloticus. Comp. Biochem. Physiol. 115A:103-109

FAURE G. and MENSING T. (2005): Isotopes: Principles and Applications; 3rd edition, John Wiley & Sons, Hoboken, New Jersey Chapter 5 – The Rb-Sr Method, page 78

GALLAHAR N. K. and KINGSFORD M. J. (1996): Factors influencing Sr/Ca ratios in otoliths of Girella elevata: an experimental investigation. J. Fish Biol. 48:174-186

GAULDIE R. W., ROMANEK C. R. (1998): Orange roughy otolith growth rates: a direct experimental test of the Romanek-Gauldie otolith growth model. Compar. Biochem. Physiol. 120A:649-653

GAULDIE R. W., THACKER C. E., WEST I. F., WANG L. (1998): Movement of water in fish otoliths. Comp. Biochem. Physiol. 120A:551-556

GAULDIE R. W., XI K., SHARMA S. K. (1994): Developing a Raman spectral method for measuring the strontium and calcium concentrations of fish otoliths. Can. J. Fish. Aquat. Sci.

GILLANDERS P. M., SANCHEZ-JEREZ P., BAYLE-SEMPERE J. and RAMOS-ESPLA A. (2001): Trace elements in otoliths of the two-banded bream from a coastal region in the south-west Mediterranean: are there differences among locations? Journal of Fish Biology (2001) 59, 350–363

GREEGOR R. B., PINGITORE Jr. N. E., LYTLE F. W. (1997): Strontianite in coral skeletal aragonite. Science 275:1452-1454

GUNN J. S., HARROWFIELD I. R., PROCTOR C. H., THRESHER R. E. (1992): Electron probe microanalysis of fish otoliths - evaluation of techniques for studying age and stock discrimination. J. Exp. Mar. Biol. Ecol. 158:1-36

HAMER P. A., JENKINS G. P. and COUTIN P. (2006): Coutin Barium variation in Pagrus auratus (Sparidae) otoliths: A potential indicator of migration between an embayment and ocean waters in south-eastern Australia. Estuarine, Coastal and Shelf Science 68 (2006) 686-702

HOFF G. R. and FUIMAN L. A. (1995): Environmentally induced variation in elemental composition of red drum (Sciaenops ocellatus) otoliths. Bull. Mar. Sci. 56:578-591

HORWITZ (1993): The function of alpha-crystallin. Investigative Ophthal visual Sci 34: 7-22

HUMPHREYS JR R. L., CAMPANA S. E. and DEMARTINI E. E.(2005):Otolith elemental fingerprints of juvenile Pacific swordfish Xiphias gladius. Journal of Fish Biology (2005) 66, 1660—1670

IKOMA T., KOBAYASHI H., TANAKA J., WALSH D. and MANN S. (2003): Microstructure, mechanical, and biomimetic properties of fish scales from Pagrus major. Journal of Structural Biology 142 (2003) 327–333

in the scales of spawning weakfish, Cynoscion regalis. CanadianJournal of Fisheries and Aquatic Sciences 60, 361-369.

INGRAM B. L. and WEBER P. K. (1999): Salmon origin in Califoria's Sacramento-San Joaquin river system as determined by otolith strontium composition. Geology 9 (1999): 851-854

KALISH J. M. (1989): Otolith microchemistry: validation of the effects of physiology, age and environment on otolith composition. J.Exp. Mar. Biol. Ecol. 132:151-178

KALISH, J.M. (1991): Determinants of otolith chemistry: seasonal variations in the composition of blood plasma, endolymph and otoliths of bearded rockcod Pseudophycis barbata. Marine Ecology Progress Series 74, 137-159.

KALISH, J.M. (1992): Stress induced changes in the concentration of elements in otoliths of Australian salmon. Journal of Experimental Marine Biology and Ecology 162, 265-277.

KENNEDY B. D., FOLT C. L., BLUM J. D., CHAMBERLINE C. P. (1997): Natural isotope markers in salmon. Nature 387:766-767

KINGSFORD M. J. and GILLANDERS B. M. (2000): Variation in concentrations of trace elements in otoliths and eye lenses of a temperate reef fish, Parma microlepis, as a function of depth, special scale, ans age. Marine Biology (2000) 137: 403-414

KNUDSON K. J., TUNG T. A., NYSTROM K. C., PRICE T. D. and FULLGAR P. D. (2005): The origin of the Juch'uypampa Cave mummies: strontium isotope analysis of archaeological human remains from Bolivia. Journal of Archaeological Science 32 (2005) 903-913

KÖLBL J. (2008):Die Forelle. Verband Österreichischer Forellenzüchter. available online: http://www.forellenzuchtverband.at, date: 08-01-06

LIMBURG K. E. (1995): Otolith strontium traces environmental history of subyearling American shad Alosa sapidissima. Mar. Ecol. Prog. Ser. 119:25-35

LO-YAT A., MEEKAN M., MUNKSGAARD N., PARRY D., PLANES S., WOLTER M. and CARLETON J. (2005): Small-scale spatial variation in the elemental composition of otoliths of Stegastes nigricans (Pomacentridae) in French Polynesia. Coral Reefs (2005) 24: 646–653

MARKWITZ A., GRAMBOLE D., HERRMANN F., TROMPETTER W.J., DIOSES T. and GAULDIE R.W. (2000): Reliable micro-measurement of strontium is the key to cracking the life-history code in the fish otolith. Nuclear Instruments and Methods in Physics Research B 168 (2000) 109-116

MAYER Jr. F. L., MARKING L. L., BILLS T. D., HOWE G. E. (1994): Physicochemical factors affecting toxicity in freshwater:294 hardness, pH, and temperature. In: Hamelink JL, Landrum PF, Bergman HL, Benson WH (eds) Bioavailability: physical, chemical and biological interactions. Lewis Publishers, London p 5-21

MILLER J. A. (2007): Scales of variation in otolith elemental chemistry of juvenile staghorn sculpin (Leptocottus armatus) in three Pacific Northwest estuaries. Mar Biol (2007) 151:483–494

MILTON D. A., TENAKANAI C. D. and CHENERY S. R. (2000): Can the Movements of Barramundi in the Fly River Region, Papua New Guinea be Traced in their Otoliths? Estuarine, Coastal and Shelf Science (2000) 50, 855–868

MONTASER A. (1998). Inductively coupled plasma mass spectrometry. Wiley-VCH.

MORITA K., ARAI T., KISHI T. and TSUBOI J. (2005): Small anadromous Salvelinus malma at the southern limits of its distribution. Journal of Fish Biology (2005) 66, 1187–1192

MORSE J. W. and MACKENZIE F. T. (1990): Geochemistry of sedimentary carbonates. Elsevier Pub, NY 580 pp

MUHLFELD C. C. and MAROTZ B. (2005): Geochemical Signatures in Scales Record Stream of Origin in Westslope Cutthroat Trout. Transactions of the American Fisheries Society (2005)134:945–959

N. N. (2008): Bachforelle. avaiable online: http://de.wikipedia.org, date: 08-01-06

N. N. (2008a): Regenbogenforelle. avaiable online: http://de.wikipedia.org, date: 08-01-06

N. N. (2008b): Fische unserer Region. Fischereiverband Leoben. avaiable online: http://www.fischerei.co.at/, date: 2008-01-06

N. N. (2008c): meristics. avaiable online: http://en.wikipedia.org, date: 08-01-07

N. N.(2007) “The 1995 update to the atomic mass evaluation” by G. Audi and A.H. Wapstra, Nuclear Physics A595 vol. 4 p.409-480, December 25, 1995.”: http://atom.kaeri.re.kr:, date: 2007-11-05

NAGIEC M., CZERKIES P., GORGYCZKO K., WITKOWSKI A., MURAWSKA E. (1995): Mass-marking of grayling, Thymallus thymallus, larvae by fluorochrome tagging of otoliths. Fish. Manage. Ecol. 2:185-195

NELMS Simon (2005): Inductively coupled plasma mass spectrometry handbook, Oxford (UK), Blackwell Publishing

NEW WAVE RESEARCH (2007): UP 193 Solid-State Laser Ablation System. Available online: http://www.new-wave.com, date: 08-01-22

NU INSTRUMENTS (2005): Nu Plasma Manual, page 5

NU INSTRUMENTS (2008): Nu Plasma HR, http://www.nu-ins.com, date: 08-03-16

OHIRA Y., SHIMIZU M., URA K. and TAKAGI Y.(2007): Scale regeneration and calcification in goldfish Carassius auratus: quantitative and morphological Processes. FISHERIES SCIENCE 2007; 73: 46–54

OLSSON P. E., KLING P., HOGSTRAND C. (1998): Mechanisms of heavy metal accumulation and toxicity in fish. In: Langston WJ, Bebianno MJ (eds) Metal Metabolism in Aquatic Environments. Chapman and Hall, London, p 321-350

OUTRIDGE P. M., CHENERY S. R., BABALUK J. A. and REIST J. D. (2002): Analysis of geological Sr isotope markers in fish otoliths with subannual resolution using laser-ablation-multicollector-ICP-mass spectrometry. Environmental Geology (2002) 42: 891-899

PAPADOPOULOU C., KANIAS G. D., KASSIMATI E. (1980): Trace element content in fish otoliths in relation to age and size. Mar. Poll. Bull. 11:68-72

PATTERSON H. M., KINGSFORD M. J. and McCULLOCH M. T. (2005): Elemental signatures of Pomacentrus coelestis otoliths at multiple spatial scales on the Great Barrier Reef, Australia. Mar Ecol Prog Ser (2004) 270: 229–239

PATTERSON H. M., KINGSFORD M. J. and McCULLOCH M. T. (2005): Resolution of the early life history of a reef fish using otolith chemistry. Coral Reefs (2005) 24: 222–229

PERSSON P.,. BJO¨RNSSON B. TH and TAKAGI Y. (1999): Characterization of morphology and physiological actions of scale osteoclasts in the rainbow troutJournal of Fish Biology (1999) 54, 669–684

POPPER A.N., J. RAMCHARITAR and S.E. CAMPANA. 2005. Why otoliths? Insights from inner ear physiology and fisheries biology. Mar. Freshwater Res. 56:497-504.

PROCTOR C. H. and THRESHER R. E. (1998) Effects of specimen handling and otolith preparation on concentration of elements in fish otoliths. Mar. Biol. 131:681-694

ROOKER J. R., SECOR D. H., ZDANOWICZ V. S., DE METRIO G. and RELINI L. O. (2003): Identification of Atlantic bluefin tuna (Thunnus thynnus) stocks from putative nurseries using otolith chemistry. Fish. Oceanogr. 12:2, 75–84

ROSMAN K. J. R. and TAYLOR P. D. P (1997): Isotopic compositions of the elements 1997, International Union of Pure and Applied Chemistry

ROSMAN K.J.R. and TAYLOR P.D.P. (1997): Isotopic compositions of the elements 1997; subcommittee for isotopic abundance measurements, commission on atomic weights and isotopic abundances, inorganic chemistry division, international union of pure and applied chemistry, page 19; available online: www.iupac.org, date: 2007-11-05

SADOVY Y. and SEVERIN K. P. (1992): Trace elements in biogenic aragonite: correlation of body growth rate and strontium levels in the otoliths of the white grunt, Haemulon plumieri (Pisces: Haemulidae). Bull. Mar. Sci. 50:237-257

SADOVY, Y., SEVERIN, K. (1992): Trace elements in biogenic aragonite: correlation of body growth rate and strontium levels in the otoliths of the white grunt, Haemulon plumieri (Pisces: Haemulidae). Bulletin of Marine Science 50, 237-257.

SADOVY, Y., SEVERIN, K. (1994): Elemental patterns in Red Hind (Epinephelus guttatus) otoliths from Bermuda and Puerto Rico reflect growth rate, not temperature. Canadian Journal of Fisheries and Aquatic Science 51, 133-141.

SCHULTHEIS G. (2003): Analysis of isotope ratios in anthropological and archaeological samples by high resolution inductively.

SCHWARCZ H. P., GAO Y., CAMPANA S., BROWNE D., KNYF M., BRAND U. (1998): Stable carbon isotope variations in otoliths of Atlantic cod (Gadus morhua). Can. J. Fish. Aquat. Sci. 55:1798-1806

SECOR D. H., HOUDE E. D. (1995): Larval mark-release experiments: potential for research on dynamics and recruitment in fish stocks. In: SECOR D.H., DEAN J. M. and CAMPANA S. E. (eds) Recent Developments in Fish Otolith Research. University of South Carolina Press, Columbia, SC p 423-444

SECOR, D. H., DEAN, J. M. and LABAN E. H. (1992): Otolith removal and preperation formicrostructural examination. P. 19-57. *In* Stevenson, D.K. and Campana, S. E. [ed.] Otolith microstructureexamination and analysis. Can. Spec. Publ. Fish. Aquat. Sci. 117.

SIE S. H., THRESHER R. E. (1992): Micro-PIXE analysis of fish otoliths: methodology and evaluation of first results for stock discrimination. Internat. J. PIXE 2:357-379

SIMKISS K. (1974): Calcium metabolism of fish in relation to ageing.In: Bagenal TB (ed) The Ageing of Fish. Unwin Brothers Ltd., Surrey, England p 1-12

THOMAS R. (2002): A Beginner‘s Guide to ICP-MS. Part X — Detectors. Spectroscopy 17(4). Available online: www.spectroscopyonline.com , date: 2008-03-10

THORROLD S. R., CAMPANA S. E., JONES C. M., SWART P. K. (1997): Factors determining delta C-13 and delta O-18 fractionation inaragonitic otoliths of marine fish. Geochim. Cosmochim. Acta 61:2909-2919

THORROLD S. R., JONES C. M., SWART P. K. TARGETT T. E. (1998): Accurate classification of juvenile weakfish Cynoscion regalito estuarine nursery areas based on chemical signatures in otoliths. Mar. Ecol. Prog. Ser. 173:253-265

THORROLD S. R., JONES G. P., PLANES S. and HARE J. A. (2006): Transgenerational marking of embryonic otoliths in marine fishes using barium stable isotopes. Can. J. Fish. Aquat. Sci. (2006) 63: 1193–1197

THORROLD S. R., LATKOCZY C., SWART P. K. and JONES C. M. (2001): Natal homing in a marine fish metapopulation. Science (2001) vol 291: 297-299

TOMAS J., AUGAGNEUR S., ROCHARD E. (2005): Discrimination of the natal origin of young-of-the-year Allis shad (Alosa alosa) in the Garonne–Dordogne basin (south-west France) using otolith chemistry. Ecology of Freshwater Fish 2005: 14: 185–190

WATSON J.T (1985): Introduction to mass spectrometry, pages 244-247

WEBER P. K., BACON C.D., HUTCHEON . D.,INGRAM B. L. and WOODEN J. (2005): Ion microprobe measurement of strontium isotopes in calcium carbonate with application to salmon otoliths. Geochimica et Cosmochimica Acta (2005), Vol. 69, No. 5, pp. 1225–1239

WELLS B. K., RIEMAN B. E., CLAYTON J. L. and HORAN D. L. (2003a): Relationships between water, otolith, and scale chemistries of westslope cutthroat trout from the Coeur d’Alene River, Idaho: the potential application of hard-part chemistry to describe movements in fresh water. Transactions of the American Fisheries Society 132:409–424.

WELLS B. K., THORROLD S. R. and JONES C. M. (2003b): Stability of elemental signatures in the scales of spawning weakfish, Cynoscion regalis. Canadian Journal of Fisheries and Aquatic Sciences 60:361–369.

WELLS, B.K., THORROLD, S.R., JONES, C.M., 2003. Stability of elemental signatures

WISE S. A. and WATTERS R. L. (2007): Certificate of Analysis Standard Reference Material® 987 Strontium Carbonate (Isotopic Standard); National Institute of Standards & Technology, available online: https://srmors.nist.gov, date: 2007-11-05

WRIGHT P. J., NEAT F. C., GIBB F. M., GIBB I. M. AND THORDARSON H. (2006): Evidence for metapopulation structuring in cod from the west of Scotland and North Sea. Journal of Fish Biology 69 (Supplement C), 181–199

ZITEK A., STURM M., WAIDBACHER H. and PROHASKA T. (2008): Retrospective assignment of brown trout (Salmo trutta f.f L.) and rainbow trout (Oncorhynchus mykiss Walbaum 1792) to life stage specific habitats based on chronological patterns of elements (88Sr/43Ca, 23Na/43Ca) and Sr isotopic ratios (87Sr/86Sr) in otoliths using LA-ICP-MS: preliminary results. In preparation for publication.

6 Appendix

6.1 List of Figures

6.2 List of Tables